Investigating the Hi-G Dryer System on coarse Daberas slurry material

by

Warren John Lloyd Olivier

Thesis presented in partial fulfilment
of the requirements for the degree

of

MASTER OF SCIENCE IN ENGINEERING
(CHEMICAL ENGINEERING)

in the Faculty of Engineering
at Stellenbosch University

Supervisor
Dr R Els

March 2015

Declaration

By submitting this thesis electronically, I declare that the entirety of the work contained therein is my own, original work, that I am the sole author thereof (save to the extent explicitly otherwise stated), that reproduction and publication thereof by Stellenbosch University will not infringe any third party rights and that I have not previously in its entirety or in part submitted it for obtaining any qualification.

Warren JL Olivier

Date: 04 February 2015

Abstract

Namdeb Diamond Corporation is constantly investigating and investing in technologies to continuously improve performance and productivity. Diamond mining operations have been taking place for more than a hundred years – ever since the first diamond was discovered in 1908. Diamonds are a scarce and finite resource. As current resources are being depleted, the Namdeb exploration team are exploring areas not previously considered feasible. One such resource is the Sendelingsdrift resource, situated about 20 km from Daberas, one of the current Namdeb operations along the Orange River.

When an environmental assessment was conducted, it was discovered that the Sendelingsdrift area was environmentally sensitive in terms of constructing a slimes dam, creating difficulties for slurry processing. Thus the Derrick Hi-G Dryer Fines Recovery System was considered as a probable solution; unfortunately it was found that the slurry discharge would be too coarse for this technology.

The Hi-G Dryer technology has never been tested with a coarse slurry feed. The Daberas processing plant produces slurry of -3 mm particles, which is very coarse compared to the 75 µm particles with which the Hi-G Dryer system normally operates. Testing was conducted at Daberas by directing the Daberas wet-sizing underflow as feed to the Hi-G Dryer system. The majority of the testing was done under production conditions, which proved to be very difficult.

The results of the initial supplier-designed Hi-G Dryer processing system produced an oversize moisture content of 17%, which was better than that which the supplier had claimed but not as good as that which the existing Daberas degrit system produced. After studying the system parameters and optimising certain parameters, a proposed Hi-G Dryer system was recommended for coarser slurries. The new process parameters generated improved results, with an oversize moisture content of 13% – better than the Daberas dewatering system benchmark. The Hi-G screen oversize material also proved to be conveyable and was quantified with oversize yield stress test results. Overall system

efficiency was improved after the recommended modifications to the design had been made and a simulation had been conducted to understand the impact of certain parameters on the overall system.

Opsomming

Die Namdeb Diamantmaatskappy is voortdurend daarop ingestel om die maatskappy se prestasie en produktiwiteit te verbeter, veral deur in nuwe tegnologie te belê. Daar word sedert die eerste diamant in 1908 gevind is, diamante langs die Oranjerivier ontgin. Diamante is egter 'n skaars en beperkte hulpbron. Namate die hulpbron uitgeput word, word die Namdeb-span genoodsaak om gebiede te ondersoek wat voorheen nie as ekonomies ontginbaar beskou is nie. Die Sendelingsdriftgebied, wat sowat 20 km van Daberas, een van Namdeb se huidige ontginningsgebiede langs die Oranjerivier, geleë is, is so 'n gebied.

Tydens die omgewingsevaluering is egter gevind dat die Sendelingsdriftgebied uiters omgewingsensitief is vir die oprigting van 'n slikdam. Dit het aanleiding gegee daartoe dat die Derrick *Hi-G Dryer Fines Recovery System* as 'n moontlike oplossing vir die probleem oorweeg is. Ongelukkig was die afvoermateriaal te grof vir die *Hi-G Dryer*-tegnologie.

Die *Hi-G Dryer*-tegnologie is nog nie vantevore met growwe flodder getoets nie. Die Daberas-aanleg lewer flodder van -3 mm-partikels, wat baie growwer is as die 75 µm-partikels waarmee die *Hi-G Dryer*-stelsel gewoonlik werk. Die stelsel is by die Daberas-aanleg getoets deur die stelsel met growwe ondervloei te voer. Die grootste gedeelte van die toetswerk moes onder produksietoestande gedoen word, wat dit baie moeilik gemaak het.

Desondanks was die resultate gunstig. Die aanvanklike prosesuitleg het 'n produkvog van 17% opgelewer, wat beter was as wat die verskaffer van die tegnologie verwag het. Dit was egter nie so goed soos die voginhoud wat die bestaande Daberas-stelsel gelewer het nie. Ná optimalisering van die stelsel het die voginhoud tot 13% verbeter – beter as die huidige Daberas-ontwateringstelsel. Die ontwaterde materiaal was ook maklik afvoerbaar.

Die algehele doeltreffendheid van die stelsel het verbeter nadat die aanbevole aanpassings aan die ontwerp gemaak is en ’n simulasie gedoen is om die impak van sekere parameters op die stelsel as geheel te verstaan.

Acknowledgements

I want to thank my heavenly Father for this project, for the knowledge and wisdom He bestowed on me during my studies and for being part of my life.

I also like to acknowledge my loving wife, Trizelle who supported and encouraged me throughout my studies. A special thanks to Dr R Els for his patience and guidance. I would also like to thank Namdeb Diamond Corporation for their confidence in me to work on this project.

Table of contents

List of figures

List of tables

Abbreviations and nomenclature

Abbreviation	Definition
alpha	curve steepness
DMS	dense medium separation
d_{50}	partition curve material cut size
d_{50c}	corrected determined cut size
DTP	Daberas Treatment Plant
G-force	gravitational force (9.81m/s^2)
Hi-G	High-gravitational
ORM	Orange River Mines
PSD	particle size distribution
R_f	liquid fraction in underflow from feed
SSE	sum of squared errors
wt	weight

Symbol	Definition	Unit
G-force	gravitational force (9.81 m/s^2)	m/s^2
rpm	revolution per minute	rev/min
SG	specific gravity	t/m^3
t/h	feed tons per hour	t/h
m^3/hr	cubic meters per hour	m^3/hr
USGPM	United States gallon per minute	USGPM

1 Background

1.1 Project definition

It has become apparent within the Namdeb Group that there is a need for an alternative means of slimes disposal, especially within environmentally sensitive areas. Currently all DeBeers and Anglo American mines make use of thickeners from which the underflow is pumped to an environmentally approved slimes dam. Although it is an effective means of slimes disposal, the thickener together with the degrit system drastically increases the footprint of the processing plant which requires addition environmental impact assessments (EIA's) and approvals. At Namdeb, the Daberas slurry material consists of -3 mm material that reports to a degrit system in which the -0.5 mm material is thickened and deposited to a slimes dam (see Figure 1-1).

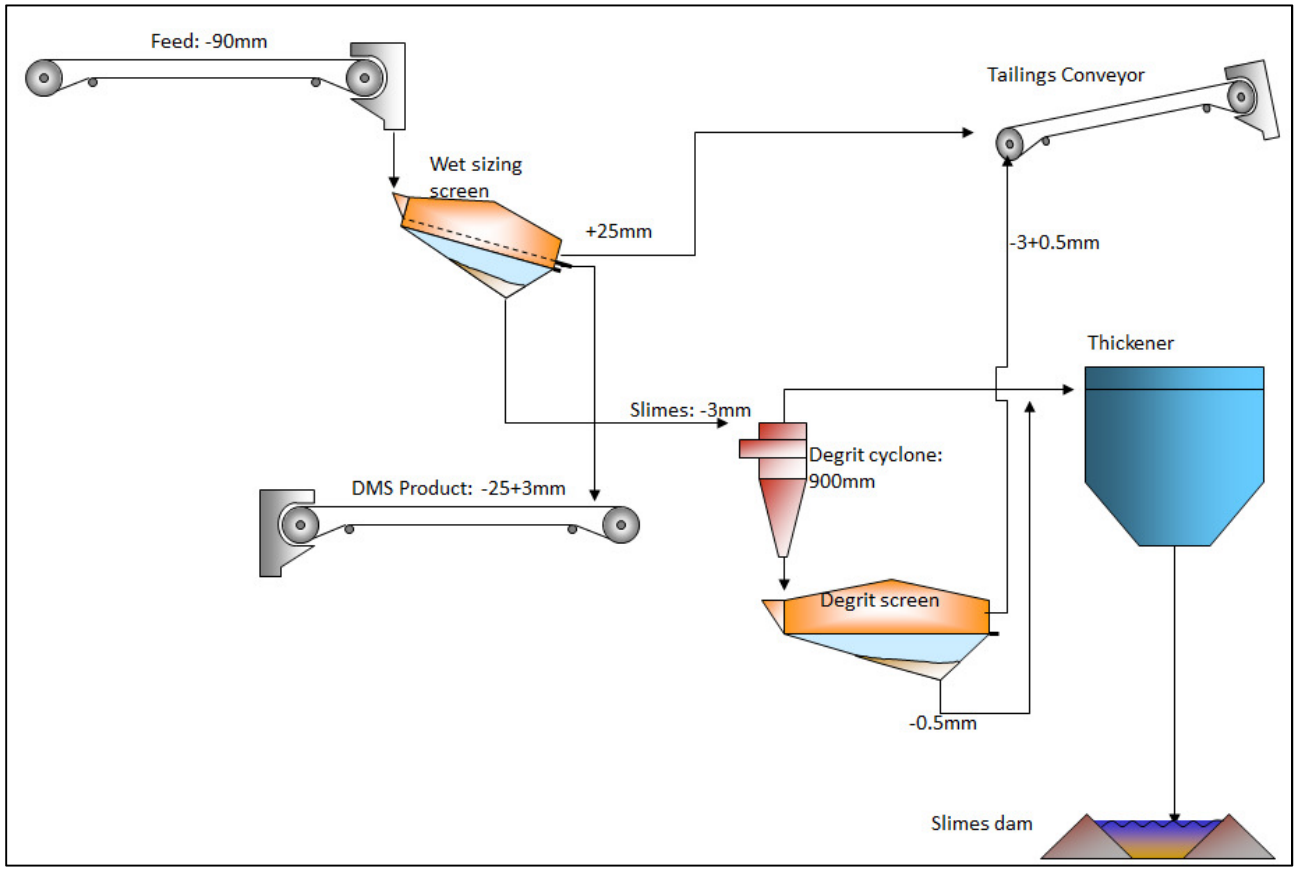

Figure 1-1: Schematic layout of the Daberas wet-sizing and degrit section

In other industrial operations, the Derrick Hi-G Dryer Fines Recovery System successfully justified the treatment of ultra-fine (38–375 µm) material from which very low-moisture oversize product was produced (Bateman, 2002) (AggMan Staff, 1999). The slurry produced as feed to the Hi-G Dryer at the Namdeb operations is much coarser (-3000µm), which creates uncertainty whether the Hi-G Dryer system technology would be suitable as an effective dewatering mechanism for coarser slurries.

Namdeb's ultimate expectation is for the Hi-G Dryer system to remove the largest possible amount of solids from the slurry and produce a low-moisture oversize product (±20% moisture) which can be conveyed easily. The study was also conducted to explore whether the Hi-G Dryer system could produce a high-quality effluent that can be used as process water.

Other benefits of the successful implementation of a coarse feed slurry Hi-G Dryer system within Namdeb operations would include:

- a reduced thickener feed capacity. Should the Hi-G Dryer system remove the majority of the solids, fewer solids would report to the thickener. This would present the potential for a smaller thickener during the design phase or a more efficient in situ thickener.
- a smaller slimes dam with less strain on the existing slimes dam
- a reduced slimes disposal footprint
- reduced unit cost of the mining operation
- ensuring the environmental integrity of Namdeb

In summary, testing was conducted to observe the dewatering capability of the Hi-G Dryer system on a coarse slurry at the Daberas processing plant in order to determine if the Hi-G Dryer system can produce a low-moisture, conveyable oversize product, a high-quality effluent and an overall efficient system.

1.2 Introduction

Derrick Corporation is a USA-based company which supplies the aggregate industry with fines recovery systems. The Derrick Hi-G Dryer Fines Recovery System consists of cluster hydrocyclones that is mounted on top of a high-G-force linear-motion screening unit. The combination of these two mechanisms alleges to produce a fines product of 75–80% solids by mass (Derrick Corporation, 2008a).

Daberas falls within the Orange River Mines area and is one of the Namdeb business units situated about 60 km from Oranjemund on the banks of the Orange River (see Figure 1-2).

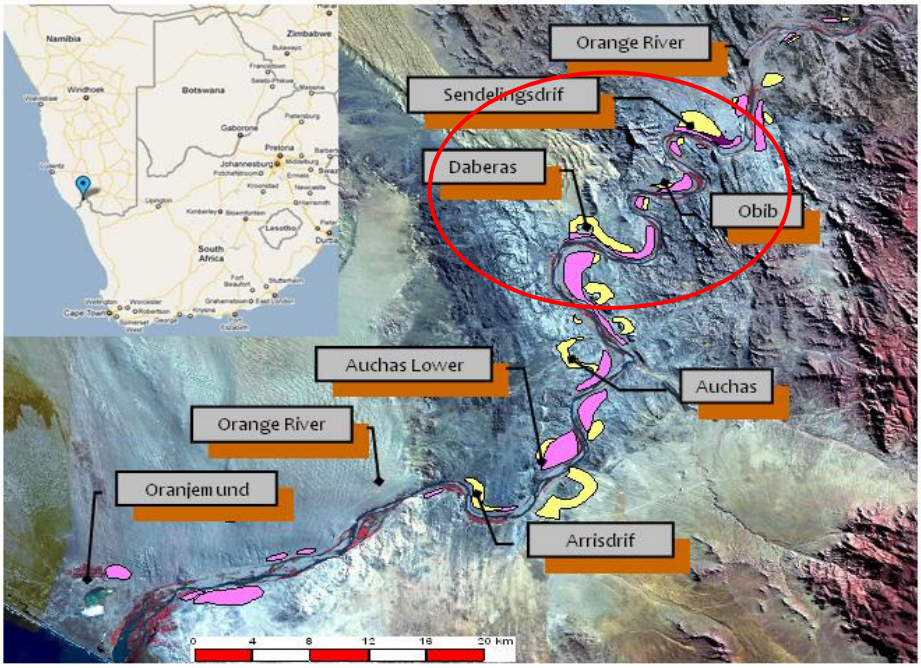

Figure 1-2: Location of river deposits

Because of the larger size diamonds mined at Daberas, it is one of Namdeb's high-revenue business units. The Daberas mine has also reached a point where most of the high-grade resources are depleted and only the low-grade resources remain. It therefore becomes imperative to invest in a technology that could reduce the cost per ton treated and thus render the low-grade resources more economical to mine. The Hi-G Dryer (see

Figure 1-3) could reduce the operational costs of sections like the thickener, degrit and slimes dam. It could even present the possibility of replacing most of these mentioned technologies by disposing of most of the fines and ultra-fines with the tailings material on the tailings dump and recycling the water produced in the plant as process water.

Figure 1-3: The assembled Hi-G Dryer unit at Daberas

The supplier adapted the process flow design of the Hi-G Dryer system for the Daberas operation in order to take the coarse particles in the slurry into account. See Figure 2-3 for a schematic layout of the design.

In the conventional Hi-G Dryer system configuration there is no primary cyclone. The supplier introduced the primary cyclone to remove the majority of the coarse particles and to densify the feed to the Hi-G screen. Normally, the feed material would be deposited directly onto the Hi-G screen and the screen undersize material would pass through twelve 125 mm cluster cyclones to remove as much ultra-fines as possible.

1.3 Project goals and objectives

The aim of this study is to determine whether the Hi-G Dryer system would be able to treat the coarser Daberas slurry material; produce a stable, low-moisture, conveyable oversize product; produce an effluent with good process water quality; and produce an efficient overall system. In order to achieve this goal the following objectives were set:

- Determine the best solids product moisture content produced by the system
- Evaluate the clarity of effluent as process water
- Determine the overall performance of the system
- Compare the Daberas degrit system to the Hi-G Dryer system
- Evaluate and optimise system parameters
- Propose the best possible Hi-G Dryer system process for a coarse slurry
- Simulate results to fully comprehend system parameters

2 Literature review

2.1 Introduction

The primary function of the Derrick Hi-G Dryer system is the efficient removal of solids from slurries. The system is thus utilised within industry to effectively recycle water or produce a low-moisture product. The designer, Derrick Corporation, claims that the Hi-G Dryer system is the most cost-effective solution for handling any fine slurry (Derrick Corporation, 2008a). The Hi-G Dryer system has been dewatering very fine slurries (38–75 µm) successfully within industry (Bateman, 2002). The Hi-G Dryer system consists of screening and cyclone technologies as separation mechanisms. The use of a Hi-G screen sets the Hi-G Dryer system apart from other conventional dewatering systems. To fully understand the system, it is imperative to comprehend the principles involved in screening, cyclone and dewatering. This section explores the theoretical background of these technologies.

2.2 The Hi-G Dryer Fines Recovery System

It is important to first understand the Hi-G Dryer system's design and function. The Hi-G Dryer system utilises both screening and cyclones for the effective dewatering of slurries. It is the combination of these technologies that contribute to effective dewatering. The Hi-G Dryer system consists of a 1.2x3 meter Hi-G screen with 20 radially mounted hydrocyclones (see Figure 2-1). This is designed to treat slurries at 30–40 t/hr. The volumetric capacity of each cluster system (twenty 125 mm cyclones) is 300–340 m^3/hr with an ideal feed density of 6–8% solids by weight. The preferred operating pressure for the cluster system is 240–260 kPa (Derrick Corporation, 2008a).

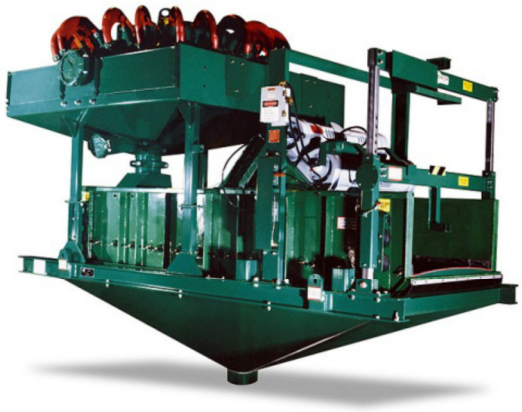

Figure 2-1: The Derrick Hi-G Dryer Fines Recovery System

The Hi-G Dryer system consists of a dual-motor, high-frequency, linear-motion vibrating screen. The Hi-G screen operates with two 1.9 kW four-pole motors that generate a linear vibrating action perpendicular through the centre of the two motors. The amplitude or stroke length of the screen is 4.3 mm at a speed of 1 750 rpm (Bateman, 2002). The combination of short stroke length and high rotational speed generates a G-force of 7.3 Gs. This can be determined by using the following equation:

$$G-force=\frac{Amplitude\times rpm^2}{2\times 900000}$$ (Meshcape Industries (Pty) Ltd, 2005) (1)

Therefore, $G-force=\frac{4.3\times 1750^2}{2\times 900000}=7.3$

It is this high G-force generated by the screen that distinguishes the system from any other dewatering system. Even though the screen is operating at high G-forces it still remains structurally intact, which is revolutionary for this technology.

The high G-forces generated on the material bed would thus allow for maximum dewatering as the bed compacts on the screen surface. It is expected that the ultra-fines are entrapped within the interstices of the bed, which acts like a filter. The material bed formed on the screen surface should also remove the denser cluster cyclone underflow and report as screen oversize.

The Hi-G Dryer system designed by Derrick Corporation for dewatering coarse slurries had the following screen parameters (see Table 2-1**Error! Reference source not found.**):

Table 2-1: Screen parameters

Screen panel type	Polyurethane
Screen panel aperture	500 µm
G-force	7.3 Gs
Amplitude	4.3 mm
Frequency	60 Hz
Speed	1750 rpm
Motor	4 pole
Dimensions	1.2x3 m
Screen orientation	Horizontal

Derrick Corporation also developed a high-capacity fines mesh, large open area urethane screen surface with superior abrasion resistance properties (see Figure 2-2). These panels have non-blinding properties which make it possible to screen material that was previously difficult to screen. The manufacturer also claims that the screen panels allow uninterrupted operation as less operator maintenance is required (Derrick Corporation, 2010).

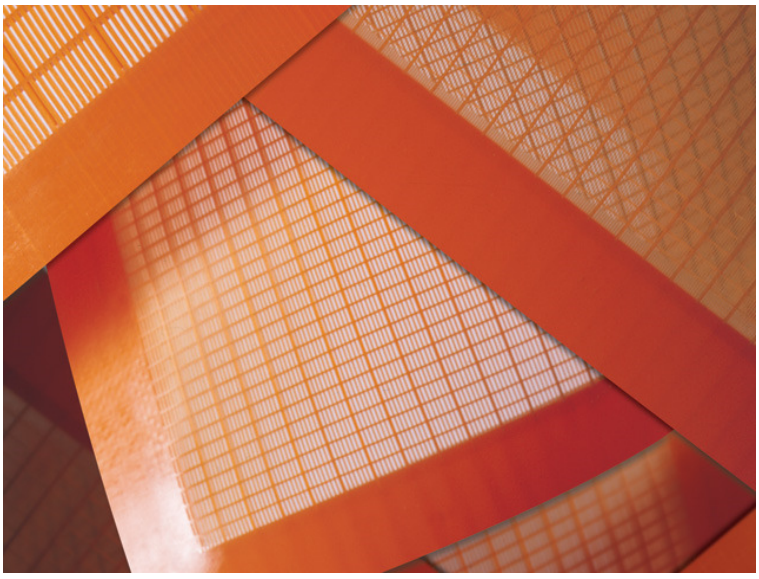

Figure 2-2: Derrick high-capacity, large open area, long-life panels

The process flow diagram of the coarse slurry Hi-G Dryer system designed by Derrick Corporation is presented in Figure 2-3 below.

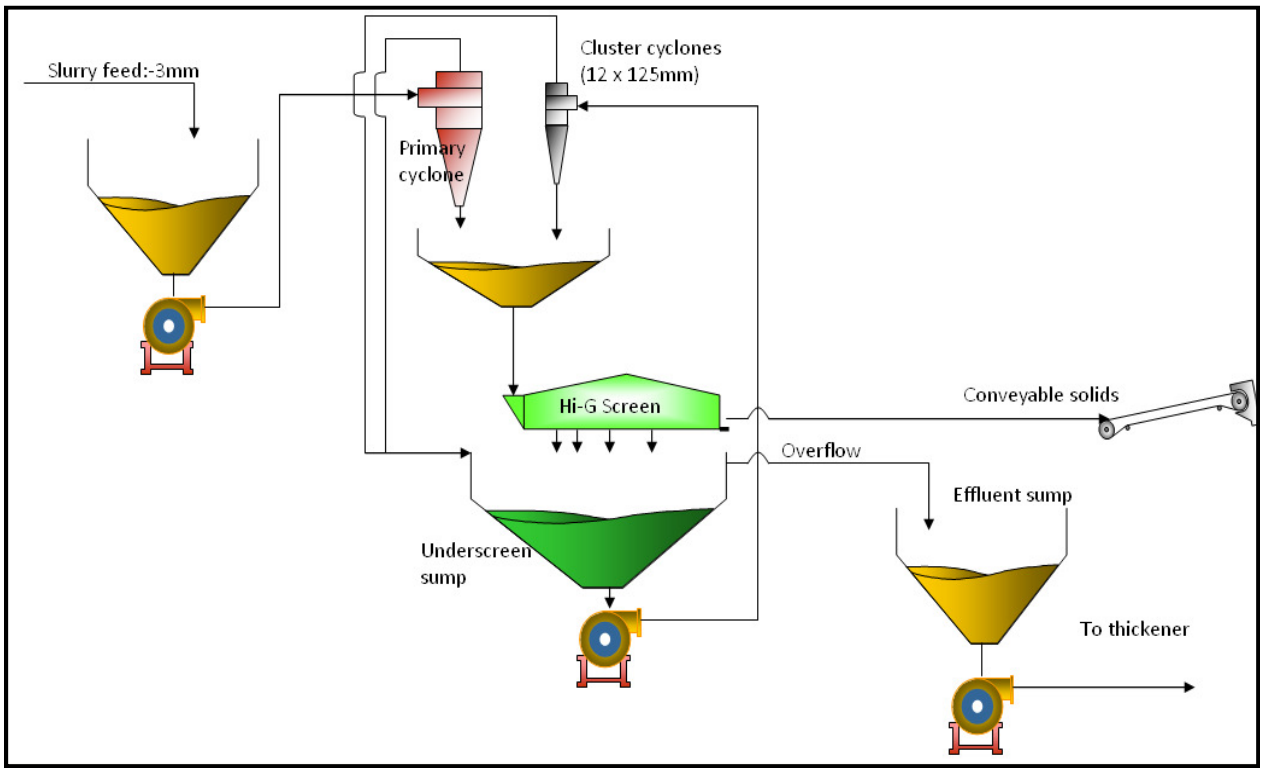

Figure 2-3: Process flow diagram for a coarse slurry Hi-G Dryer system

The Hi-G Dryer system that Derrick Corporation designed for the coarse Daberas slurry had a different flow system than other typical Hi-G dryer systems. A 250 mm primary cyclone was added to the system to remove the majority of the larger grits from the feed. These grits would be discharged onto the Hi-G screen from the primary cyclone underflow, whereas the overflow of the primary cyclone would report to the underpan of the Hi-G screen. The primary cyclone overflow together with the undersize of the Hi-G screen is pumped to twelve 125 mm cluster cyclones. The low-moisture product would then report to the tailings conveyor while the underpan sump overflow would report as effluent to the thickener (see Figure 2-3). The recommended pressure for the cluster cyclones is about 250 kPa with a slurry feed of 5–15% solids.

See Table 2-2 for the dimensions of the cluster cyclones and Figure 2-4 for a representation of the cluster cyclones themselves.

Table 2-2: Cluster cyclone dimensions

Component	Dimension
Spigot diameter	15 mm
Vortex finder	30 mm
Barrel diameter	125 mm
Inlet	52 mm

Figure 2-4: One of the cluster cyclones dismantled (left) and the 12 radially mounted cyclones above the Hi-G screen (right)

With regard to particle size distribution (PSD), this system can treat a top particle size of 2–3 mm, ideally only 2–3% smaller than 1 mm and a maximum of 20% between 500 and 1000 µm. Under these operating conditions the Hi-G Dryer can produce a 30–40 t/hr stackable, conveyable solid product with a moisture content of 70–85%. The system can recover fines from 38 µm where most 38 µm material will report to cyclone overflow. As the solid oversize material is transported over the screen surface, a cake bed is formed on the screen and compacted by the high G-forces. As per the design, 500 µm aperture screen panels are used for dewatering the coarse slurry; however, exceptions can be made for finer PSD operations to assist in cake formation.

2.2.1 Integration with Daberas process

The Daberas process plant consists of a wet-sizing section where water is introduced on two Joest screens to classify the -90 mm head-feed material into a -30+3 mm product. The -90+30 mm fraction reports to the tailings dump whereas the -3 mm slurry is pumped to a degrit section for processing. Two centre-seal slimes pumps pump the -3 mm slurry material produced at the wet-sizing section to two 900 mm hydrocyclones (see Figure 2-5**Error! Reference source not found.**).

The underflow to the hydrocyclones is discharged onto two Velco dewatering screens at the degrit section.

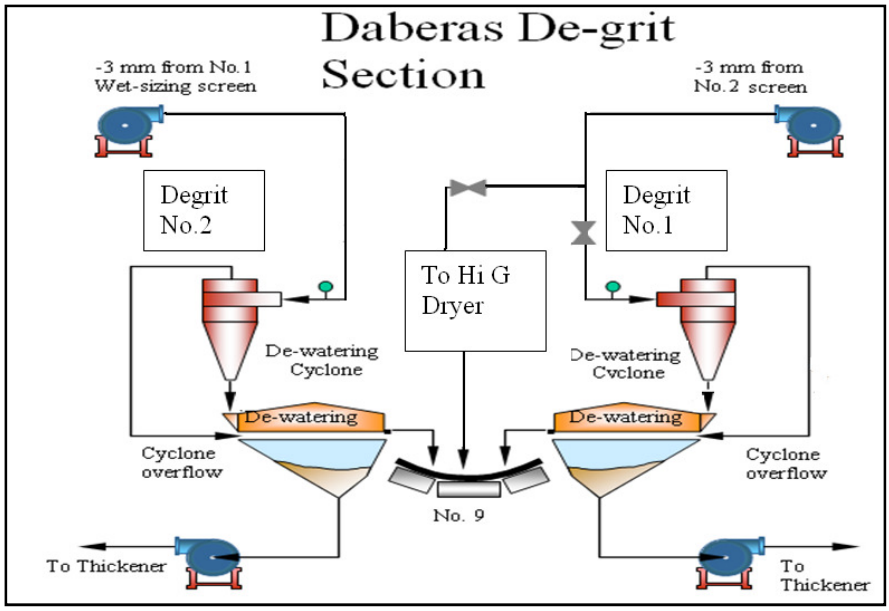

Figure 2-5: Schematic of the degrit section at Daberas

The screens' -3+0.5 mm product is discharged onto the no. 9 conveyor, which conveys the material to the tailings dump, whereas the underflow of the degrit screens and overflow of the hydrocyclones report to a thickener for further processing. The Hi-G Dryer feed line was installed on the no. 1 degrit system line, which receives feed material from the no. 2 wet-sizing screen. The two Velco dewatering screens are inclined at five degrees with 500 µm aperture panels installed. The operation of the Hi-G Dryer system is therefore

totally dependent on the Daberas processing plant's availability and operation. See Appendix II for a diagram of the overall Daberas process flow.

2.3 Screening

In order to comprehend the uniqueness of the Hi-G screen, it is necessary to understand screening technology. Thus the distinction between the Hi-G screen technology and other conventional screening technologies for dewatering can be appreciated.

2.3.1 Screening fundamentals

The basic components of a screen (see Figure 2-6) are:

- a steel frame to keep the screen surface in place;
- a screen surface which can be made of different panels like wedge wire, polyurethane or rubber panels;
- a motor and a drive to vibrate the screen in order to create the movement of the vibrating frame and ultimately the particles.

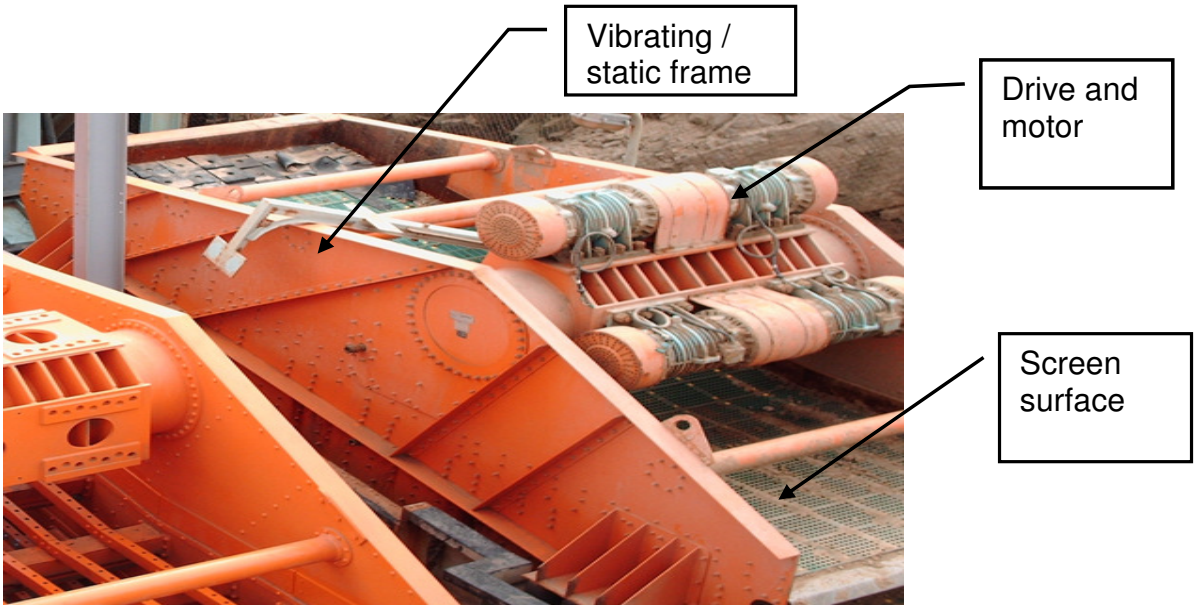

Figure 2-6: Basic components of a vibrating screen

In the mining industry a screen is commonly used to size particles according to a specific size range, but it is generally limited to material less than 250 µm due to a drop in efficiency associated with smaller particles (Russell, 1991; Wills & Napier-Munn, 2006). The most significant part of the screen is the screen surface. This surface is perforated with specific apertures according to the separation range required. Particles larger than the aperture size are retained (oversize) on the screen panel while the particles smaller than the aperture size (undersize) pass through. The purpose of screening can be to:

- prevent undersize material from entering a circuit by removing the material as it passes over the screen. Oversize would be the product and undersize would be the waste or gangue.
- remove larger waste (oversize) material by allowing the oversize to travel over the screen and the product (undersize) material to pass through the apertures.
- produce a closely sized product by removing oversize of a specific fraction and undersize of a specific fraction.

Screens can be utilised for a number of activities within industry. The Allis-Chalmers Corporation (n.d.) highlights the following uses:

- Size separation: The material is separated by size. There are different types of size separation:
    - Scalping – removing larger oversize material
    - Coarse sizing – removing a coarse fraction of material
    - Fine sizing – removing fine material fraction from material
    - Ultra-fine separation – removing ultra-fines from material
- Dewatering: Removing water from material
- Deslime: Separating wet fines from material
- Media recovery: Recovering media used in processes for use
- Trash removal: Removing foreign material such as wood or vegetation
- Washing: Washing and rinsing material
- Dedusting: Removing dust
- Conveying: Transporting material from one point to another
- Concentration: Blending material or adding material to a specific concentration

According to Allis-Chalmers (n.d.), screening involves two basic principles, namely:

- **Stratification** – The process whereby the larger particles move to the top of the vibrating material bed as the smaller particles pass through the voids of larger particles, resulting in smaller particles at the bottom of the bed.
- **Probability of separation** – The process whereby a particle would present itself to the panel aperture and can be either rejected or pass through the voids.

A number of factors can affect stratification and probability of separation, and thus screening efficiency. These factors involve the relative particle size and aperture, screen surface, screen movement, bed depth and moisture (Jianzhang & Xin, 2012; Soldinger, 2000; Venkoba Rao, Kapur & Rahul, 2003). Stratification is a very important process for separation because it allows the finer feed particles to be exposed to the apertures of the screen (Soldinger, 1999). For efficient screening to take place, the optimum bed depth of material is required. This bed depth can be controlled by manipulating the width of the screen to achieve optimum efficiency. Soldinger (2000) established a model to determine the relationship between bed thickness and particle size distribution on stratification and separation.

The probability for a particle to pass through a screen aperture in one attempt is the ratio of area available for the particle to pass through the aperture to the total area on which the particle can fall. According to Gaudin (1939), the probability of passage (P) is determined with the following equation:

$$P = \left(\frac{x_a - x}{x_a + w} \right)^2 \qquad (2)$$

where

x_a = aperture size

x = particle size

w = wire diameter

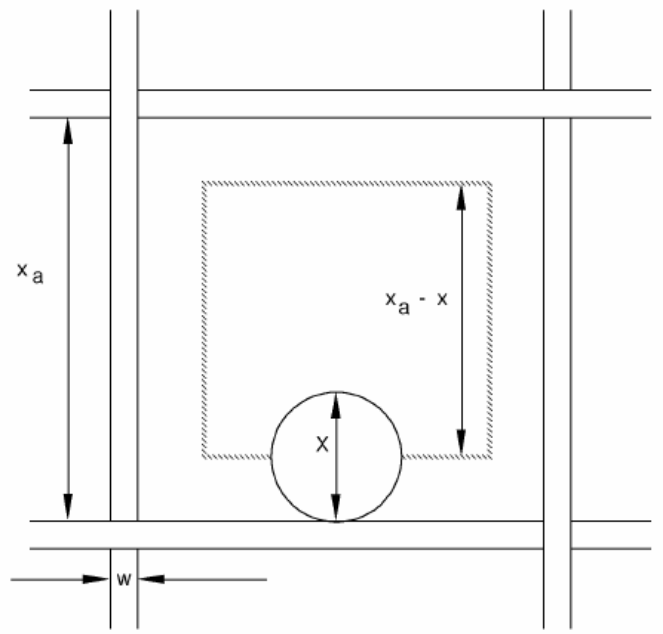

Figure 2-7: Relative dimensions of particle and aperture as per Equation 2

Equation 2 would thus imply that the probability of a particle passing through a screen aperture would be significantly more should aperture size increase, particle diameter decrease and wire diameter decrease as can be observed in Figure 2-7. The prime purpose of allowing motion of a screen is to enhance stratification by lifting the material off the screen and to repeatedly present the particle to the screen apertures for passage. The vibration of the screen also imparts an impulse force on each particle:

$$I = m_p v \tag{3}$$

where

I = impulse

m_p = particle mass

v = launch velocity

Should the launch velocity be the same for all particles, it can be deduced from Equation 3 that the larger particles receive more impulse and are carried to the top of the material bed. The smaller particles are thus closer to the screen.

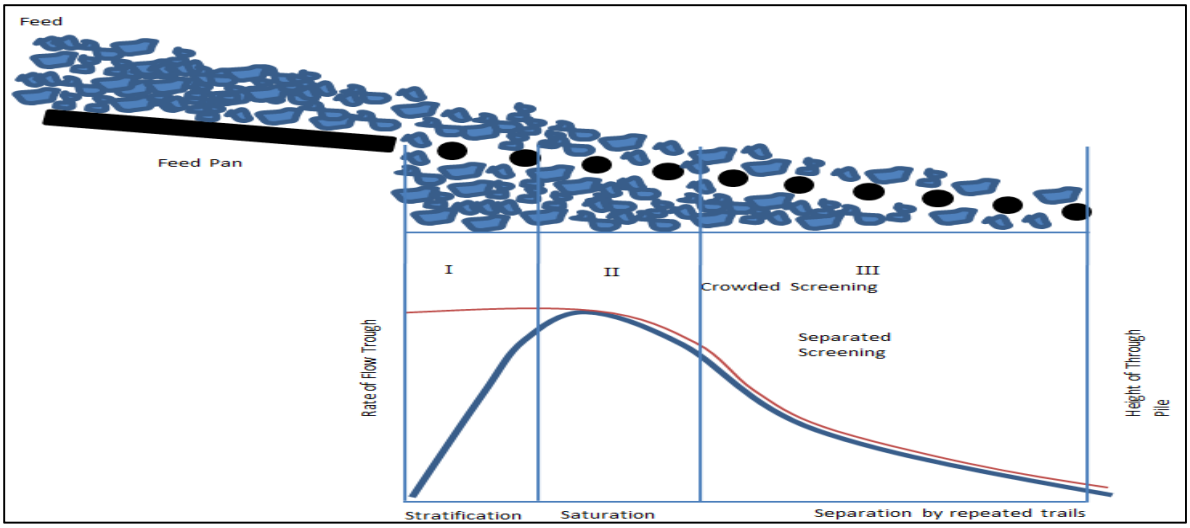

Figure 2-8: Stratification and separation along the length of the screen

As seen in Figure 2-8, the feed particles are introduced at the feed pan of the screen. As the material migrates over the screen surface, stratification initially occurs during phase I. During this phase the finer particles pass through the material bed and voids to the screen surface. During phase II the majority of the material is removed from the material bed as the highest degree of probability occurs (saturation screening). During phase III the probability of passage is reduced because either the majority of the particles are near size or the particles are larger than the apertures on the screen (Wills & Napier-Munn, 2006).

Vibration screening can have different applications depending on the frequency and amplitude applied. The particles are ejected and then returned to the screen as steeply as possible (see Figure 2-9). It is expected that the particles would move forward half to one full aperture per vibration (De Pretto, 2000).

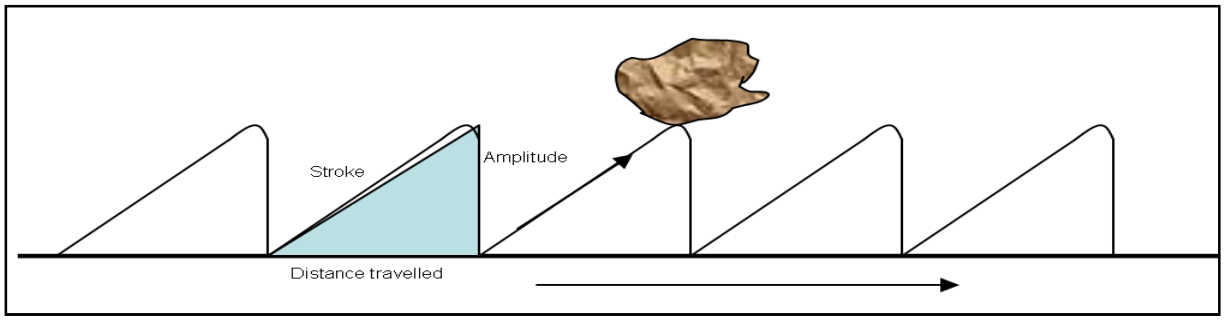

Figure 2-9: Stroke, amplitude and frequency of particles travelling over screen surface

For fines screening, it is conventional for the frequency of vibration to increase and the amplitude to decrease as the aperture size decreases (see Figure 2-10). Therefore, for fines screening to be effective, a screen with low amplitude and high frequency would be required (Rogers & Brame, 1985; Wills & Napier-Munn, 2006).

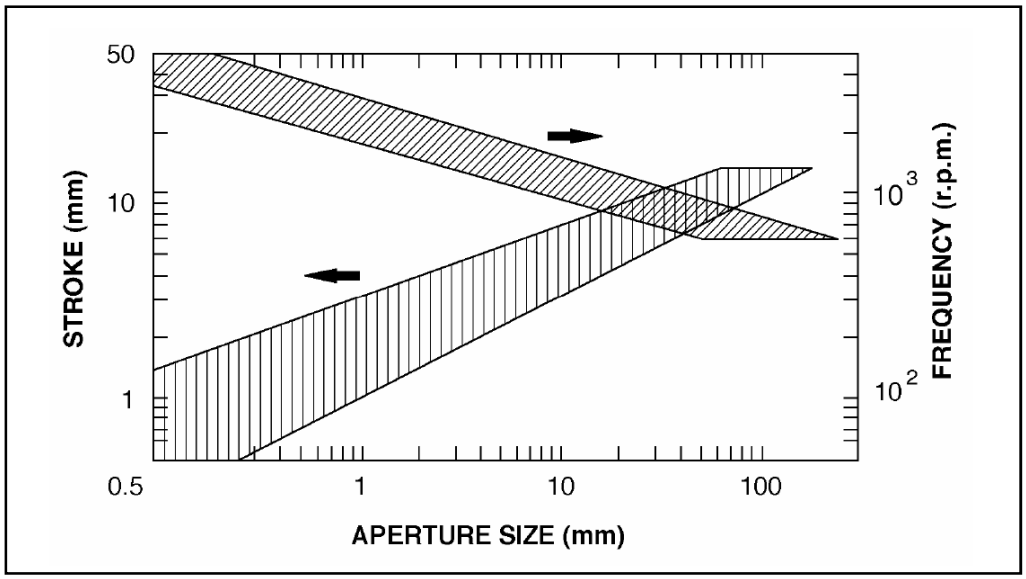

Figure 2-10: The relationship between aperture size, amplitude (stroke length) and frequency

2.3.2 Techniques for screening fines

There are various technologies within industry that are based on the principles of fines screening. It is relevant to investigate other fines screening techniques to fully appreciate the significance of the Hi-G Dryer system. The challenge with fines screening is the limited open area of the screen deck which tends to blind and misplace undersize particles as oversize.

Fines screening can be classified into two categories, namely static and dynamic screening.

Sieve bends such as the Dutch State Mines (DSM) sieve bends are static screens that are commonly used for dewatering and are widely accepted within the mineral industry for

screening wet fines material. Sieve bends consist of a concave curve wedge-bar screening surface with apertures perpendicular to material flow (see Figure 2-11).

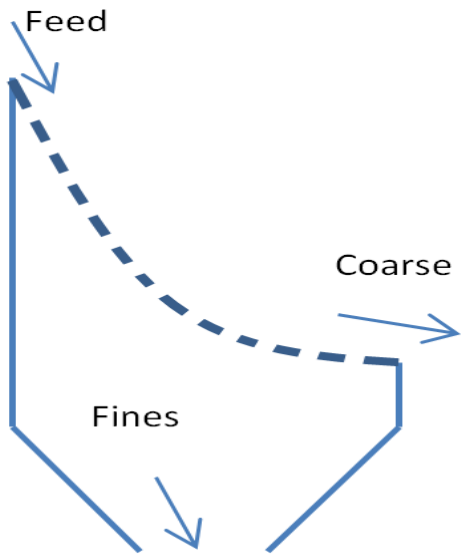

Figure 2-11: Schematic of a sieve bend

The slurry is fed from the top of the screen and enters the sieve tangentially. The bottom of the screen, which is the discharge end, is at a 45° angle from the feed end. As the feed moves over the screen, a thin layer of water and solids is removed, which report through the openings to the undersize. The water flow on the sieve bend helps break the cohesion between particles and significantly improves screening. Large amounts of water with low velocities are preferred (Dong & Yu, 2012). Sieve bends can be installed in conjunction with vibrating screens to enhance dewatering. Sieve bend separation can be taken down to 50 µm with capacities of 180 m^3/hr (Wills & Napier-Munn, 2006). The primary purpose of sieve bends is to remove as much water as possible. The screening size is considered as half of the actual aperture size and therefore a sieve bend can be classified as a probability screen. The factors that influence the performance of sieve bends are feed rate, solids concentration, particle size distribution in feed, the amount of near-size material and rod profile of the screen surface (De Pretto, 2000).

Banana screens are very similar to sieve bends. Banana screens (see Figure 2-12) can be either stationary or vibrating screens, depending on the application (Horton, 1997). This technology also comprises a multi-sloped screen deck and is utilised in high-capacity separation of aggregates into different size fractions. The multi-slope of the banana screen creates different cut sizes as the slope angle changes. The screen vibrates at high frequencies and can generate around 4–6 Gs of acceleration to separate particles according to size (Cleary, Sinnott & Morrison, 2009). The feed end is the steepest at around a 30–35° angle, where about 90% of the fines are removed as material travelling at speeds of 3–4 m/s. The second part of the screen is inclined at about 20–25° and the material travels at much slower speeds (1–1.5 m/s) to further remove fines. This prepares the material to the end of the screen, which is angled at 10–15°. Depending on the size, banana screens can achieve capacities of up to 2500 t/h and they operate optimally with feed material containing more than 30% fines (De Pretto, 2000).

Figure 2-12: Banana screen

The **Velco dewatering screen** was developed by Linatex for dewatering slurry material. The Daberas process plant at Namdeb has two Velco dewatering screens in operation to assist with the slimes disposal circuit. The screen has a 45° angle back deck at the feed section of the screen with slotted panels perpendicular to the directions of the flow (see Figure 2-13). This acts as a vibrating draining panel. The rest of the screen deck is inclined at 5° to the discharge to allow for bed formation and effective dewatering. The lowest point of the screen is where the sloping back and main decks meet and a pool of partially dewatered slurry is generated.

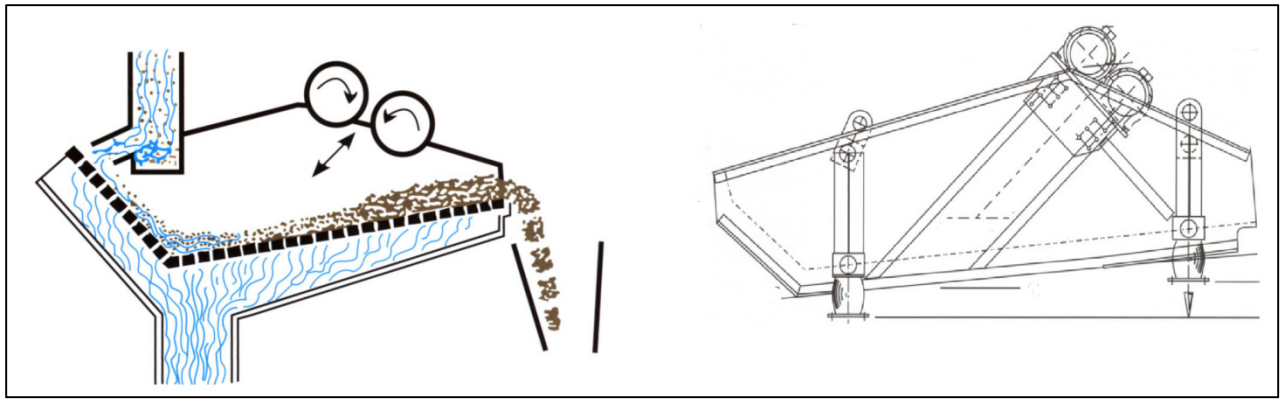

Figure 2-13: Velco screen technology and screen proportions

As the material migrates from this lowest point, a cake is formed on the screen which acts as a filter bed. This allows only fine particles to pass through the apertures. The vibration of the screen moves the cake along the screen surface for further dewatering, depending on the porosity of the bed, until it is discharged over the product weir. The vibrations of the screen are produced by two exciter motors operating at 980 rpm or 1 460 rpm, which generate about 2.1 Gs and 4.7 Gs, respectively. Velco screens have been utilised for various applications, namely scalping oversize from suspensions and slurries, sizing and dewatering (Linatex, 2006).

Derrick Corporation, manufacturer of fines screening equipment and screen surface technology, has mastered the art of dewatering systems and has developed a range of high-frequency, low-amplitude vibrating screens. The advantage of working at high-frequency, low-amplitude parameters is that the forces generated disrupt the fluid surface tension, promoting screen and particle surface interaction. Derrick Corporation products range from technologies such as the Derrick Stack Sizer and Hi-G Dryer system to repulp screens.

The Derrick Stack Sizer is a highly efficient wet particle fines screen that operates at high capacity on a very small footprint. This technology is most suitable for separation of particles ranging from 6.3 mm to 38 µm. In some operations, the Stack Sizer operates with 500 µm apertures at 300 t/hr and still achieves efficiencies between 90 and 95%. The Stack Sizer comprises five individual screen decks that are positioned one over the other

and operate in parallel. A single feed is distributed to the five separate feed points. Two vibrating motors cause the five screen decks to vibrate in a high-frequency linear motion. In conjunction with Derrick's high-capacity urethane screen panels, very efficient high-capacity screening is achieved on wet fine particles (Derrick Corporation, 2008b). Derrick Corporation also developed a dewatering screen called the Derrick Vacu-Deck screen. This technology introduces a low-horsepower blower that creates a slight vacuum and pulls air through the material bed. More drainage should take place as air moves through the bed.

2.4 Classification cyclones

The majority of modern dewatering circuits comprise classification cyclone technology. A study of this technology is imperative as hydrocyclones form part of the Hi-G Dryer system dewatering process. Classification fundamentals will be explored with the focus on hydrocyclone classifiers.

2.4.1 Classification fundamentals

Classification involves the separation of particles of different size, shape and gravity by allowing them to settle within a fluid medium. To better appreciate classification, consider particles in a column with a raising fluid. The particles in the column can either rise or sink if their terminal velocities are greater or less than the upward velocity of the fluid. Particles are separated according to this principle. The factors that influence the separation of these particles are particle properties, properties of the fluid, external acceleration forces and flow regime.

Particle properties with regard to classification are:

- size of the particle
- density of the particle
- shape of the particle

- surface roughness

The fluid in which the particle is submerged can also influence separation (Neesse & Dueck, 2007) in terms of:

- viscosity
- percentage of solids
- stability of the medium
- density of the fluid

Particles in a fluid can settle by means of either free settling, where there is no interference between particles, or hindered settling, where particle crowding becomes more apparent. With free settling there are predominantly three forces that are acting on a particle as it settles (see Figure 2-14). These are the gravitational force (F_g) or centrifugal force (F_c), which act downwards, the upward buoyant force due to water displacement (F_b) and the upward drag force (F_d).

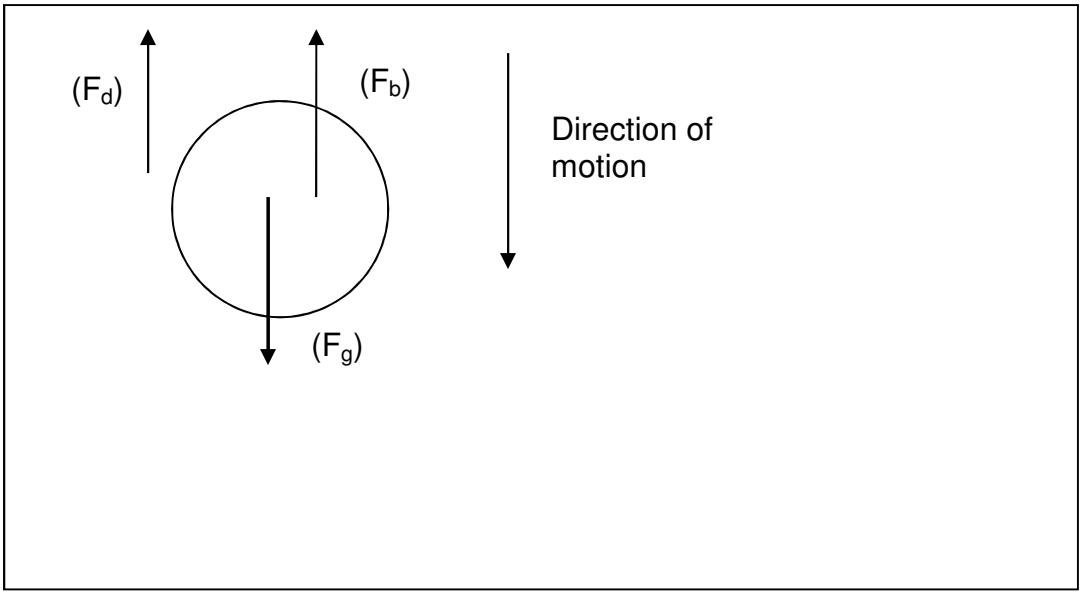

Figure 2-14: The forces acting on a particle during settling

The particle would initially accelerate until terminal velocity is reached and the forces balance. Using Newton's law, the following equation can be derived by balancing the forces:

$$m \times \frac{dv}{dt} = \frac{mg(\rho_s - \rho_f)}{\rho_s - F_d} \quad (4)$$

The drag force depends on whether the flow regime is turbulent or laminar. Stokes' law (Stokes, 1891; Tavares, Souza, Lina & Possa, 2002) assumes that the drag force is due to the viscous resistance of the fluid, resulting in the following equation:

$$F_d = 3\pi d\eta v \quad (5)$$

where

η = fluid viscosity

v = terminal velocity

The mass of a spherical particle can be defined by the following equation:

$$m = \frac{\pi d^3 \rho}{6} \quad (6)$$

By substituting Equations 5 and 6 into Equation 4 and assuming terminal velocity, the following expression can be deduced from Stokes' law:

$$v = \frac{gd^2(\rho_s - \rho_f)}{18\eta} \quad (7)$$

Newton assumed that the drag force is entirely due to turbulent resistance and deduced the following equation:

$$F_d = 0.55\pi d^2 v^2 \rho_f \quad (8)$$

By substituting Equations 6 and 8 into Equation 4, an expression for Newton's law can be derived:

$$v = \left[\frac{3dg(\rho_s - \rho_f)}{\rho_f} \right]^{0.5} \quad (9)$$

Stokes' law is valid for particles smaller than 50 µm and Newton's law is valid for particles with a diameter of more than 0.5 cm.

Simplifying Stokes' and Newton's laws, the following equation is generated which demonstrates that the terminal velocity of a particle is a function of particle size and density:

$$\frac{d_1}{d_2} = \left[\frac{\rho_{s2} - \rho_f}{\rho_{s1} - \rho_f} \right]^n \quad (10)$$

where

n = 0.5 for small particles obeying Stokes' law

n = 1 for larger particles obeying Newton's law

According to Equation 10, the density of the particles being classified has a greater effect on the coarser particles obeying Newton's law than on finer particles obeying Stokes' law.

Hindered settling arises when particle interference becomes more prominent and slurry or fluid becomes very viscous (Tavares et al., 2002). Considering Equation 9, as the density of the fluid increases, the effect of particle density on classification would increase whereas the effect of particle size on classification would decrease. The hindered settling ratio is therefore always greater than the free settling ratio due to the denser pulp.

2.4.2 Types of classifiers

Three types of classifiers are used in industry. These are mechanical classifiers (which mechanically classify the material and usually work against gravity, essentially making use

of free settling), sedimentation classifiers (which allow particles to settle out in a pool of water) and hydraulic classifiers (which require particles to settle against the upward flow stream of a medium, making use of hindered settling and thus utilising the effect of density on separation) (Kelly & Spottiswood, 1989; Osborne, 1988). See Table 2-3 for a summary of different types of classifiers (Kelly & Spottiswood, 1989).

Table 2-3: Summary of different types of classifiers

Classifier	Type	Description	Size (m)	Limiting particle size	Max. feed size	Feed rate (t/hr)	Application
Bowl classifier	Material transported mechanically. Sedimentation classifier.	Similar to slope tank classifiers, with settling in a circular tank with a rotating mechanism to scrap sand.	Width: 0.3 to 6.0 Diameter: 1.2 to 15 Max. length: 12	150 µm to 45 µm	12 mm	5 to 225	Used for closed circuit grinding where clean sand is necessary.
Cylindrical tank classifier	Material transported mechanically. Sedimentation classifier.	Effectively an overloaded thickener. Rotating rake feed sand to central underflow.	Width: – Diameter: 3 to 45 Max. length: –	150 µm to 45 µm	6 mm	5 to 625	Simple, but gives inefficient separation. Used for primary dewatering where separation involves large feed volumes.
Hydraulic cylindrical tank classifier	Material transported mechanically. Fluidiser bed classifier.	Hydraulic form of overload thickener.	Width: – Diameter: 1 to 40 Max. length: –	1.4 mm to 45 µm	25 mm	1 to 150	Two-product device giving very clean sand and requiring little hydraulic water. Used for washing, desliming and closed circuit grinding.
Cone classifier	Material transported non-mechanically (gravity). Sedimentation classifier.	Similar to cylindrical tank classifier but only conical.	Width: – Diameter: 0.6 to 3.7 Max. length: –	600 µm to 45 µm	6 mm	2 to 100	Low cost. Used for desliming and primary dewatering.
Hydraulic cone classifier	Material transported mechanically. Fluidiser bed classifier.	Upper section open with conical lower section.	Width: – Diameter: 0.6 to 1.6 Max. length: –	400 µm to 100 µm	6 mm	10 to 120	For closed circuit grinding to reclassify hydrocyclone underflow.
Hydrocyclone	Material transported non-mechanically (gravity/pressure). Sedimentation classifier.	Centrifugal action generating high separation forces.	Width: – Diameter: 0.01 to 1.2 Max. length: –	300 µm to 5 µm	1400µm to 45 µm	0.2 to 20 m^3/min	Cheap device used for closed circuit grinding. Gives very efficient separation.
Scrubber	Material transported mechanically. Sedimentation classifier.	Rotating drum.	Width: – Diameter: 1.5 to 1.4 Max. length: 3 to 10		450 mm	700	Similar to log washer, but lighter application.
Elutriator	Material transported non-mechanically (gravity/pressure). Fluidised bed classifier.	Tube with hydraulic water fed near bottom to produce hindered settling. Sands withdrawn from base.	Width: 0.5 to 6.0 Diameter: – Max. length: 12	2.4 mm to 100 µm	10 mm	4 to 120	Efficient separation, but requires 3 t hydraulic water/ton of sand. Produces clean sand into narrow size ranges.

2.4.3 Hydrocyclones

A hydrocyclone is an extremely simple static mechanical device with no moving parts that utilises the centrifugal force on particles to accelerate their settling rate. The purpose is to separate or classify a material feed into a coarse and a fine fraction. A typical hydrocyclone is cylindroconical with a feed inlet tangential to the cylindrical section (see Figure 2-15).

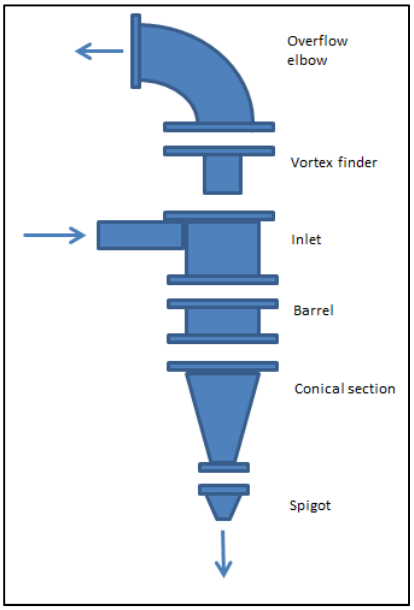

Figure 2-15: Components of a hydrocyclone

The diameter and lower angle of the central cone have a significant effect on the sharpness of separation (Chu & Luo, 1994; Kilavuz & Gulsoy, 2011). The opening at the cone underflow is known as the spigot or apex. The coarse fraction of the feed material is discharged through the spigot, which is critical to the cyclone's performance. The top of the cylindrical section is closed with a flat plate through which an overflow or vortex finder projects. The vortex finder extends into the feed chamber, preventing the short-circuiting of the feed directly into the overflow. The fine fraction of feed material, together with most of the water, is discharged through the vortex finder. As the slurry material enters the hydrocyclone, it forms a spiral or vortex in the cyclone due to the tangential feed

configuration, thus creating the centrifugal forces required for separation (see Figure 2-16).

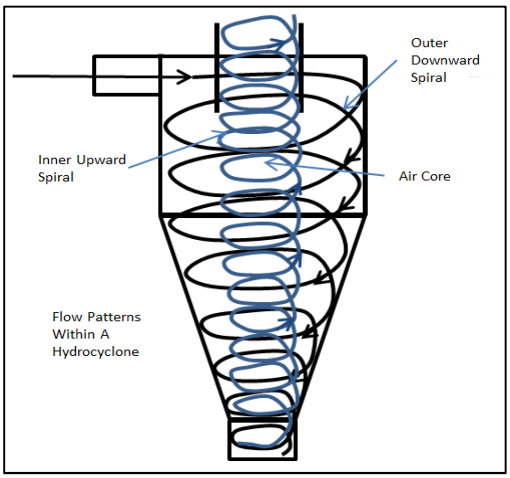

Figure 2-16: Flow patterns in a hydrocyclone

The faster settling particles, which are often the larger particles, migrate to the walls of the cyclone and report downwards towards the spigot. The smaller, lighter fraction moves to the vortex, which consists of a low-pressure zone along the vertical axis of the cyclone, and migrates upwards to the cyclone overflow. The high pressure caused by high feed velocity often yields a finer separation, depending on the cyclone's size.

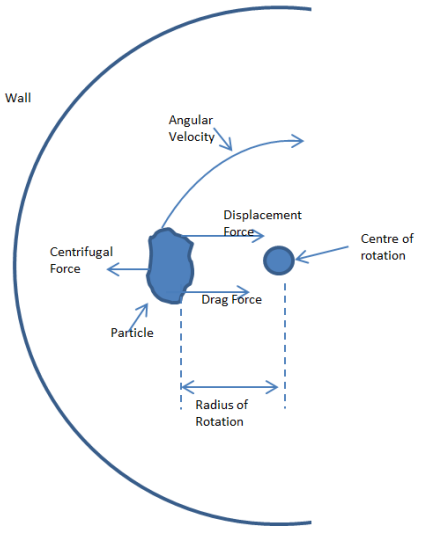

Figure 2-17: Separation forces in a hydrocyclone

Equilibrium orbit theory can be used to predict cyclone performance. As observed in Figure 2-17, the particle is moving along a radius and therefore is subjected to two main forces, namely centrifugal force and drag force. At equilibrium these two forces are equal. Differently sized particles therefore move along different radii. Some particles move along the outer wall of the cyclone whereas other particles move close to the vortex. Within the cyclone there exists a plane of zero vertical velocity (Kawatra, Bakshi & Rusesky, 1996), known as the envelope of zero velocity (see Figure 2-18). At the envelope of zero velocity a particle has equal probability of either reporting to the vortex finder as overflow or to the spigot as underflow. The size of particles at the envelope of zero velocity is known as the cut size (d_{50}).

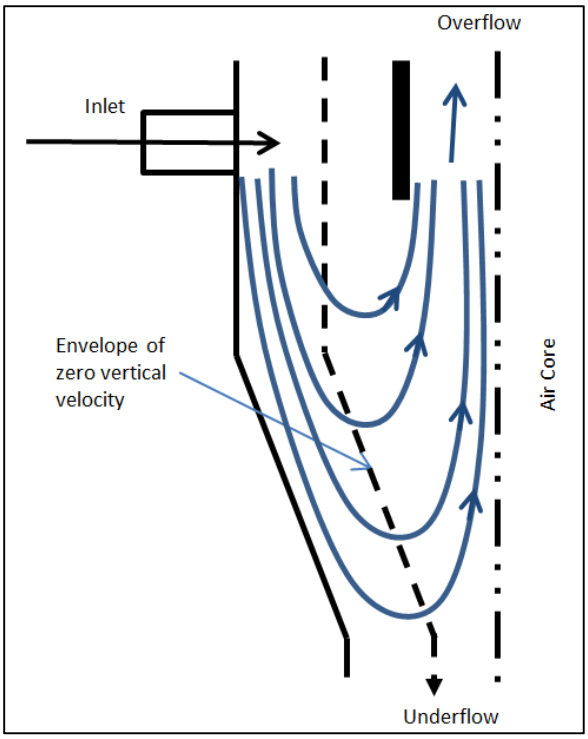

Figure 2-18: A demonstration of the envelope of zero velocity and particle flow

The equation for the centrifugal force of a spherical particle as observed in Figure 2-17 is:

$$F_c = \pi \frac{d^3}{6}(\rho_s - \rho)\frac{\omega^2}{r} \qquad (11)$$

Assuming laminar flow (Stokes' equation) as observed in Equation 7 as the drag force (F_d), the cut size or d_{50}-size particle can be determined as the two forces are equal at equilibrium:

$$d_{50} = \left[\frac{18 \mu v_r r}{(\rho_s - \rho)\omega^2} \right]^{0.5} \quad (12)$$

Based on work by Plitt (1976), it can be assumed that the envelope of zero vertical velocity is at a radius of one-sixth of the cyclone radius. There are other theories that also try to explain the cut size of a cyclone, such as retention time theory, which considers the time the particle migrates outwards and down to the spigot, and crowding theory, which emphasises the effect of spigot size on the separation of particles.

It is necessary to use reliable models to express cyclone efficiency to simulate performance. Efficiencies can be expressed on a partition curve which represents the distribution of various size fractions to the overflow and underflow products during classification.

Inefficiencies can be due to short-circuiting or misplacement of coarse material to overflow or more commonly the entrainment of fine particles in water to underflow. Material of all size ranges tend to short-circuit due to the liquid of the coarse product in direct proportion to the fraction of feed water reporting to the underflow (Kelsall, 1953). Due to the short-circuiting, the actual efficiency (E_a) needs to be corrected (E_c). E_c is the correction of the partition curve due to the entrainment of fine particles in water underflow (see Figure 2-19).

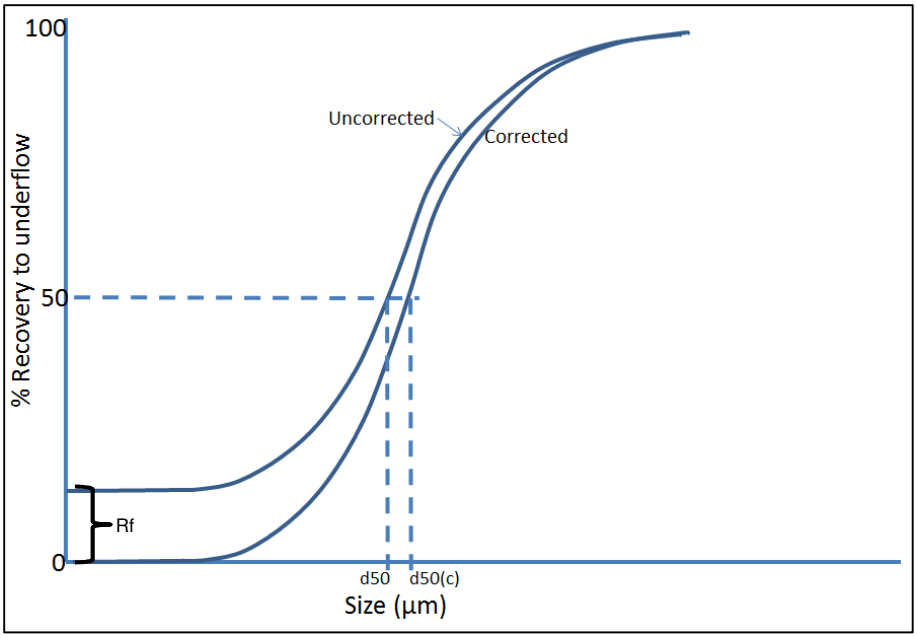

Figure 2-19: The difference between a corrected partition curve and an uncorrected partition curve

The relationship between E_a and E_c can be expressed with the following equation:

$$E_c = \frac{E_a - R_f}{1 - R_f} \quad (13)$$

where

E_a = the actual fraction of particles reporting to the underflow

E_c = the fraction of particles referring to the coarse product

R_f = the liquid fraction in the underflow from the feed

The d_{50} and sharpness of separation are very significant parameters for determining the efficiency and separation of hydrocyclones (Gupta & Yan, 2006). The d_{50} refers to the cut point or cut size where actual separation takes place. At the cut point the material has a 50% change to report either to the overflow or underflow (Svarovsky, 1984). This can also be observed in the schematic of a partition curve in Figure 2-20.

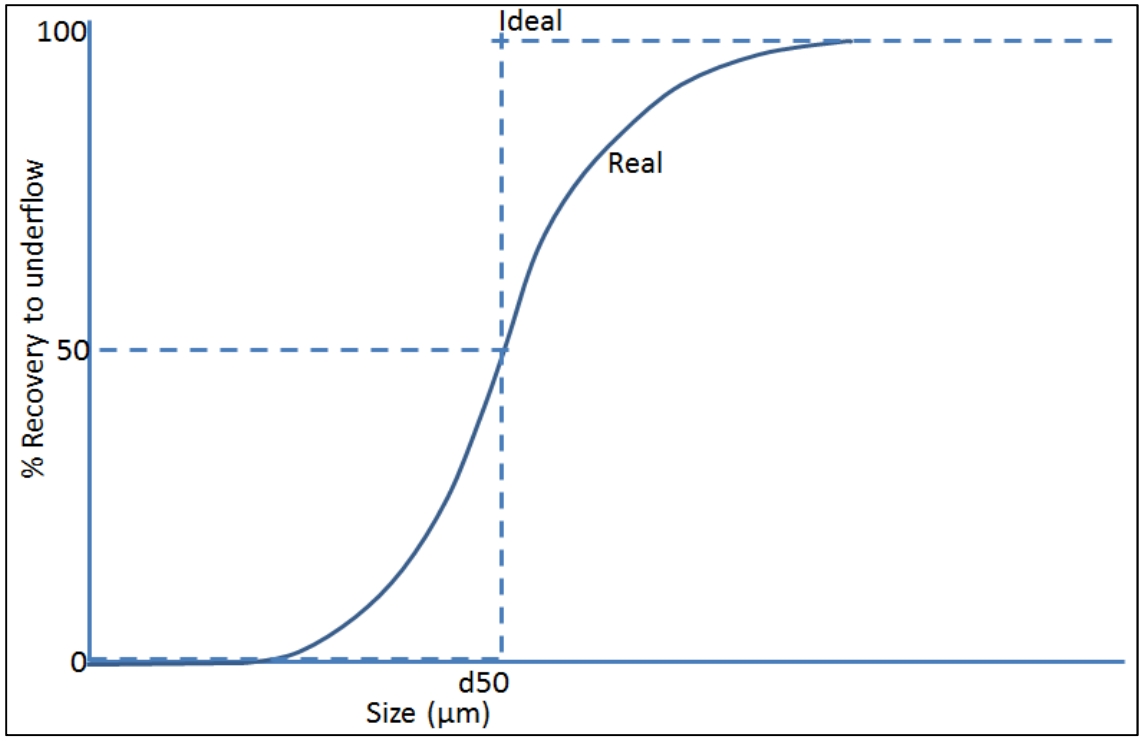

Figure 2-20: Schematic of a partition curve illustrating d_{50}

The slope of the partition curve gives an indication of how efficient recovery is. The closer the curve is to the vertical, the more efficient the cyclone is. The efficiency of separation is also known as the imperfection (I) and is determined by the following equation:

$$I = \frac{d_{75} - d_{25}}{2d_{50}} \quad (14)$$

where

d_{75} and d_{25} = the percentage recovery at 75% and 25% of the particle size on the partition curve

The imperfection for cyclones ranges between 0.2 and 0.6 with an average of about 0.3 (Gupta & Yan, 2006). The d_{50c} is the cut size of the E_c corrected curve. The d_{50c} is normally greater than the d_{50}, depending on the R_f value, as illustrated in Figure 2-19.

There are various models that can express d_{50c} relative to cyclone dimensions. Two of the most common models were proposed by Plitt (1976) and Lynch (1965). Plitt predicted the cut size using the following dimensions:

$$d_{50c} = \frac{F_1 \times 39.7 \times D_c^{0.46} \times D_i^{0.6} \times D_o^{1.21} \times \eta^{0.5} e^{(0.063 \times \%Vs)}}{D_u^{0.71} \times h^{0.38} \times Q_f^{0.45} \left(\frac{\rho_s - 1}{1.6} \right)^k} \quad \text{(Plitt, 1976)} \quad (15)$$

while Lynch used the following:

$$d_{50c} = \frac{14.8 \times D_c^{0.46} \times D_i^{0.6} \times D_o^{1.21} \times e^{(0.063 \times \%Vs)}}{D_u^{0.71} \times h^{0.38} \times Q_f^{0.45} (\rho_s - \rho_m)^{0.5}} \quad (16)$$

where

D_c = cyclone diameter (cm)

D_i = inlet ratio (equivalent circle diameter)

D_o = vortex finder ratio

D_u = spigot diameter (cm)

h = free vortex height (cm)

d_{50} = cut size (μ)

η = viscosity (cP)

ρs = particle density (t/m^3)

%Vs = percentage volumetric solids

Q_f = l/min

The solids content has an exponential effect on the cut size. This can be contributed to the effect of hindered settling on underflow crowding. The vortex finder diameter is proportionally related to the cut size, according to Equations 14 and 15. This means that if the vortex finder diameter increases, so will the particle cut size, as a larger vortex is formed, extracting more fines material to the overflow. The spigot diameter has an inverse effect on the cut size. The reason for this is that more fines material reports to the vortex finder as spigot diameter is reduced, due to underflow crowding. The free vortex height has an effect on the retention time of the particles in the cyclone. Increasing the vortex height increases the retention time and allows fine particles to move to the outer sides of the cyclone towards the underflow, thus decreasing cut size. (Arterburn, 1982)

Plitt and Lynch also proposed corrected efficiency models as an expression of particle size. The Plitt model (Plitt, 1976; Plitt & Kawatra, 1979) puts it as follows:

$$E_c = 1 - e^{[-0.6931(\frac{d}{d_{50c}})^m} \quad (17)$$

while the Lynch model (Lynch & Rao, 1975) represents it as follows:

$$E_c = \frac{e^{[a(d/d_{50c})]} - 1}{e^{[a(d/d_{50c})]} + e^a - 2} \quad (18)$$

where

d_{50c} = particle size where separation takes place

m and a(alpha) = sharpness of the separation

Finch (1983) also reported a “fish hook” effect at the fine end of the partition curve (see Figure 2-21). This effect was noticed predominantly in the smaller size cyclones and is due to the bypass of a high percentage of fines fraction to underflow (Neesse, Dueck & Minkov, 2004). The effect is based on flow forces, which enrich fine particles around the settling coarser particles boundary layer (Majumder, Yerriswamy & Barnwal, 2003; Schubert, 2010).

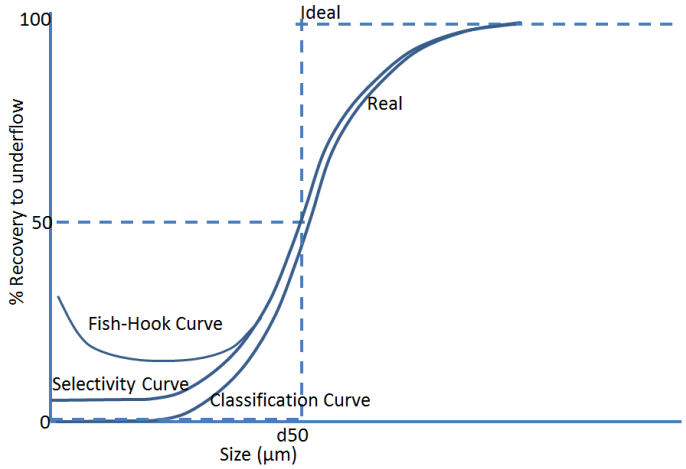

Figure 2-21: A comparison between different partition curves, including a fish-hook partition curve

In industry, hydrocyclones have proven to be very efficient for separating fine particles and are widely used in closed-circuit grinding operations. Hydrocyclones have a wide range of uses, such as the washing of coal, desliming, degritting and thickening (Wills & Napier-Munn, 2006).

2.5 Dewatering principles

The idea behind effective dewatering is producing a solids product that is significantly low in moisture and a water product that is essentially free of solids.

When water comes in contact with particles, it is bound in different ways. There are different types of moisture that particles occupy, which can be defined as follows (De Pretto, 2000):

- **Free or surface moisture content** – The water adheres to the particle surface by adhesion forces, or is retained in cracks and fissures in the particles. The water can easily be removed from the particle surface by air-drying.
- **Water absorption** – The water absorption capacity is the maximum internal moisture content that the particle can contain. The moisture content can be obtained by calculating the difference between the mass of particles in the absolutely dry state and the mass of particles in the water-saturated state.
- **Internal or inherent moisture content** – The moisture that is entrapped within the particles and the pores of the particles. This moisture cannot be removed by ordinary drying and is therefore removed by heating at 105 ℃ until the mass is constant.
- **Total moisture content** – The combination of surface moisture and internal moisture content. This can be obtained by deducting the mass of the feed material in its absolutely dry state from the mass of the feed material in its moist state, which can be expressed as percentage.

In practice, the surface moisture can be removed easily by means of mechanical methods or gravity, whereas the inherent moisture can only be removed by means of exposure to heat. Using only mechanical methods to remove surface moisture from particles is not possible because of the strong hydrogen bonds or surface tension of water to the surface of solids. The main dewatering focus of this project would be the effective removal of surface moisture.

De Pretto (2000) describes the relationship between particle size and the surface moisture retained. This has an effect on the ease by which the surface moisture on the particles is removed. Larger particles retain less surface moisture due to a smaller surface area compared to smaller particles of the same mass. Smaller particles therefore create more surface area for water to bind, which makes mechanical dewatering difficult. More energy is therefore required to break the surface tension for smaller particles to overcome the hydrogen bonds on and between particles. The high G-forces applied by the Hi-G Dryer screen would be significant in breaking these bonds and effectively dewater particles.

Dewatering methods can inherently be classified into three groups, namely sedimentation, filtration and drying. Sedimentation relies more on the density differences between the solids and liquids. Large particles would settle more rapidly under gravity whereas as ultra-fine particles require coagulation and flocculation to assist in their settling process. Examples of sedimentation devices are thickeners, hydrocyclones and centrifuges.

In the filtration process, solids are removed from the liquid by passing the liquid through a filtering medium. Dewatering screens can be considered a filtration process because the liquid would pass through the screen panels and the dewatered particles would be left behind on the panel surface. It can be assumed that some liquid will still be entrapped within the interstices and surface of the solids (De Pretto, 2000).

Thermal drying, which is usually used for concentrate drying within the diamond industry, is a very expensive drying method. This method is usually used after mechanical drying and removes the inherent moisture (De Pretto, 2000).

A general rule for dewatering screens is that two-thirds of all water should be removed over one-third of the length of the screen (Lamb, 2000). Lamb also highlights the screening parameters that affect the dewatering process:

- **Particle shape** – This determines the dewatering ease of the particles. The interstitial space for drainage is more for spherical or cubical shapes, while flat shapes hinder drainage.
- **Solids concentration and size distribution** – The dewatering process is also affected by the formation of the filter bed, which is created initially by coarser particles larger than the aperture size. This could also be a result of bridging of smaller particles to arrest percolation of solids with the drainage fluid.
- **Aperture shape and size** – The dewatering process and amount of material lost to drainage fluid is also a result of the screen deck type. An ideal surface would be a wedge wire cross-flow deck, but polyurethane panels can be utilised because of their high wear resistance qualities. Slotted apertures orientated with the flow of material effectively have more drainage capability, followed by slotted apertures across the flow of material and square holes.
- **Open area** – This determines the drainage capacity of the screen. The larger the open area, the greater the drainage capacity of the screen.
- **Operating frequency, amplitude and screen slope** – The frequency and amplitude have a direct effect on transportation and drainage. The rate of travel is a result of the angle of throw and acceleration, but can also be influenced by inclination of the screen. Inclination of the deck against the direction of flow can increase drainage. In an effort to reduce the moisture content of the dewatered product, the vibrating screen usually operates at a high frequency to increase drainage forces. In addition, the screen is designed in such a way that a deep bed of solids forms on it. The thickness of the bed creates pressure within the bed that reduces the interstitial volume and thus assists in the removal of liquid.

These parameters will be investigated and monitored when conducting the Hi-G Dryer screen dewatering study.

The following parameters should be considered for dewatering cyclones:

- **Cyclone diameter** – Cyclone diameter is proportional to cut size. It is expected that a smaller diameter cyclone would be more efficient for dewatering because the d_{50} is expected to be much lower compared to larger diameter cyclones.
- **Solids concentration** – The higher the solids concentration, the coarser the separation. This is relative to slurry viscosity and can therefore be affected by particle size and shape. A lower solids concentration would be best suited to dewatering.
- **Pressure drop across the cyclone** – This is the difference between the feed pressure and overflow pressure. A higher pressure drop would give a finer separation, whereas a lower pressure drop would give a coarser separation.
- **Density difference between solids and liquid** – A big difference would give a finer separation, which would positively affect dewatering.

In summary, when selecting a cyclone for dewatering it is optimal to have a small diameter cyclone, fed at a low solid concentration, a high pressure drop across the cyclone and a big difference between solids and liquid (Arterburn, 1982).

2.5.1 Yield stress

Ultimately the product of the Hi-G Dryer should be disposed of in an economical and environmentally acceptable way. Derrick Corporation claims that the Hi-G Dryer can produce a solids moisture product of 75–80% solids by mass (AggMan Staff, 1999). It is important to understand the behaviour of the solids product produced to determine if it is possible to convey the material. The conveyability of the solids product can be related to the yield stress of the product.

Yield stress is a force required for the deformation of the material. At yield stress the material starts behaving plastically and the flow is initiated if the yield stress on the material is exceeded. Yield stress can be determined directly or indirectly. The most reliable method for measuring yield stress directly is using a vane viscometer to measure torque over time. An indirect measurement of yield stress can be performed with a slump

test. A slump test can be used to determine the flow behaviour of the material in terms of slump height measurement. A cylinder with height equal to diameter and both ends open is used. The material is firstly put into the cylindrical mound and removed vertically. The distance between the top of the mould and the slumped sample is then measured (see Figure 2-22).

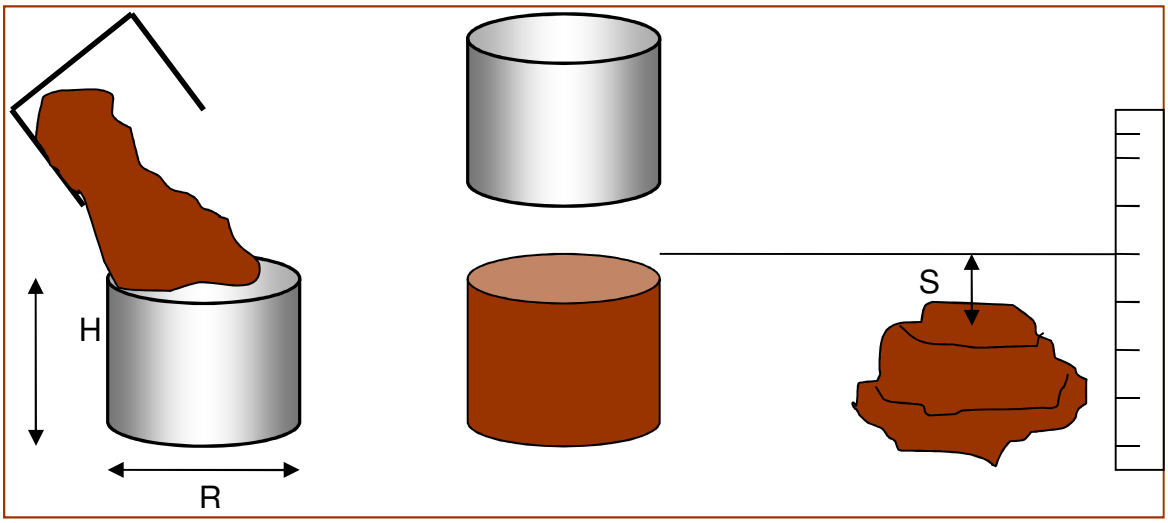

Figure 2-22: Slump test dimensions

The slump test alone cannot provide the yield stress. A correlation to convert the dimensionless slump height measurement to yield stress for a cylindrical container was determined by Pashias, Summers, Glenister and Boger (1996). The correlation consists of the following implicit equation:

Dimensionless slump height: $$S' = \frac{S}{H} \quad (19)$$

50c rheometer correlation: $$\tau'_y = 0.5 - 0.5\sqrt{S'} \quad (20)$$

Dimensionless yield stress: $$\tau'_y = \frac{\tau_y}{\rho g H} \quad (21)$$

where

τ'_y = dimensionless yield stress

S' = dimensionless slump height

S = slump height (m)
τ_y = yield stress (Pa)
H = height of slump container (m)
ρ = material density
g = 9.81 (m/s)

Should the screen solids oversize have a high moisture content, it would easily deform and thus produce a low yield stress.

2.5.2 Water quality

It is imperative to measure the water quality of the effluent produced by the Hi-G Dryer system to determine if the water can be reused in the system as process water. A clarity wedge (see Figure 2-23) is a simple instrument that can be used to measure the water clarity of the effluent and then relate it to the raw water and thickener overflow. This method can be used to determine clarification, thickening and sedimentation performance of slurry according to ISO 10086 (Oscillation Pty Ltd, 2012). The clarity wedge has a scale on its rear surface and the clarity can be observed by reading the highest value visible through the liquid.

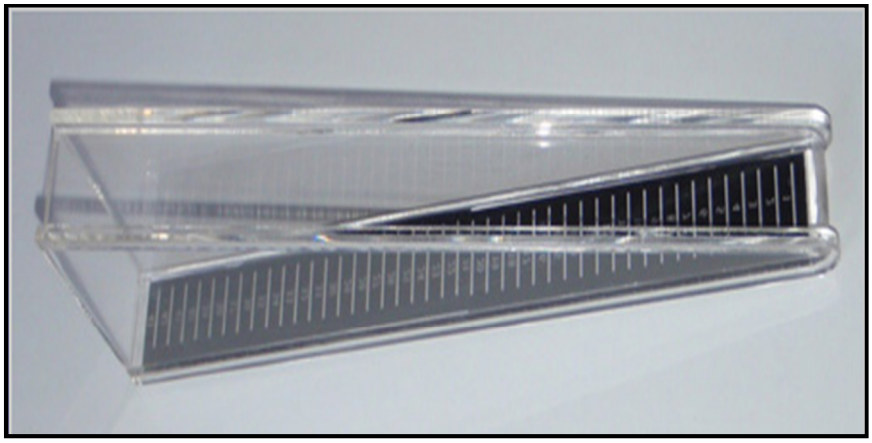

Figure 2-23: A clarity wedge

3 Experimental plan

3.1 Introduction

After researching the technologies involved with regard to the Hi-G Dryer system, it was commissioned at the Daberas processing plant. The assembly was done according to the supplier's process design specifications (see Figure 2-3) and the system was fed coarse Daberas slurry produced from its wet-sizing section. To ensure feed consistency, the material resource that the Daberas plant processed during the course of the testing was mined from Zone 13. It was imperative to only take samples during steady-state conditions at the relevant sampling points. The researcher processed and analysed the samples at the Daberas plant laboratory using the procedures and equipment identified.

It was imperative initially to assess the supplier's process layout so as to comprehend the advantages and disadvantages of the system. After assessing the system, the theoretically acquired information about the system parameters needed to be applied in order to design and optimise a system that would best suit coarse slurry application. The sampling campaign, equipment required and test procedures are highlighted in this section.

3.2 Sampling campaign

Samples were taken at the different sampling points on the Hi-G Dryer system to determine the following parameters:

- **Moisture content of screen oversize** – A material sample was taken at the Hi-G screen oversize to determine the product moisture, yield stress and PSD.
- **Water (effluent) quality** – Water samples were taken at the Hi-G effluent sump overflow, thickener overflow and raw water tank to compare water quality.
- **Cyclone efficiencies** – Samples were taken at the cyclone overflow and underflow to determine the d_{50} and separation sharpness.

- **Effect of PSD of ore on operation** – Samples were taken at the feed, product, primary cyclone overflow and underflow, cluster cyclone overflow and underflow, and effluent.

3.3 Equipment used

The following equipment were used during testing:

- Seven 10-litre buckets for taking samples
- A calibrated Unical field scale to determine mass in the field
- A calibrated laboratory scale to determine wet mass and PSD
- An HDPE pipe with height equal to diameter for slump test
- A ruler to determine slump height
- An oven to dry the samples
- A sieve shaker and screens to classify material into their relative size ranges
- A clarity wedge to determine the relative clarity of the water
- A volumetric flow meter to determine the material flow entering the Hi-G Dryer

3.4 Experimental plan objectives

It was imperative to first evaluate the existing supplier design. After evaluation of the design, it was necessary to apply the researched system parameters to design and optimise a process that would best suit the coarse Daberas slurry. The dewatering parameters presented in Table 3-1 were considered for optimising the system:

Table 3-1: Dewatering parameters considered for optimising the system

Dewatering parameters for screen	**Dewatering parameters for cyclones**
Particle shape	Cyclone diameter
Solids concentration	Solids concentration
Size distribution	Pressure drop
Aperture shape	Density difference between solids and liquid

Aperture size	
Open area	
Operating frequency	
Amplitude	
Screen slope	

3.5 Moisture content sampling and analysis

The following two procedures were used to sample and analyse moisture content.

3.5.1 Moisture content determined by oven drying

Material was collected in buckets at different sampling points and analysed in the Daberas laboratory using the following procedure:

1. After taking the sample, the total wet mass of the sample was determined and recorded.
2. The sample was left to stand for 60 minutes to allow solids to settle.
3. Some of the water was decanted.
4. The sample was put in a metal tray, marked and transferred to an oven.
5. The sample was dried for about 6 hours at 105 ℃.
6. The particle size distribution was determined by sizing the dry sample into the following sieve sizes: 4, 2.8, 2.0, 1.4, 1.0, 0.5, 0.3, 0.212, 0.15, 0.106, 0.075, 0.045 mm.
7. The different size fractions were totalised to determine the total dry mass.
8. The moisture content was calculated as percentage moisture or percentage solids using the following equations:

$$\%\ Moisture\ \ Content = \frac{Wet\ \ Mass - Dry\ \ Mass}{Wet\ \ Mass} \times 100 \qquad (22)$$

$$\%\ Solids\ (mass) = \frac{Dry\ Mass}{Wet\ Mass + Dry\ Mass} \times 100 \quad (23)$$

3.5.2 Moisture content determined by volume

The second method for sampling moisture content entailed using a 5-litre bucket. The procedure was as follows:

1. The sample was collected in a 5-litre container.
2. Total sample mass was determined using an in-field scale and bucket mass was subtracted.
3. Equation 27, a predetermined equation that relates the volume of the bucket and material mass to the percentage solids by mass, was applied.

The following equations were used to determine the percentage solids by mass:

$$\%\ Solids\ (mass) = \frac{Dry\ Mass}{Wet\ Mass + Dry\ Mass} \times 100$$

If dry mass = $\mathbf{M_s = \rho_s \times V_s}$, where $\boldsymbol{\rho_s}$ = solids density and $\mathbf{V_s}$ = volume of solids,
wet mass = $\mathbf{M_w = \rho_w \times V_w}$, where $\boldsymbol{\rho_w}$ = water density and $\mathbf{V_w}$ = volume of water,
and total mass = $\mathbf{M_t = \rho_t \times V_t}$, where $\boldsymbol{\rho_t}$ = total density and $\mathbf{V_t}$ = total volume,
then:

$$\%\ Solids\ (mass) = \frac{\rho s \times Vs}{(\rho s \times Vs) + (\rho w \times Vw)} \times 100 \quad (24)$$

Using: $\mathbf{M_t = M_s + M_w}$

$$Mt = \rho s Vs + \rho w Vt - \rho w Vs \quad (25)$$

By solving Equation 25 in terms of Vs, the follow equation is determined:

$$Vs = \frac{Mt - \rho w Vt}{(\rho s - \rho w)} \quad (26)$$

By substituting Equation 26 into Equation 24 and simplifying it, the following equation is produced:

$$\%Solids\ \ (mass) = \left[\left(\frac{\rho s}{\rho s + \rho w}\right) - \left(\frac{\rho s \times \rho w}{\rho s - \rho w}\right)\frac{Vt}{Mt}\right] \times 100 \quad (27)$$

Equation 27 was used to determine the different solids by mass for different feed rates by taking the mass and volume into account. The density of the solids and liquid were also verified.

3.6 Cyclone efficiency and particle size distribution

The cyclone efficiency was determined by formulating a partition curve (see Section 2.4.3) from the cyclone samples taken. For consistency, the Lynch model was used because it makes use of non-linear regression to predict the partition curve. The particle size distribution was also determined by analysing the dried sized samples. These parameters were then used to conduct the mass balances and simulate parameters.

3.7 Clarity test

The quality of the water was measured using a clarity wedge (see Figure 2-23). Water samples were taken at the raw water sump, effluent sump and thickener overflow for comparison. A measurement was then read from the wedge scale based on the highest visible value (see Section 2.5.2).

3.8 Yield stress

To determine the transportability of the low-moisture oversize product, an in-field yield stress was conducted on the sample (see Section 2.5.1). Should the sample contain a large amount of water, it would easily deform and thus produce a low yield stress. On the other hand, less deformation would be inherent in a low-moisture sample, which would

thus produce a high yield stress. A high yield stress would mean that the oversize product is conveyable at inclined conveyor angles.

3.9 Mass balance

LIMN: The Flowsheet Processor is an Australian developed flowsheeting software package developed by David Wiseman. It is a process flowsheet processor which utilises the Microsoft Excel spreadsheet as a calculation platform. The flowsheet of the Hi-G Dryer system was modelled in LIMN (see Figure 3-1) to produce a mass balance for comparison and to simulate the impact of identified parameters on the Hi-G Dryer system. The actual partition data would be plotted and fitted with the Lynch model by using solver to change alpha, Rf and cut size to produce the best fit for the actual partition data on the model with a minimum SSE.

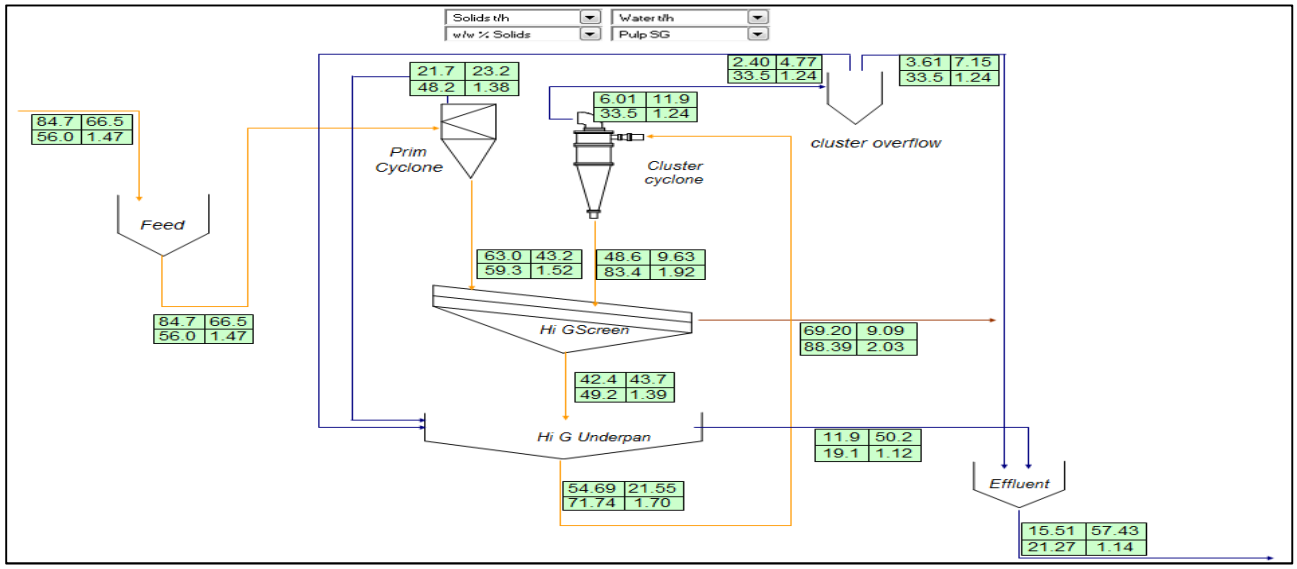

Figure 3-1: Example of an emblematic Hi-G Dryer flowsheet in LIMN

3.10 Plant operating parameters

Availability at the Daberas process plant had a large influence on Hi-G Dryer testing, as the Hi-G Dryer system tied in directly with the wet-sizing section. Testing was done only when the plant was running under steady-state conditions. The sampling was done at the

operating parameters listed in Table 3-2. When the plant operated within these conditions for more than 10 minutes, it was considered that the system reached steady state and a sample was taken.

Table 3-2: Operating conditions of the Hi-G Dryer

Plant feed to wet-sizing	200–300	t/hr
Hi-G feed	80,100, 120	m^3/hr

Based on the Zone 13 PSD presented in Figure 3-2, it is deduced that about 42% of the material fed to wet-sizing potentially reported to the degrit section for dewatering, depending on the wet-sizing screening performance. The average Zone 13 material density was determined in the laboratory to be about 2.37±0.06 SG.

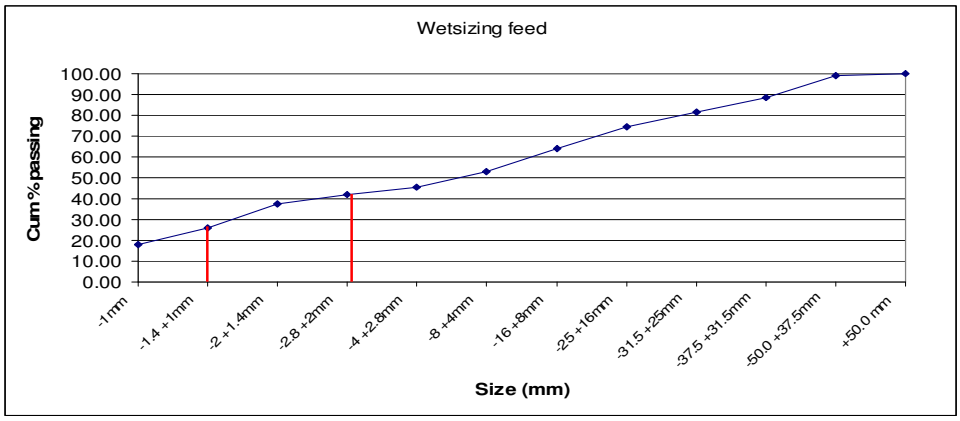

Figure 3-2: Particle size distribution of Zone 13 material to wet-sizing section

3.11 Safety

Namdeb is very strict regarding the safe operation of all equipment. It was therefore important to ensure that the Hi-G Dryer system was operated safely. It was ensured that the operating panel made provision for lock-out procedures when any maintenance, adjustments and mechanical work was done on the Hi-G Dryer system. A safety audit was also conducted by the Daberas safety officer to make sure that the system complies with Namdeb safety standards. An operational procedure was developed for the system to ensure that the integrity of the equipment was maintained.

4 Results and discussion

It should be noted that the majority of the testing was conducted during the Daberas plant production setup. Testing could only be carried out when the plant was operational and a steady-state condition was achieved. This resulted in extensive delays in the project. The experiments were firstly conducted to substantiate the supplier's system design performance. Secondly, the studied system parameters were optimised to produce a system that would be best suited to a coarse slurry process.

These results were then compared to the current Daberas degrit system's performance, which served as benchmark for a coarse dewatering system. A few tests were also conducted in Buffalo, USA, to evaluate some parameters. Only the raw data results were obtained and results were further processed to substantiate the individual performance of the screen. These results were also used to simulate the system in order to comprehend the impact of some parameters.

4.1 Initial Hi-G Dryer system

The supplier designed the initial Hi-G Dryer system (see Figure 2-3) for the coarse Daberas slurry. The slurry material from the Daberas wet-sizing section undersize was fed to a feed sump and pumped to a 250 mm hydrocyclone. A 250 mm primary cyclone is not normally included in the Hi-G Dryer system design, but in this case it was incorporated to account for the coarse particles in the system. The supplier argued that the solids concentration from the wet-sizing section to the Derrick screen could be too low and thus impede the material bed formation. A higher percentage solids to the screen could assist with material bed formation and ultimately with dewatering. The overflow of the 250 mm cyclone reported to the screen underpan and together with the screen undersize was pumped to the cluster cyclones for further classification.

It was expected that some settling would take place in the screen underpan sump before overflowing to the effluent sump. The settling would therefore allow for a clearer overflow.

During testing it was noted that the screen underpan sump slurry was very turbulent, therefore very little settling took place. The underflow of the cluster cyclones together with the primary cyclone underflow reported to the Hi-G screen for dewatering. The screen oversize material moisture was quantified and compared to the Daberas degrit section. The quality of the effluent was also measured to establish if it meets the requirement as plant process water.

4.1.1 Product moisture results of initial layout

According to the results presented in Figure 4-1, the Hi-G Dryer system produced oversize product moisture of less than 30%. This confirms Derrick Corporation's claim that the Hi-G Dryer system can produce an oversize moisture content of 25–30% and less. The results show that an average screen product moisture content of 17.2% was obtained. The overall solids lost to effluent were about 3% of the feed, which is very good. About 97% of the solids reported as Hi-G screen oversize and were conveyed to the Daberas tailings dump for disposal.

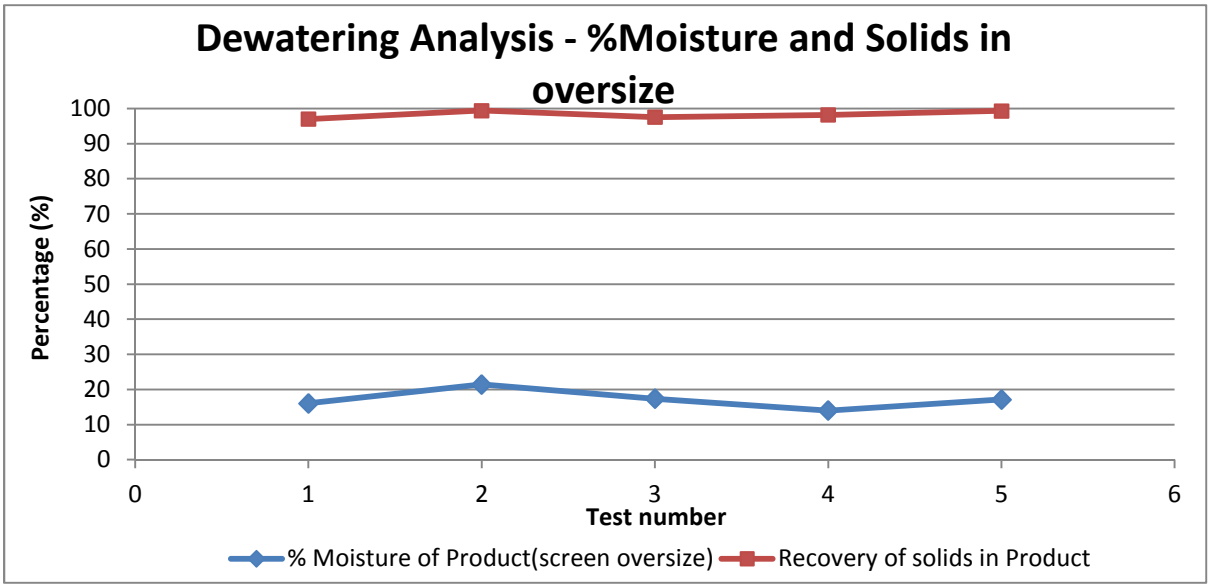

Figure 4-1: Product moisture and recovery results for the initial layout

Even though the drainage on the screen was good, about 50% of the screen surface was effectively covered with slurry, thus making only 50% available for effective dewatering (see Figure 4-2). The general rule for effective dewatering at Namdeb is that the majority of the water should be removed on at least one-third of the screen surface. The operation therefore does not conform to the internal dewatering standard.

Figure 4-2: The Hi-G dewatering screen surface while in operation (initial layout)

The oversize product was conveyable and easy to transport to the tailings dump, but it was observed that the yield stress test results on the oversize product of the Daberas degrit section were better than those of the Hi-G Dryer system (Figure 4-3).

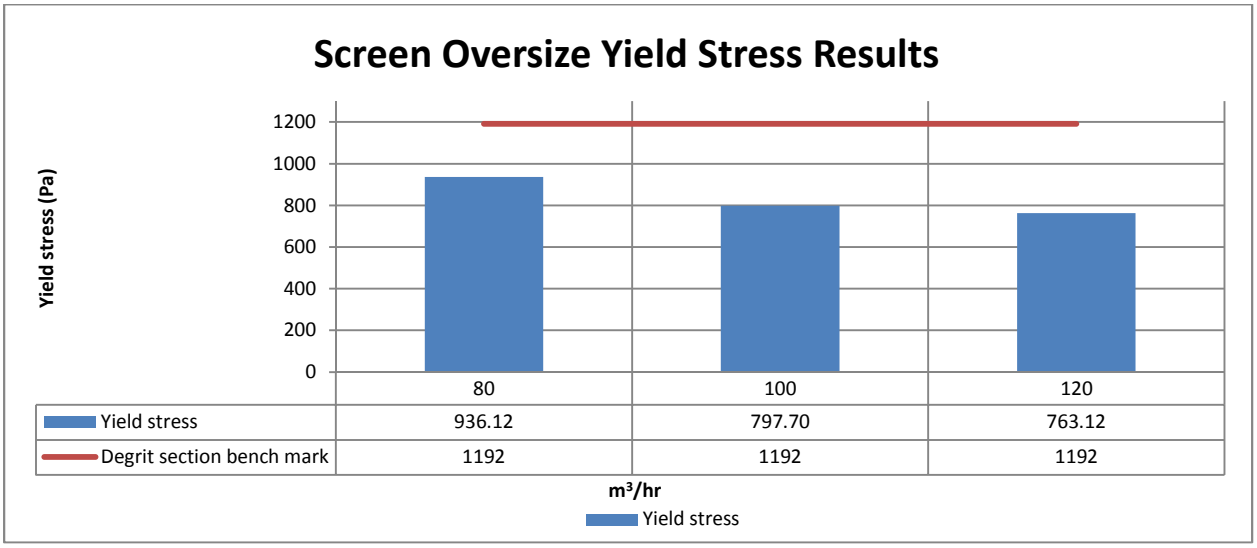

Figure 4-3: Yield stress test results for initial layout

The yield stress test results show that the Hi-G Dryer product was about 21% less stable than the Daberas degrit product. The oversize product only becomes totally unstable at 500 Pa, therefore the product is still transportable. It is also evident from the results that the product became more unstable as the feed rate increased. This could be as a result of the high slurry volume on the screen surface as the feed rate increased. This meant that a large amount of fines could have been screened through to the undersize, resulting in poor cake formation, which caused the product to be coarser and thus less stable. Another reason for the lower yield stress could be the solids concentration obtained. The lower the moisture, the more stable the product.

Figure 4-4 below demonstrates the particle size distribution of the product oversize material over the screen. When comparing the oversize product to the feed, the oversize product was found to be slightly finer.

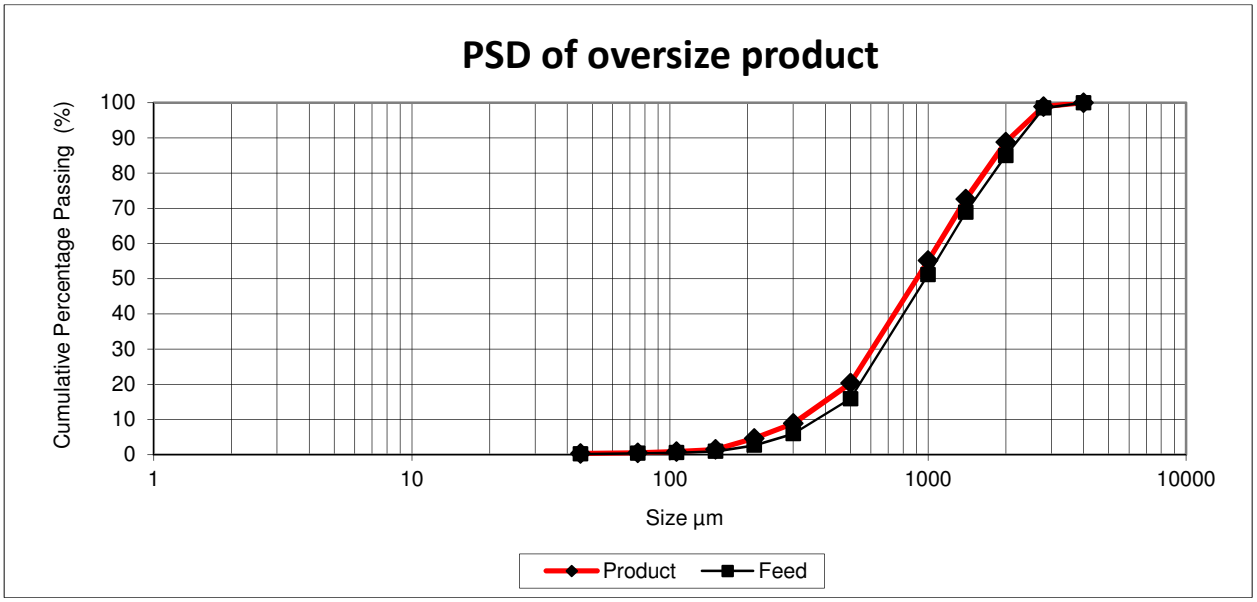

Figure 4-4: Oversize product particle size distribution

It can be concluded that some fine particles are removed to the product through bed filtration. A material bed, which can be observed on the screen in Figure 4-5, should act as a filter bed to trap ultra-fine particles. A finer product, based on PSD, underlines the fact that fine particles could be trapped between the voids of the larger particles, creating this

slight shift in the graph. It should also be noted that the shift is very small, proving that the lower yield stress test results were not due to less fines in the product. Product instability could therefore be due to less moisture in the Daberas degrit oversize product.

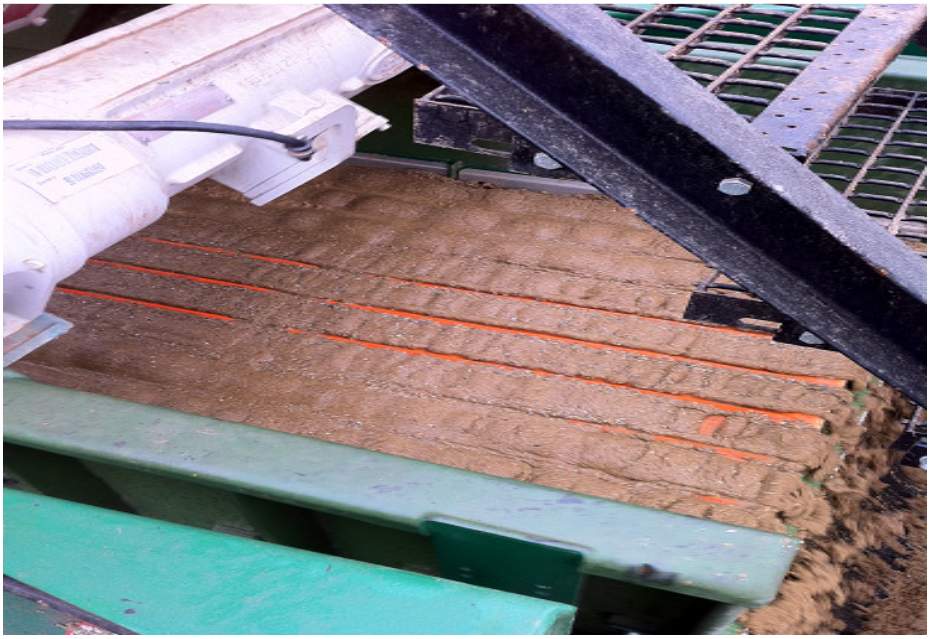

Figure 4-5: Product material discharge of the Hi-G Dryer screen

The Hi-G Dryer system performance was compared to that of the Daberas degrit system. The Daberas degrit system had a slightly better performance in terms of moisture compared to the initial process layout. The Hi-G Dryer screen had a horizontal orientation and it was decided to incline the screen at 6 degrees in order to improve results. The Velco screens at the Daberas degrit section have a 5-degree incline to allow the formation of the filter bed cake. Even after inclining the Hi-G screen at 6 degrees, the Velco screens at Daberas still produced a slightly dryer product, as deduced from Figure 4-6.

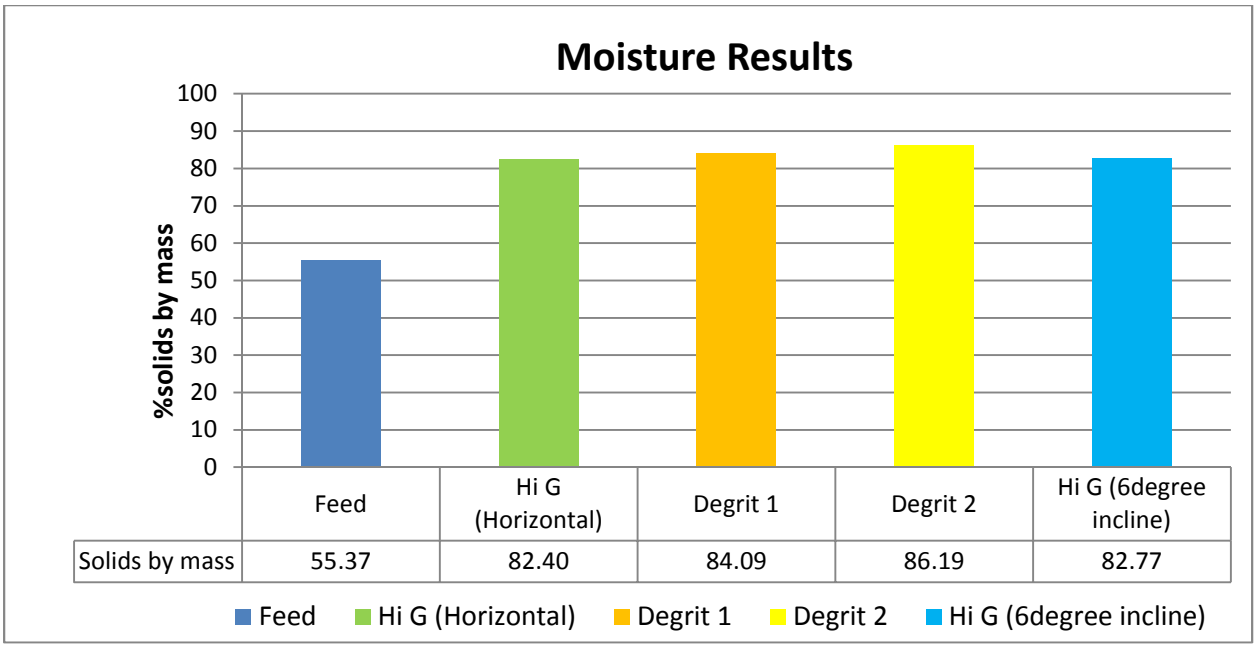

Figure 4-6: Degrit performance compared to that of the Hi-G Dryer

Figure 4-7 shows that the particle size distribution (PSD) of the product oversize is very similar to that of the degrit Velco screens, which is based on a similar dewatering principle as the Hi-G screen. Both dewatering screens have very similar parameters apart from the difference in G-forces, which makes similarities in the particle size distribution very likely.

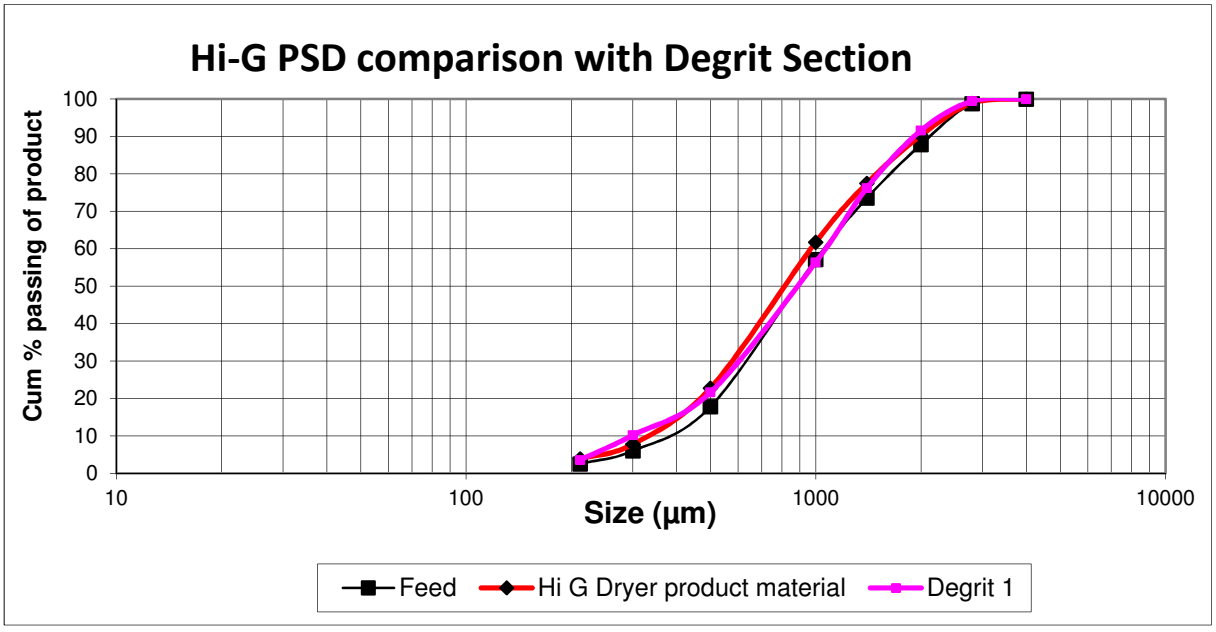

Figure 4-7: PSD: Hi-G Dryer vs degrit section

The Velco screen product oversize particle size distribution does indicate a slight shift that could encourage some entrapment of fine particles to the screen oversize, but it is very small and therefore negligible. The similarity between the particle size distributions in Figure 4-7 has more to do with the fact that dewatering is more prominent then classification.

4.1.2 Water quality results of initial layout

The percentage solids by mass in the effluent varied between 1 and 3% (see Figure 4-8), which is a good result. However, there was a large amount of misplaced material reporting to the screen underpan sump due to the inefficiencies experienced at the primary cyclone and cluster cyclones. The high volumes of slurry entering the underpan sump caused a great deal of turbulence in the underpan, which also hindered the particles from settling in the underpan. This contributed to larger particles reporting to the overflow into the effluent sump.

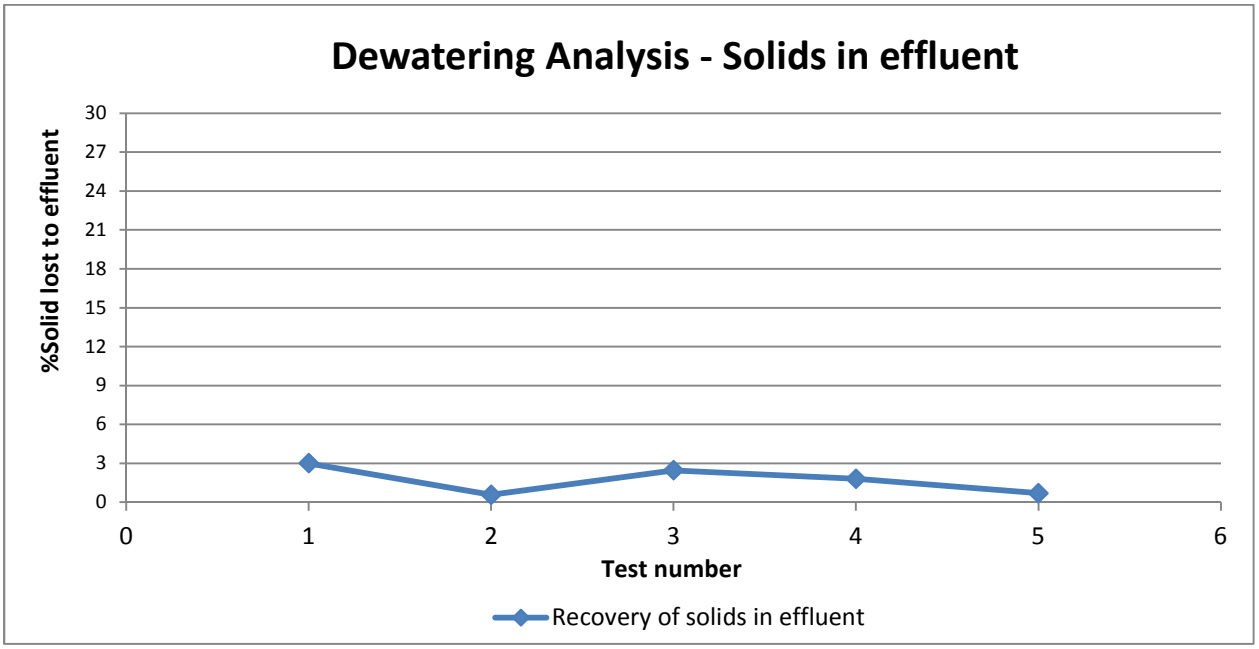

Figure 4-8: % Solids lost to effluent

It is evident from the particle size distribution of the effluent (see Figure 4-9) that a large amount of large particles were reporting to the effluent overflow. As the panel aperture size was 500 µm, particles greater than 500 µm should not be evident in the effluent. This highlights a great concern regarding the Hi-G Dryer system performance.

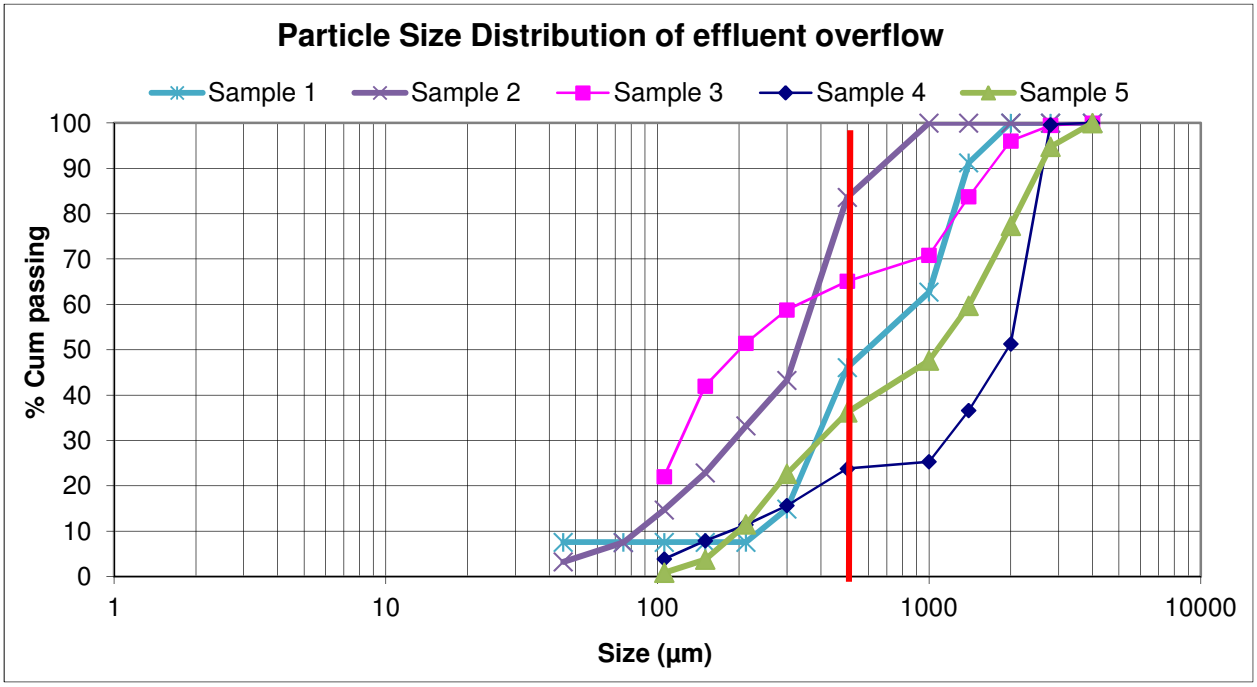

Figure 4-9: PSD indicates large particles in the effluent overflow

When investigating the reason for the misplaced material, it became clear that the primary cyclone and cluster cyclones were underperforming. The primary cyclone and cluster cyclones were constantly under roping conditions, which was the reason for the misplaced material. The inefficiencies of the primary cyclone had a direct influence on the performance of the cluster cyclones and because of the high turbulence in the screen underpan the misplaced oversize particles were lost to the effluent.

The effluent of the Hi-G Dryer was compared to that of the current Daberas degrit system, the thickener overflow and the raw water. The Daberas degrit overflow reports to a thickener for further processing. The clear thickener overflow water is used at the wet-sizing section as process water. Should the Hi-G Dryer system produce a similar water quality, it would have great benefits.

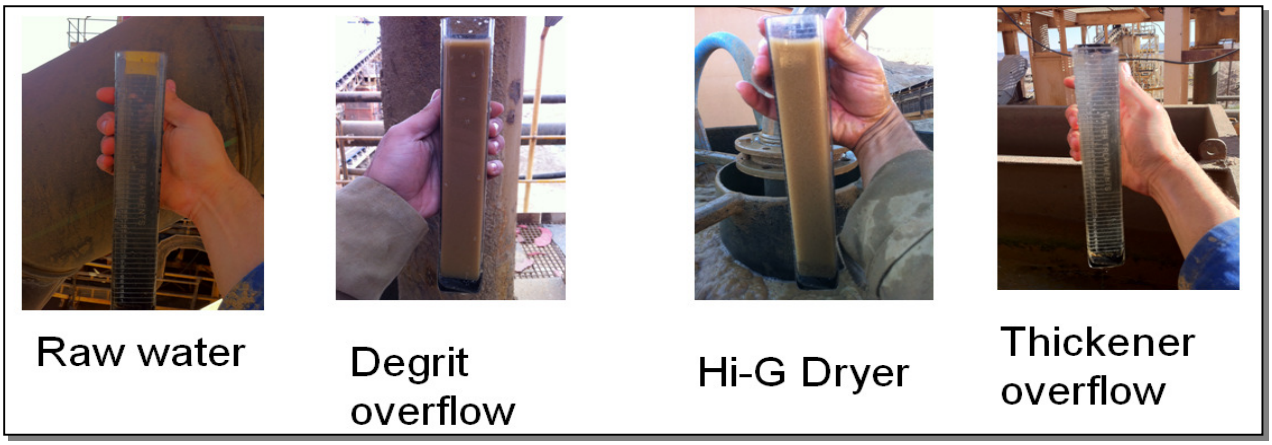

Figure 4-10: Water quality test results

As observed in Figure 4-10, there were a large number of unstable solids in the Hi-G Dryer effluent that could not be removed by the hydrocyclones and the screen. This was very similar to the Daberas degrit overflow before the thickener stage. The visually unstable solids and particle size distribution of the effluent confirm inefficiencies of the Hi-G Dryer system.

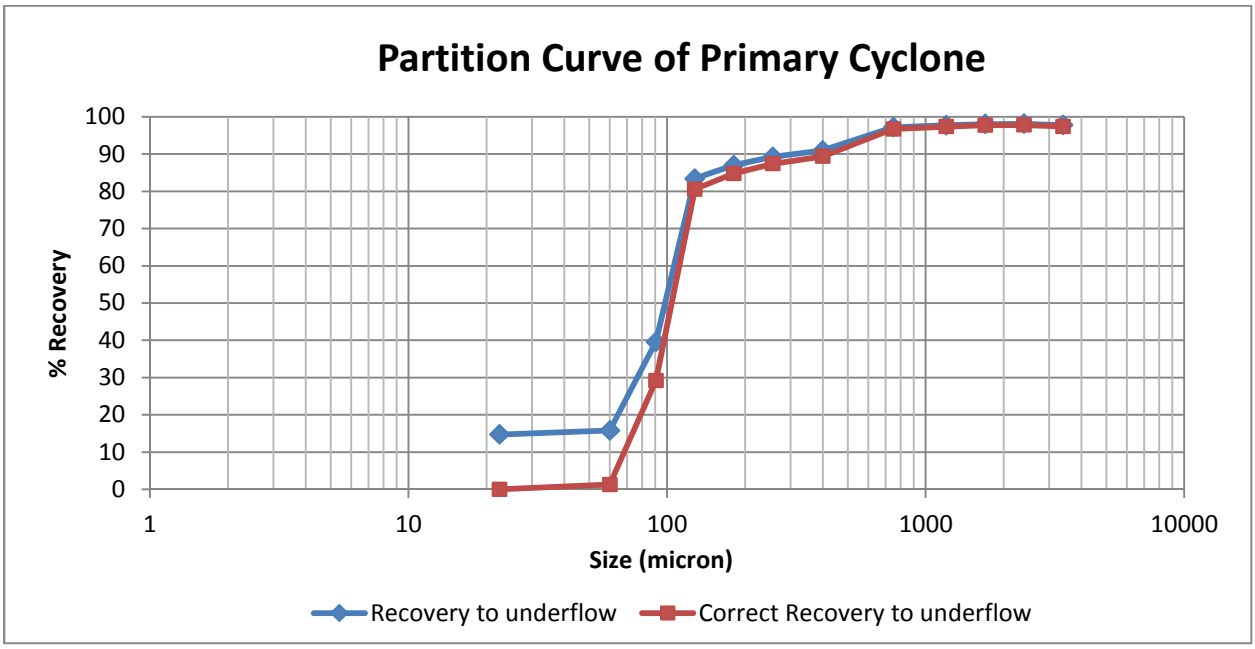

Figure 4-11: Efficiency of the primary cyclone

The test results confirmed that the performance of the primary cyclone was inefficient as it misplaced particles over the entire size range (see Figure 4-11). Although it had a d_{50c} of 100 µm and an Imperfection (I) of 0.2 which is very good, it had no D_{100}. The misplaced material had a huge impact on the cluster cyclones, which resulted in blockages and inefficiencies of the cluster cyclones.

Figure 4-12: The primary cyclone under roping conditions discharging with the cluster cyclones

Figure 4-13 shows how the misplaced material from the primary cyclone negatively affected the cluster cyclones' performance, which was very poor. There was misplaced material over the entire size range and even more at the larger sizes. The larger particles that were misplaced via the primary cyclone overflow reported as feed to the cluster cyclones. The misplace material negatively affected to cluster performance by causing spigot crowding and blockages. The cluster cyclones were close to roping conditions, which resulted in misplaced material to the overflow. Particles larger than 1 mm should not be in the cluster cyclone partition curve, but due to the poor primary cyclone performance it is present and negatively affected the performance of the cluster cyclones as observed in Figure 4-13. The Imperfection was calculated to 0.72 with no D_{100}, thus confirming the poor cyclone performance.

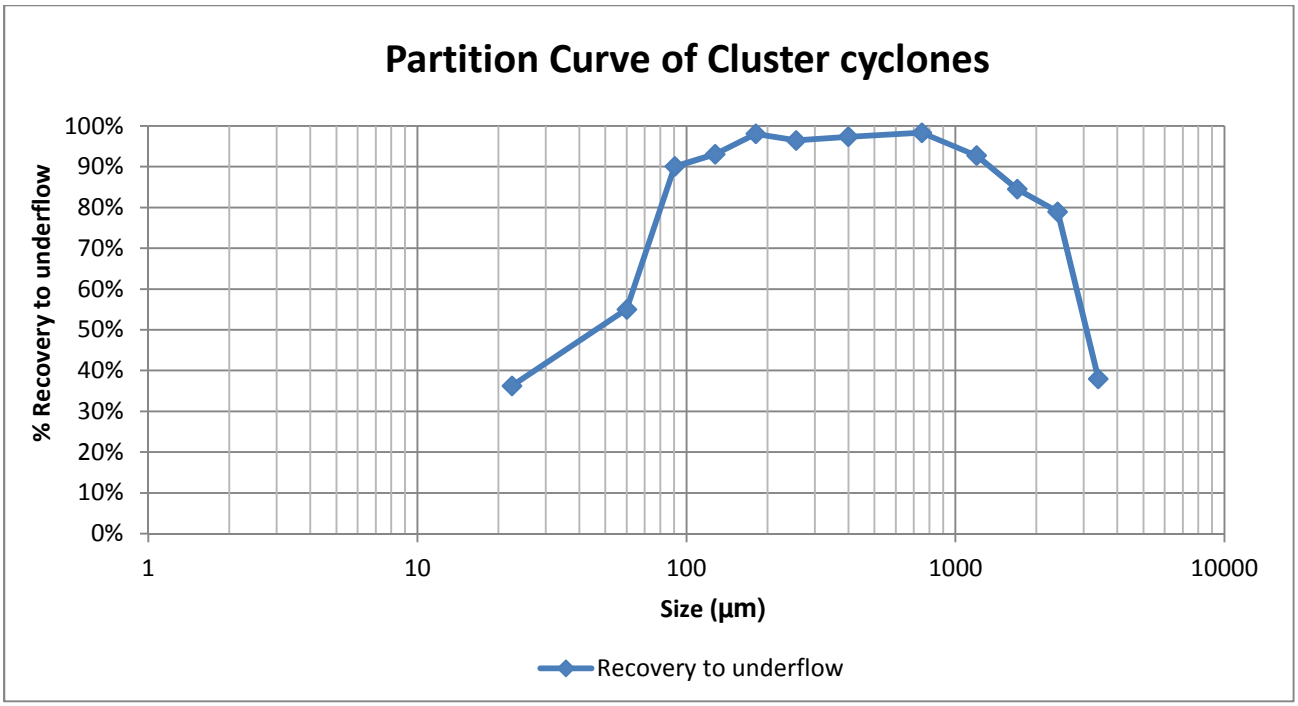

Figure 4-13: Cluster cyclone performance

After observing the inefficiencies of the system, modifications were made based on the dewatering parameters studied in the literature. The problem areas were identified and modifications were made to enhance or optimise the performance of the system.

4.1.3 Problems with initial layout

The following problems were discovered during testing on the initial layout:

- The primary cyclone was inefficient and misplaced a large amount of material to the cyclone overflow which reported to the screen underpan. The screen underpan material was then pumped to the cluster cyclones, resulting in blockages and poor cluster cyclone performance.
- The primary cyclone was the bottleneck of the system and was constantly roping at higher feed rates, misplacing more material to the cluster cyclones.
- There was a great deal of turbulence in the underpan due to primary cyclone overflow and screen undersize, which resulted in more coarse and fines material reporting to the effluent overflow.

- The slurry on the Hi-G screen covered more than 50% of the screen surface, resulting in a smaller effective dewatering area.

The parameters that could have an effect on the system in order to address the problems identified are summarised in Table 4-1.

Table 4-1: Dewatering parameters that could be changed to optimise system performance

Parameter	**Action**	**Comment**
Particle shape	Cannot change	The Daberas coarse material is being tested. The particle shape has to remain constant for testing.
Solids concentration	Cannot change	The feed solids concentration from the wet-sizing section is also kept constant to test and compare the systems.
Size distribution	Cannot change	The Daberas coarse material is being tested. The feed particle size distribution has to remain constant for testing.
Aperture shape	Cannot change	Only slotted panels are produced by the supplier.
Aperture size	Can change	Can change to 180 μm panel.
Open area	Can change	Depending on the aperture size selected.
Operating frequency	Cannot change	It is related to the G-forces which are beneficial to the Hi-G system.
Amplitude	Cannot change	It is related to the G-forces which are beneficial to the Hi-G system.
Screen slope	Can change	Can change to 6 and 12 degree angles.

4.1.4 Initial layout conclusion

The initial process layout did produce very good screen product oversize moisture results which compare well to the current degrit system and confirm the dewatering ability of the Hi-G screen. The oversize product had a moisture content of about 17.2% and was easily conveyable. Inefficiencies were mainly due to the primary cyclone misplacing material to

the overflow and consequently having a negative effect on the cluster cyclones' performance.

The Hi-G effluent had very unstable ultra-fines and unfortunately coarse particles also reported to the effluent. The high turbulence experienced in the screen underpan hindered the settling of the particles and also resulted in larger particles reporting as overflow to the effluent. More than 50% of the screen surface was covered with slurry, which negatively effects dewatering. The dewatering parameters studied in the literature assisted the action taken to address these problems identified in order to optimise the system.

4.2 New process layout

After considering the problems encountered with the previous setup, mainly three modifications of the system parameters were considered. The first was bypassing the primary cyclone, followed by inclining the screen at 12 degrees and lastly replacing the 500 µm aperture panels with 180 µm aperture panels. The changes were in line with the dewatering parameters considered in Table 4-1. Each modification had a predetermined expectancy:

- **Bypassing the primary cyclone** – It was expected that fewer oversize particles would be misplaced by the primary cyclone and a better bed depth would be built, thus improving bed filtration. Improved cluster cyclone performance was also expected.
- **Inclining the Hi-G screen at 12 degrees** – Inclining the screen would reduce the area used for water drainage and also improve the material bed construction, thus allowing bed filtration with a much dryer product (see Figure 4-14).
- **Replacing 500 µm panels with 180 µm panels** – This is to create a thicker bed to allow for improved water filtration. The reduction in aperture size would also reduce the amount of material going to the cluster cyclones, thus improving cyclone efficiencies, and allow the Hi-G Dryer screen to remove the majority of the grits.

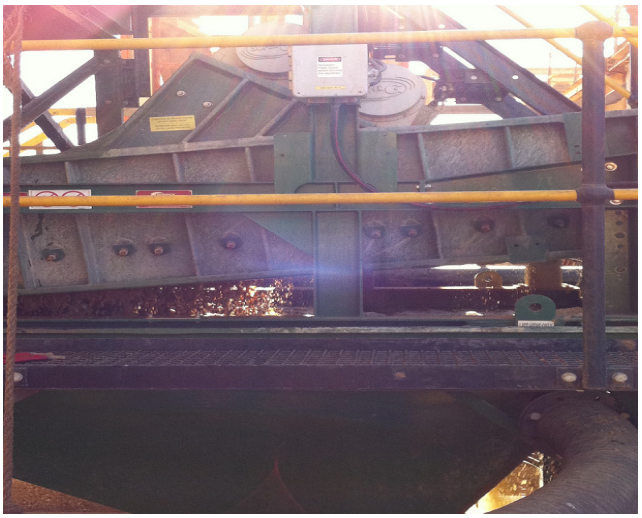

Figure 4-14: An inclined Hi-G Dryer screen at Daberas

In the new process layout (see Figure 4-15), the cluster cyclone overflow reported to both the effluent sump and the Hi-G screen underpan. The cluster overflow split was balanced to allow for enough fluid to prevent the cluster cyclone pump from surging so that no overflow reports to the effluent sump. One of the advantages of preventing overflow of the screen underpan sump is that no solids would be lost to the overflow, should high turbulence be experienced in the screen underpan. The effluent quality is therefore more dependent on the efficiency of the cluster cyclones.

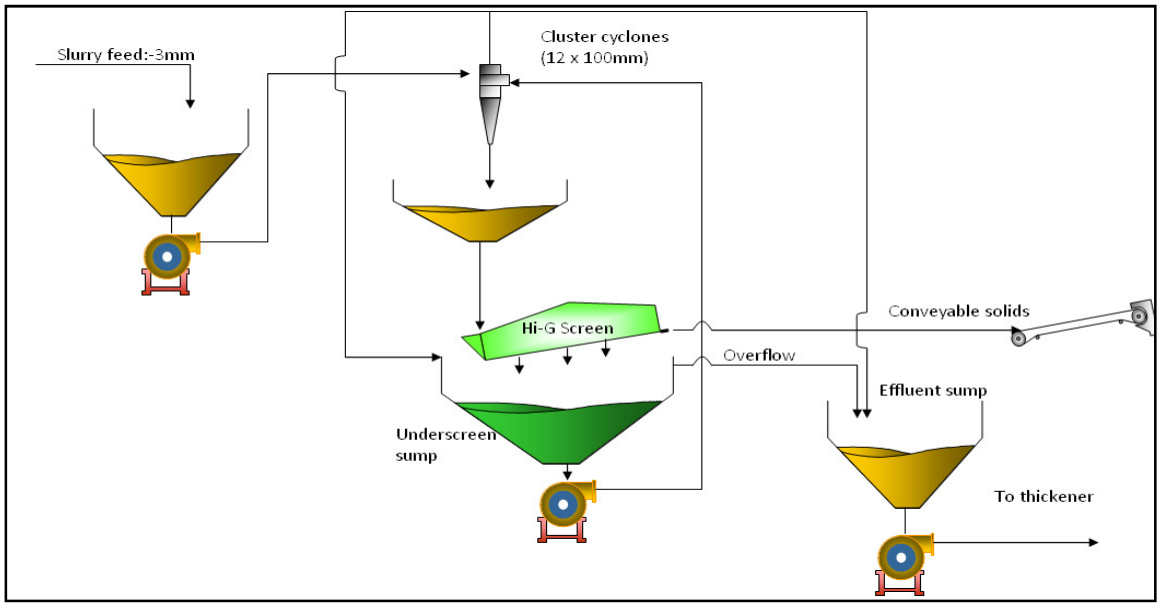

Figure 4-15: The new proposed process layout

As indicated in Figure 4-16, each modification brought about an improvement with regard to moisture content and solids recovery to product. Bypassing the primary cyclone had little effect on the moisture results compared to the initial process layout. Bypassing the primary cyclone and inclining the screen at a 12 degree angle had a slightly better effect on moisture results. The moisture content dropped to below 20% and the overall recovery of solids to product oversize was about 98%.

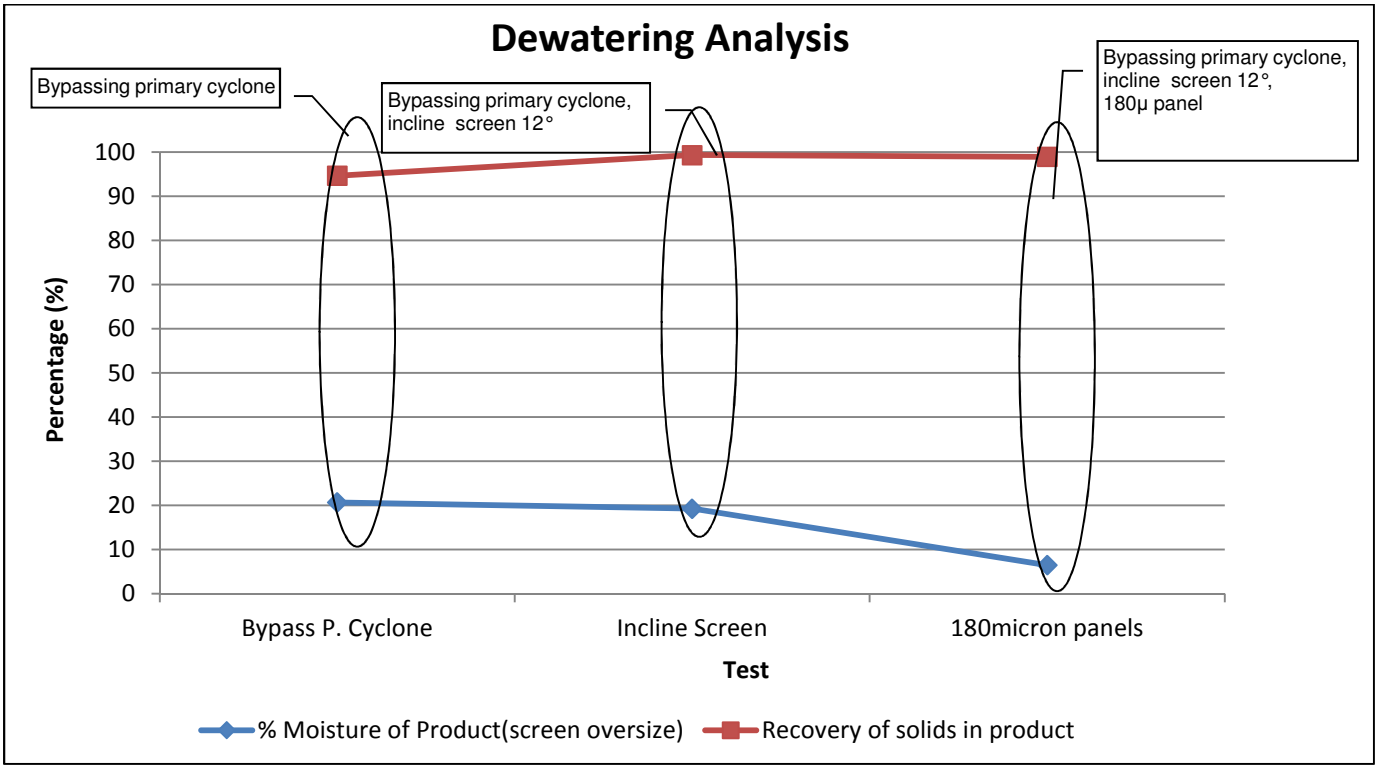

Figure 4-16: Moisture analysis after all three modifications

The best results were obtained after all three modifications were completed. After the installation of the 180 µm panels, the moisture content was reduced to below 10% with an overall solids recovery of 98%. More tests were conducted at a feed of 80 m^3/hr to determine the repeatability of the testing. The results are presented in Figure 4-17. An average of 13.8% moisture in the oversize product was obtained after all the modifications were done according to the new process layout.

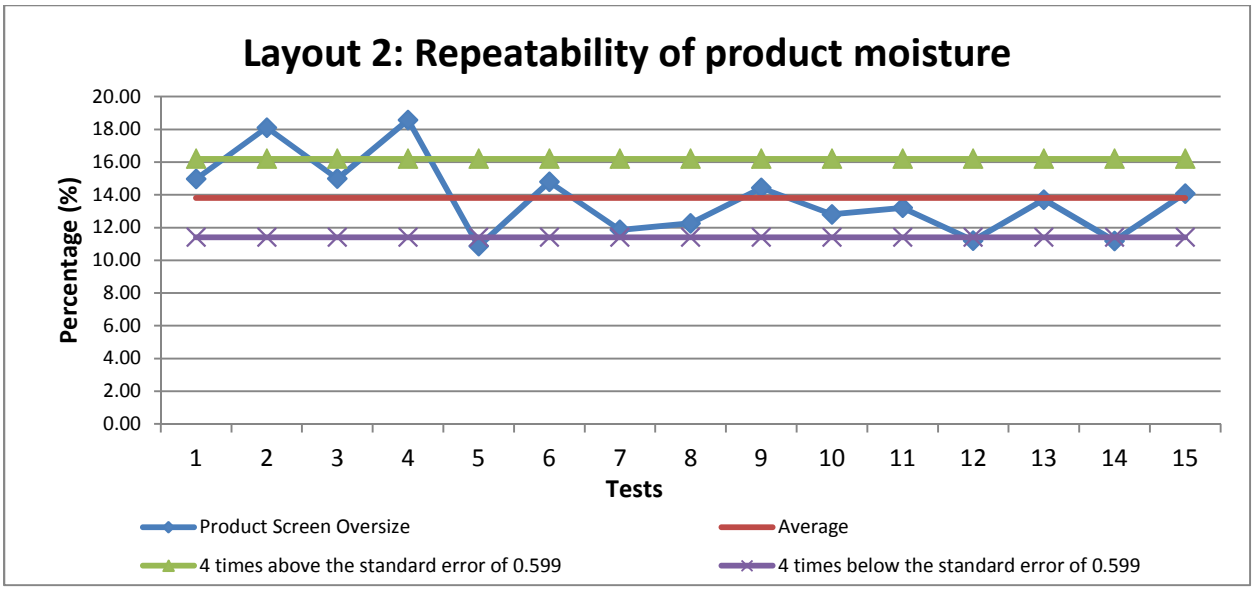

Figure 4-17: Stability of product moisture results

A much thicker bed was also formed (see Figure 4-18). The thicker bed could have assisted the dewatering process and the overall recovery of solids.

Figure 4-18: A much thicker material bed formed on the screen

The particle size distributions presented in Figure 4-19 demonstrate how the fine particles behaved after each modification. After inclining the screen, a shift to a fine particle size distribution was observed. This was due to an improved material bed, assisting the entrapment of finer particles. After the 180 µm panels were installed, the particle size distribution shifted slightly to a coarse distribution. The smaller apertures allow more material to the oversize and the slight shift to coarse distribution can be attributed to the fact that less oversize is lost to undersize.

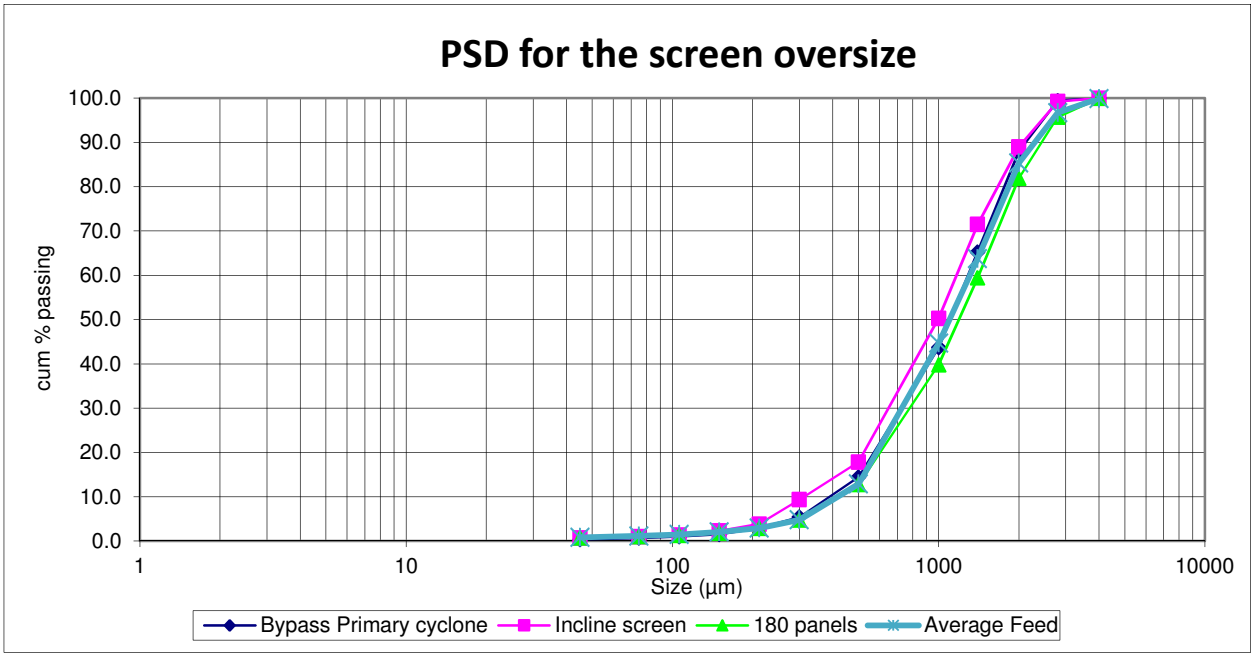

Figure 4-19: The PSDs of the three modifications tested

The screen oversize product stability also improved, as shown in Figure 4-20. This compares well to the current Daberas product stability. A much better material bed was formed due to the modifications. When the feed rate was increased, more material was available for material bed formation, resulting in improved stability of the product. This suggests that there should be no concern regarding the transportability of the material to the tailings dump.

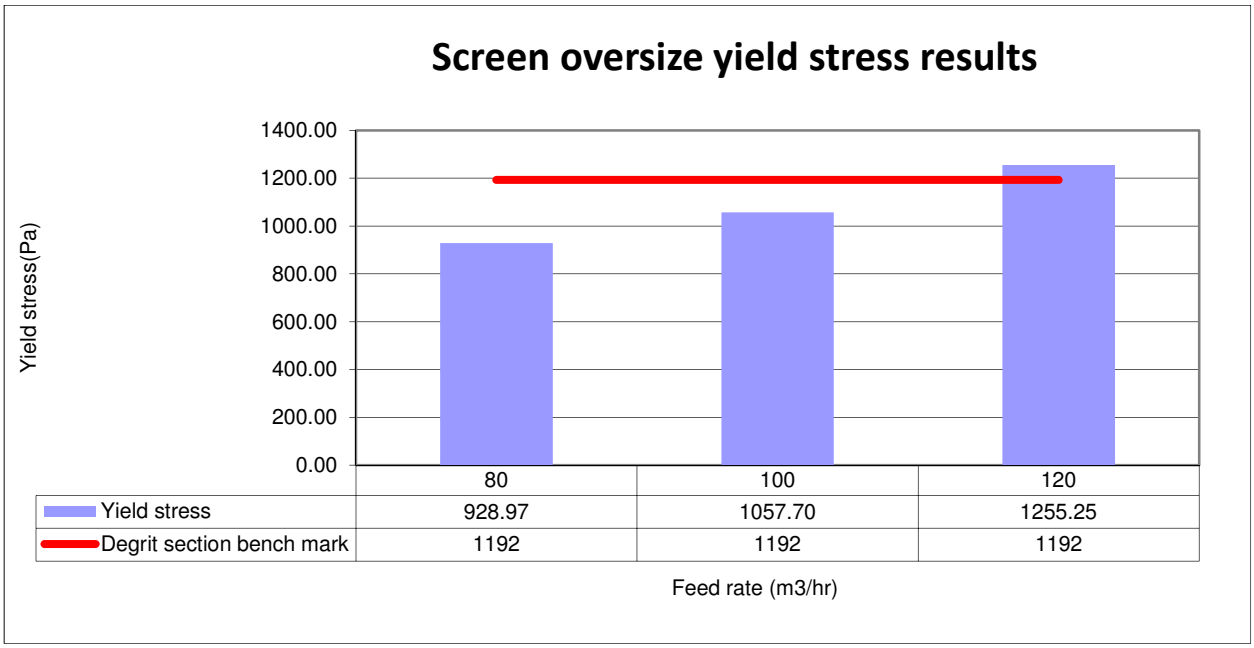

Figure 4-20: Yield stress after all three modifications

The modified Hi-G Dryer system produced an improved moisture content compared to that of the Daberas degrit system (see Figure 4-20). The 13.8% moisture content in the screen oversize confirms Derrick Corporation's claim that the Hi-G Dryer can effectively produce an oversize product of 30% solids by mass and less. The Hi-G Dryer system has proved to be a viable means of dewatering the coarse Daberas material.

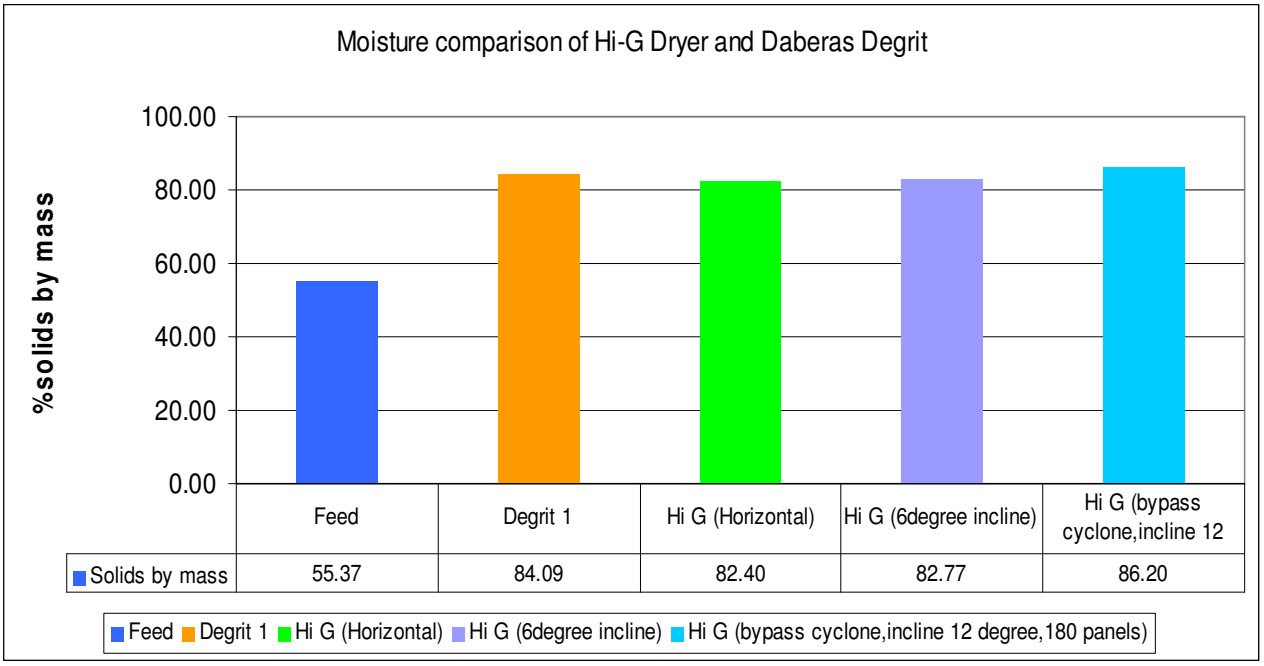

Figure 4-21: Hi-G system product moisture compared to degrit and some modifications

4.2.1 New process layout water quality results

The clarity results indicated that there still was a large amount of ultra-fines in the effluent (see Figure 4-22). The effluent is therefore not viable as process water due to the stability of the ultra-fines in the water. The stable ultra-fines will have a very negative impact on dense medium separation (DMS) performance further on in the process, should it be used as process water. The Hi-G Dryer effluent would therefore still require a thickening stage to produce a clearer supernatant, should it be reused as plant process water.

Figure 4-22: Effluent clarity from the Hi-G Dryer

The screen removed the majority of the larger particles from the system, putting less strain on the cluster cyclones. There were no particles larger than 1.4 mm reporting to the cluster cyclones. Due to the smaller apertures, particles smaller than 500 µm reported to the effluent sump, as observed in Figure 4-23. This is a much better result compared to the initial process layout.

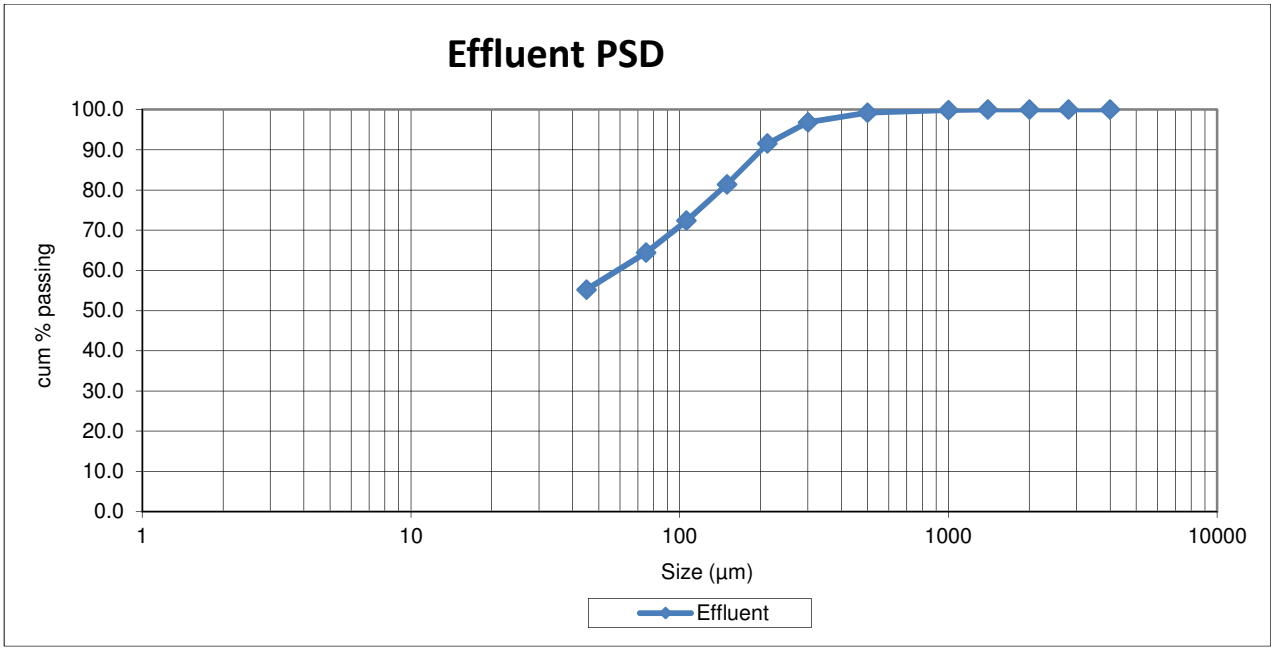

Figure 4-23: Particle size distribution of the effluent

Figure 4-24 demonstrates the performance of the cluster cyclones after each modification. The efficiency of the cluster cyclones improved compared to the previous process layout. The majority of the fines reported to the cluster cyclone underflow with no problematic misplaced particles present. The best cluster cyclone performance was obtained after all three modifications were made. This means there was no misplaced material from the primary cyclone to impact on cluster cyclone performance and less material from the screen undersize allowed for better performance results. The Imperfection was calculated to 0.34 with a D_{100} of 200µm, which is a remarkable improvement from the Imperfection of 0.72 that was previously found.

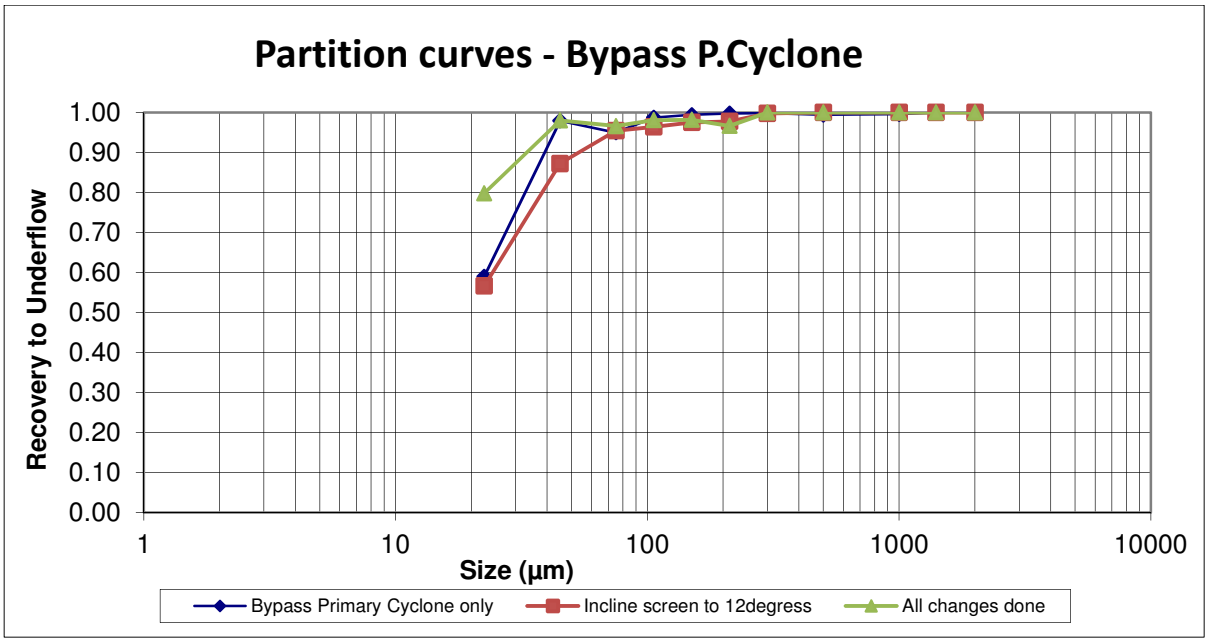

Figure 4-24: Partition curves for cluster cyclones after modifications

4.2.2 Overall Hi-G Dryer system performance under production conditions

Conducting tests under production conditions proved to be difficult, but the results obtained provided significant information regarding the applicability of the equipment for a much coarser application.

The supplier's design layout proved to be very inefficient, although good moisture results were obtained. The inclusion of a primary cyclone proved to be the cause of the inefficiencies. Results indicate that a primary cyclone should not have been included, but it is understandable that the supplier was concerned about getting a much denser feed to the Hi-G screen to allow the material bed to build. However, the primary cyclone created a bottleneck to the Hi-G Dryer and misplaced a large amount of material to the cluster cyclones, resulting in blockages which rendered the cluster cyclones ineffective. As a result, more misplaced material reported to the effluent.

After the modifications were implemented, a significant improvement in system performance was noticed. The Hi-G Dryer system produced an oversize product with a

moisture content of about 13.8% with very good stability for transportation to the tailings dump. The overall recovery of solids to the screen product oversize was 98.2%. This means that 1.8% of the Hi-G Dryer system solids reported to the effluent with a particle size distribution of less than 500 µm. The effluent could not be used as process water because of the high stability of ultra-fines in the effluent. The cluster cyclones had a d_{50c} of 16.5 µm, which is very good and compares very well with literature. According to Arterburn (1982), the ideal d_{50c} is about 13.5 µm. This information was used in the modelling of the cluster cyclone performance. These parameters were fed into the LIMN simulation used to model mass balance on the Hi-G Dryer system.

It is clear that an extra process step such as a thickener or clarifier is required for the effluent to be considered as process water. The following challenges were experienced during the testing campaign:

- There was difficulty conducting testing under production conditions as a result of delays, mainly due to the Daberas plant availability.
- It was necessary to take samples when steady-state conditions were reached. At times the feed to the Hi-G Dryer system was very low (see Figure 4-25).
- Spigot blockages were experienced at the cluster cyclones due to misplaced material and spigot crowding.
- Samples could not be taken for the screen and cyclones independently because of the closed circuit. Some testing was therefore done under laboratory conditions to investigate screen and cyclone performance independently.

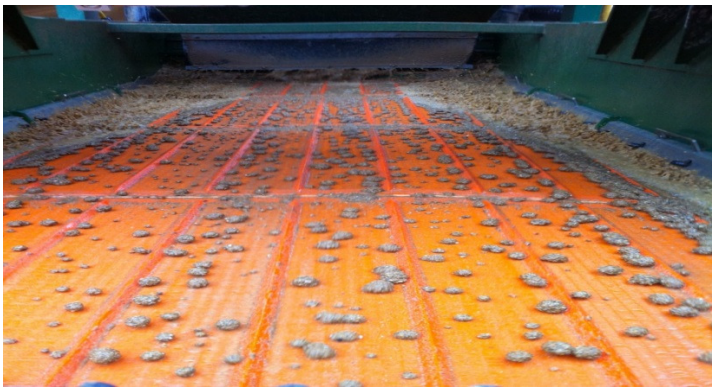

Figure 4-25: Low feed to the Hi-G Dryer system due to operational delays

4.3 Laboratory testing

Tests were also conducted at Derrick Corporation in Buffalo, USA to determine the performance of the dewatering screen and cyclones independently under ideal laboratory conditions.

Tests were conducted on the 4x8 (1.2 m wide x 2.4 m long) Hi-G dewatering screen with 4-inch hydrocyclones. To simulate the proper solids loading (discharge of one 12-way hydrocyclone cluster) on the Hi-G screen, the usable width of the Hi-G test screen was restricted to 20% of the full width. In a full-scale commercial system, all the underflow from one 12-way hydrocyclone manifold feeds a Hi-G dewatering screen. Initially the dewatering screen was fed with 50.7% solids (by weight) at a dry solids feed rate of 42.4 t/h. The undersize was diluted from 40.2% to 14.6% (by weight) to feed the 4-inch hydrocyclone.

4.3.1 Hi-G screen testing conducted under laboratory conditions

A mass balance test was conducted on a Hi-G screen only (see Figure 4-26). The testing was conducted with the original 500 µm panels. The dewatering was fed with 50.7% solids by weight at a dry solids feed rate of 42 t/hr. The screen produced oversize product moisture of 22% solids. Based on the results of the mass balance test, it can be deduced that 57.3% of the solids reported to the undersize of the screen. The high percentage solids could be the reason why the cluster cyclones were not performing effectively at Daberas.

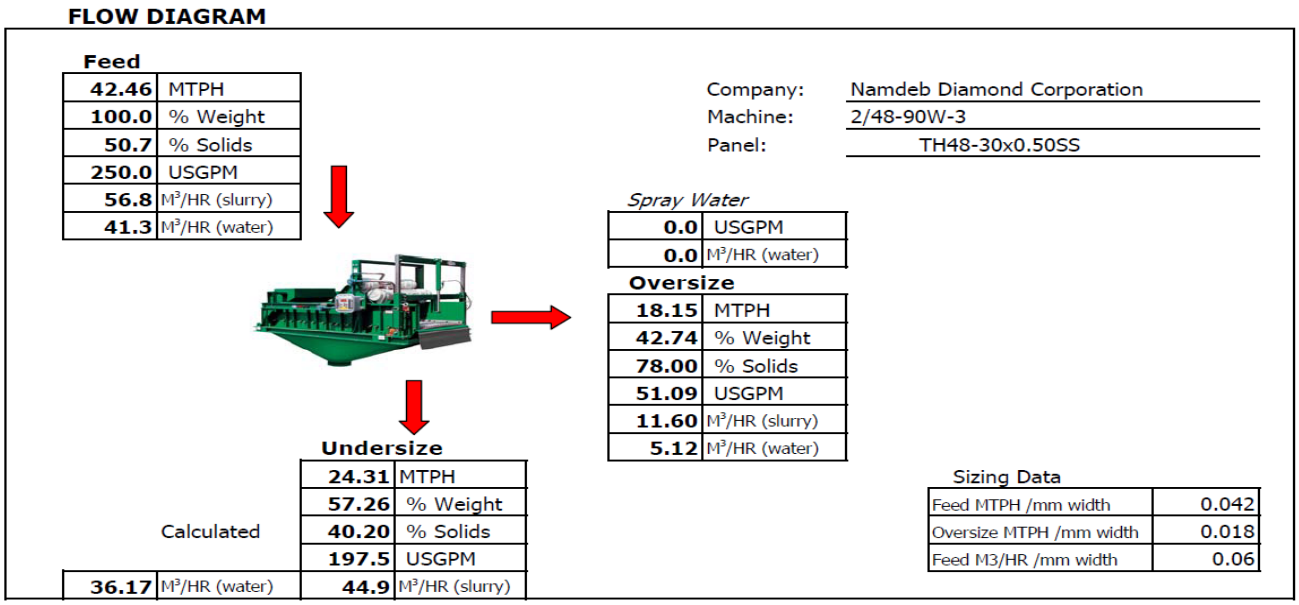

Figure 4-26: Mass balance test done on the Hi-G screen only with Daberas material

The particle size distribution of the feed, oversize and undersize of the Hi-G screen testing conducted under laboratory conditions are presented in Figure 4-27. It is clear that classification is more prominent than dewatering. This justifies using smaller aperture panels to allow for a more stable bed in order to assist dewatering.

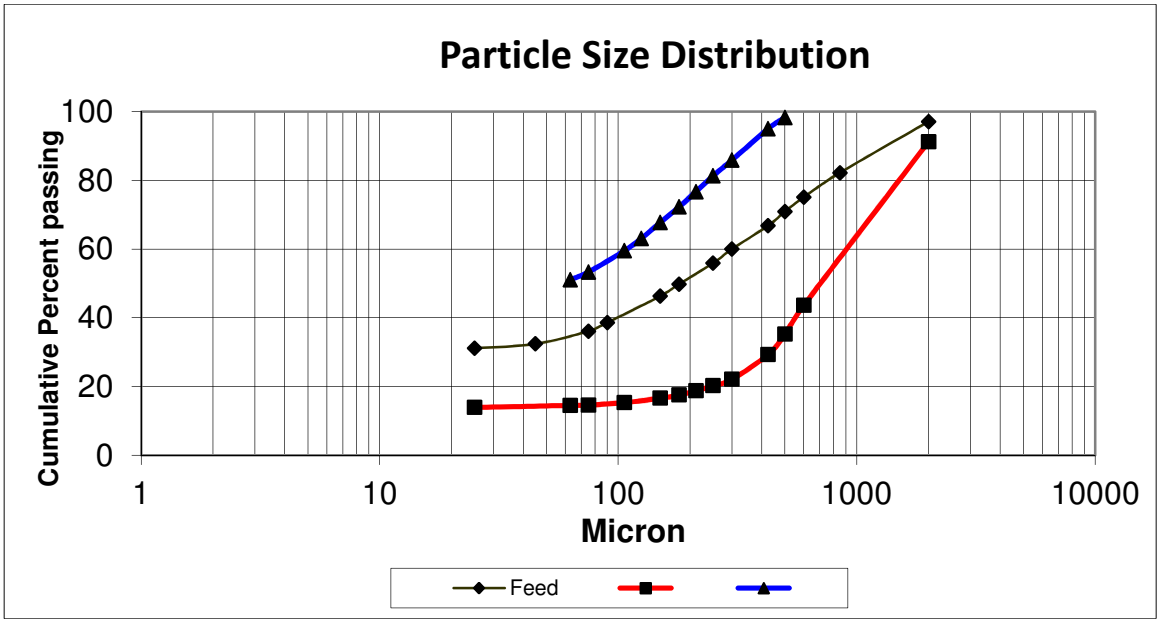

Figure 4-27: Particle size distribution of feed, oversize and undersize of Hi-G screen testing conducted under laboratory conditions

The recovery of solids to oversize is represented in Figure 4-28. Based on the graph fit, the following parameters were determined in order to populate the Lynch model (also referred to as the Whiten efficiency model) (see Equations 13 and 18):

Alpha = 1.572
d_{50c} = 580.28
R_f = 0.06
SSE = 0.027

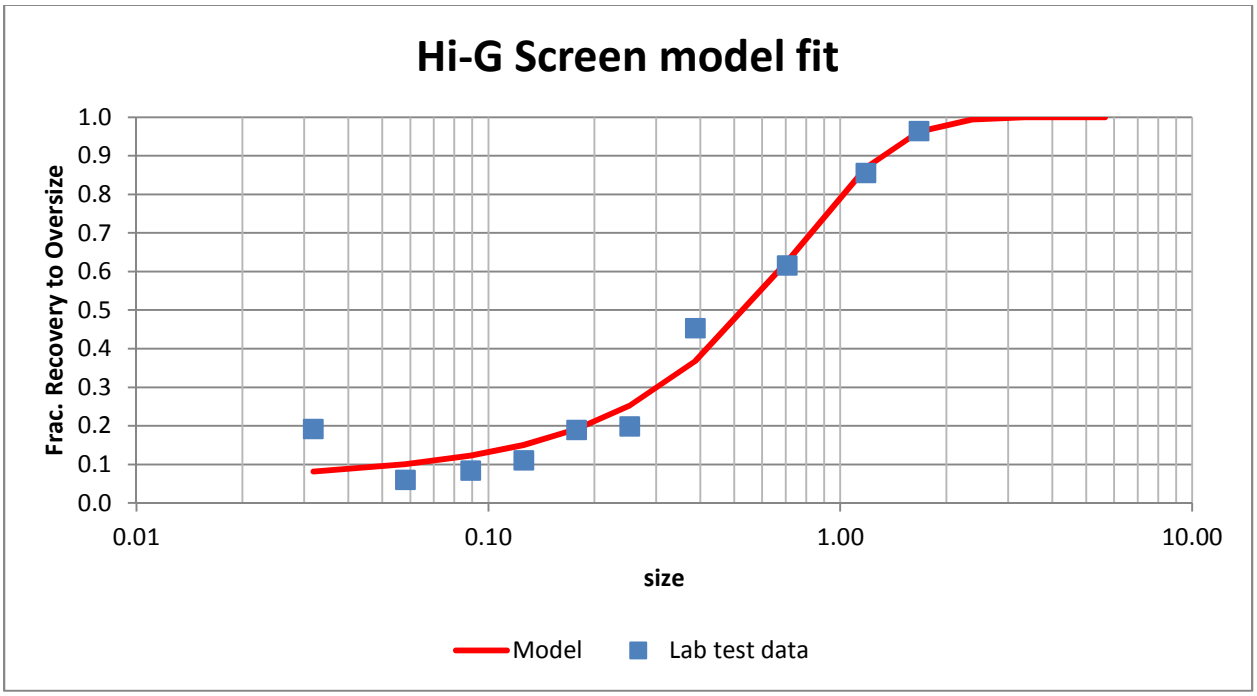

Figure 4-28: Efficiency of the Hi-G screen only under laboratory conditions

4.3.2 Cluster cyclone testing conducted under laboratory conditions

Cluster cyclone performance was also tested under laboratory conditions using material from the screen undersize. A material balance test was also conducted (see Figure 4-29). As expected, the feed particle size distribution was 100% 500 µm passing from the screen and the overflow consisted of mainly ultra-fines (see Figure 4-30).

FLOW DIAGRAM

Feed

24.29	MTPH
100.0	% Weight
14.6	% Solids
670.0	USGPM
152.2	M³/HR (slurry)
142.6	M³/HR (water)

Company: Namdeb Diamond Corporation
Machine: 12 -4" hydrocyclone
Panel:

Spray Water

0.0	USGPM
0.0	M³/HR (water)

Underflow

13.81	MTPH
56.85	% Weight
71.90	% Solids
45.47	USGPM
10.33	M³/HR (slurry)
5.40	M³/HR (water)

Overflow

10.48	MTPH
43.15	% Weight
7.09	% Solids
620.8	USGPM
141.0	M³/HR (slurry)

Calculated

137.23	M³/HR (water)

Figure 4-29: Mass balance test done on cluster cyclones

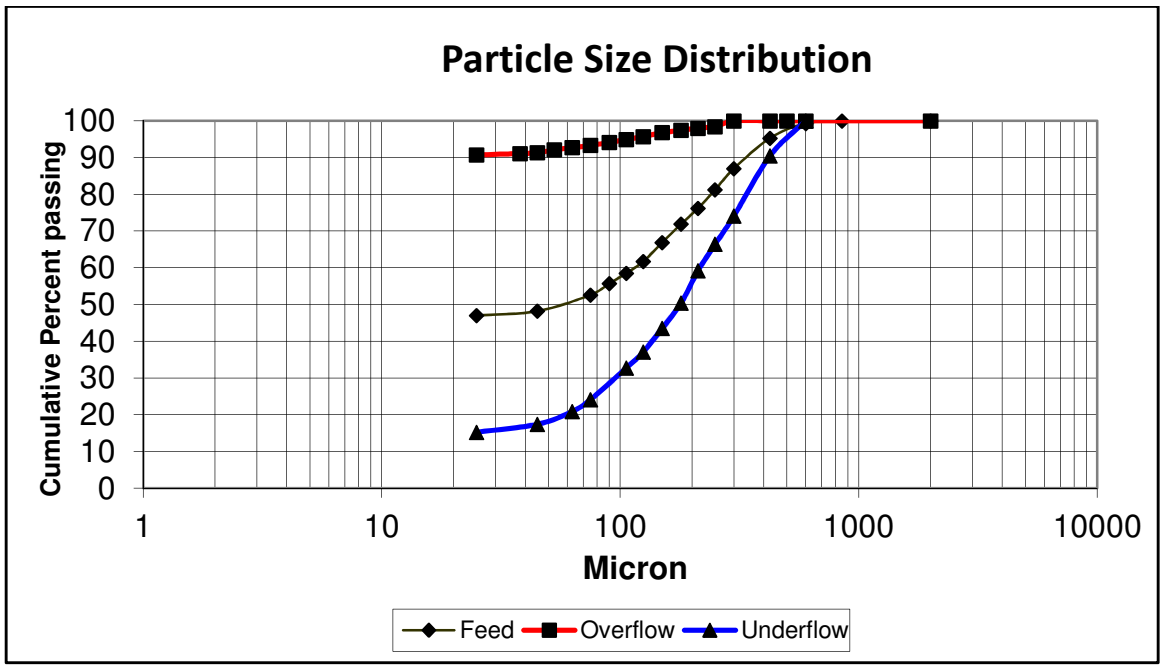

Figure 4-30: Particle size distribution results for cluster cyclones

The performance of the cluster cyclones was tested with the undersize material of the Hi-G screen as cluster feed. The results were fitted and the following parameters were determined (see Figure 4-31):

Alpha = 4.949

d_{50c} = 45.97
R_f = 0
SSE = 0.028

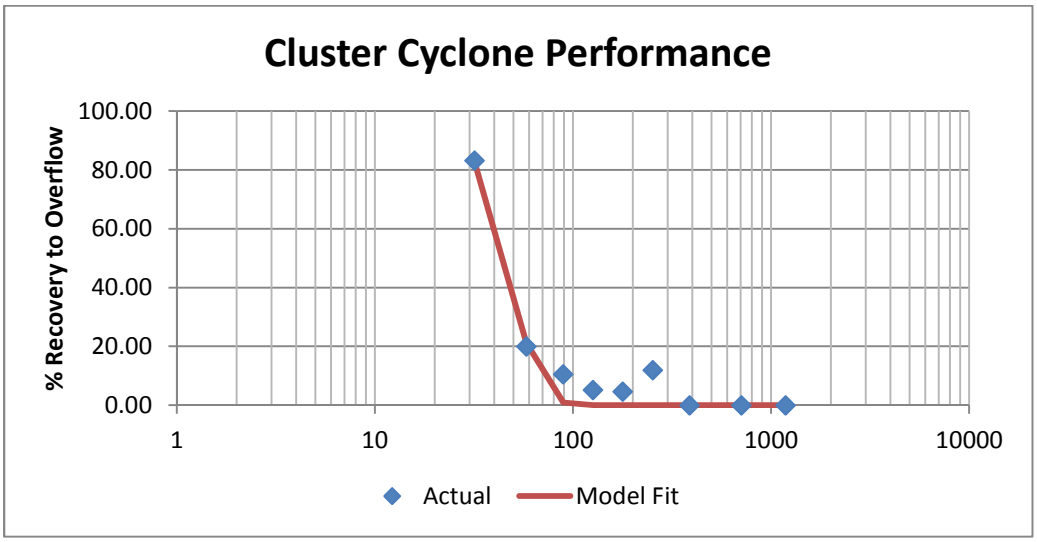

Figure 4-31: Efficiency of cluster cyclone performance with Hi-G screen undersize

A summary of the results obtained by Derrick Corporation on Daberas material is presented in Table 4-2.

Table 4-2: Derrick Hi-G dewatering screen test results at 3° angle

Equipment Type	PSI/ Opening (mm)	Feed			Underflow/Oversize				Overflow/Undersize			
		Slurry (m^3/h)	Dry Solids (MTPH)	Solids (%)	Weight (%)	Dry Solids (MTPH)	Slurry (m^3/h)	Solids (%)	Weight (%)	Dry Solids (MTPH)	Slurry (m^3/h)	Solids (%)
Dewatering Screen	0.5	56.8	42.5	50.7	42.7	18.2	11.6	78.0	57.3	24.3	44.9	40.2
12 - 4"cones	40.0	152.2	24.3	14.6	56.9	13.8	10.3	71.9	43.2	10.5	141.0	7.1

All significant performance parameters were analysed based on the raw laboratory data of both the screen and the cyclones. These parameters can therefore be considered to simulate the performance the system.

4.4 Hi-G Dryer system LIMN simulations

In order to comprehend the impact of some of the parameters on the Hi-G Dryer system, LIMN simulations were conducted. The screen and cyclone parameters based on these results were used as input to model the performance of the equipment and understand how different scenarios could affect the system.

4.4.1 Laboratory test model

The Hi-G screen could not be tested independently on-site due to the discharge of the cluster cyclones onto the screen. The independent laboratory test results of the screen were therefore considered. They yielded the model parameters presented in Table 4-3.

Table 4-3: Screen and cyclone model parameters obtained from laboratory data

	Hi-G screen	Cyclones
Nominal d_{50c} cut size (mm)	0.58	0.046
R_f – bypass fraction	0.06	0.00
Alpha – sharpness of cut	1.572	4.949

The mass balance presented in Figure 4-32 was generated based on the model parameters.

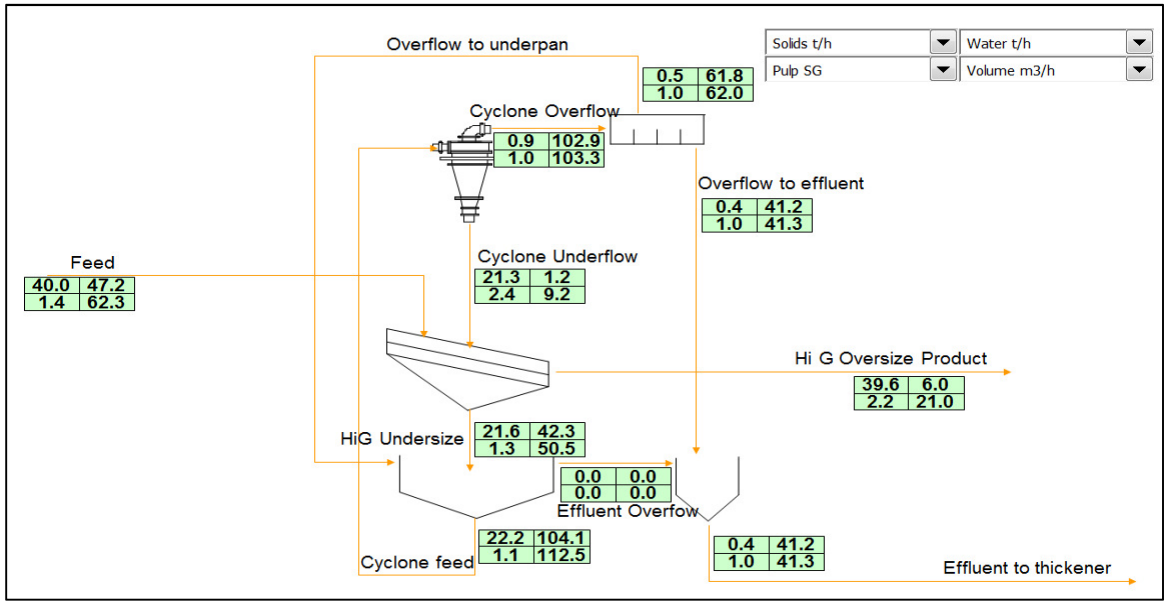

Figure 4-32: Mass balance using parameters obtained from laboratory model

4.4.2 Daberas on-site test model

To simulate the Daberas test results, the Alpha and R_f of the screen was kept the same. The cluster cyclone parameters obtained from the Daberas test results were used and the screen d_{50c} was changed to simulate the 180 µm panels (see Table 4-4).

Table 4-4: Screen and cyclone parameters obtained on-site

	Hi-G screen	Cyclones
Nominal d_{50c} cut size	0.18	0.017
R_f – bypass fraction	0.06	0.00
Alpha – sharpness of cut	1.572	1.22

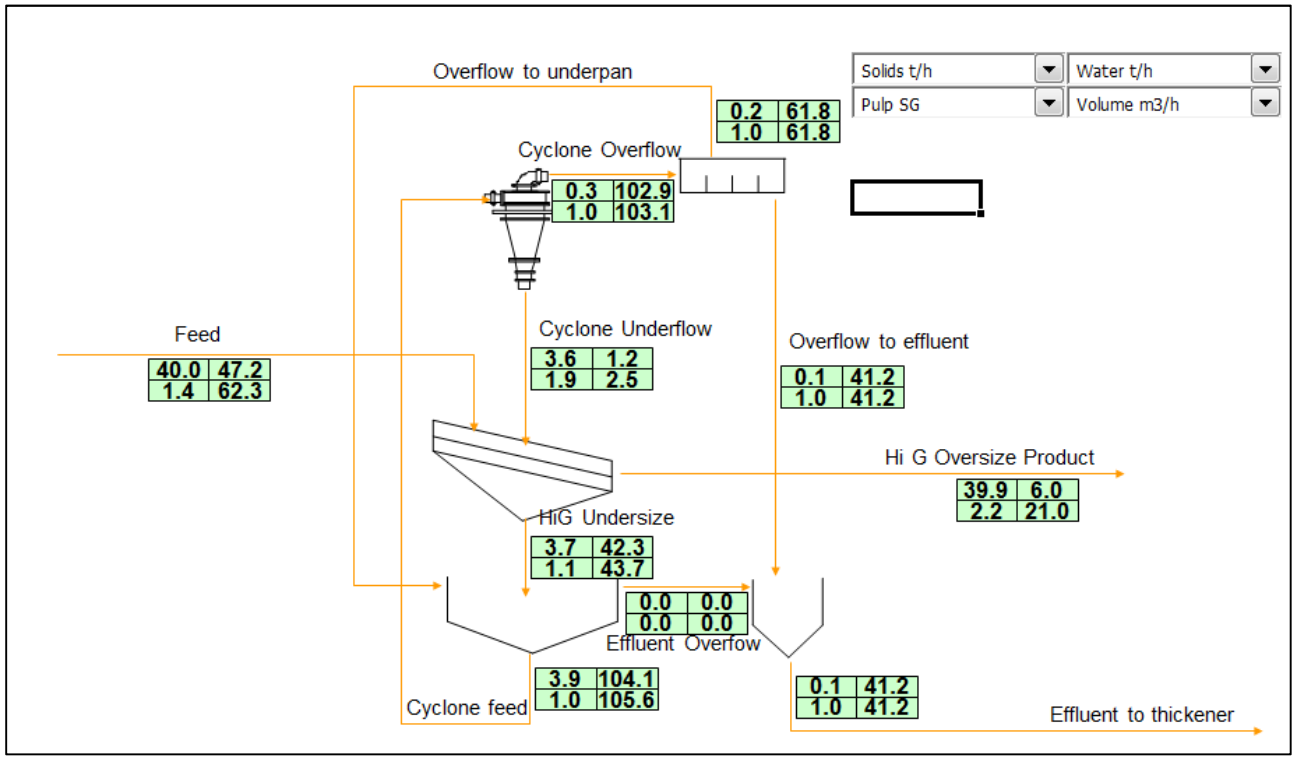

Figure 4-33: Mass balance using parameters obtained on-site

The simulation of the on-site test compares well with the laboratory simulation. Both simulations produced an overall oversize recovery of 99% with similar moisture content. The difference between the two systems is the screen cut size, which is higher in the laboratory simulation. The 180 µm panels proved to produce better results in the on-site

test, hence the difference in cut size. This means that fewer solids are fed to the screen undersize and thus the cluster cyclones.

4.4.3 Influence of Hi-G screen apertures on the system

Changing the panels from 500 µm to 180 µm contributed towards the improved performance of the system. The sensitivity of the apertures was simulated to understand the impact on the system. A change in screen apertures could have a significant effect on the feed to the cyclones (see Figure 4-34). Increasing the cut size has a significant effect on the cluster cyclones as it would increase feed to the cluster cyclones. The cluster cyclones would need to be sized accordingly to accommodate the extra volume that would be produced as a result of increased drainage through the screen. The impact of aperture size on other model outputs, such as effluent and screen oversize product, was insignificant.

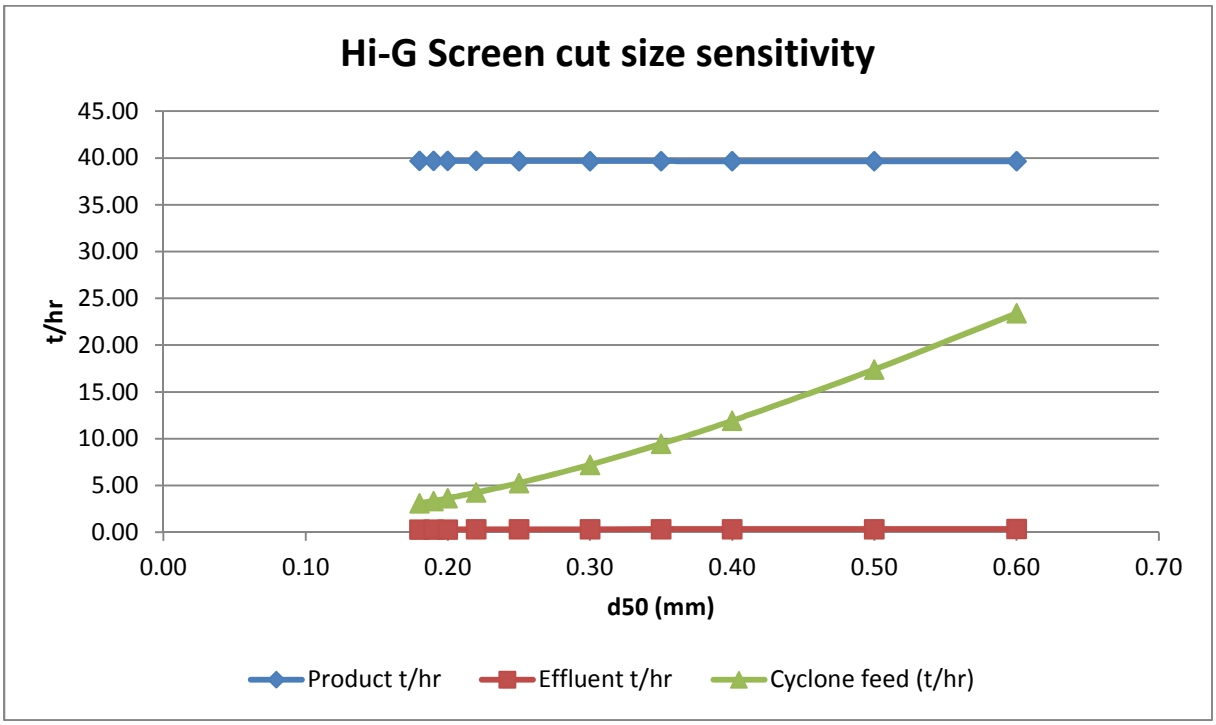

Figure 4-34: Influence of cut size on the system

4.4.4 Influence of feed rate on system

The system was simulated at different feed rates to understand the impact of feed rate on the system. The results are presented in Figure 4-35. As expected, the product oversize increased as the feed rate increased. An interesting observation was the difference between the 500 µm aperture panels and the 180 µm aperture panels as the feed rate increased.

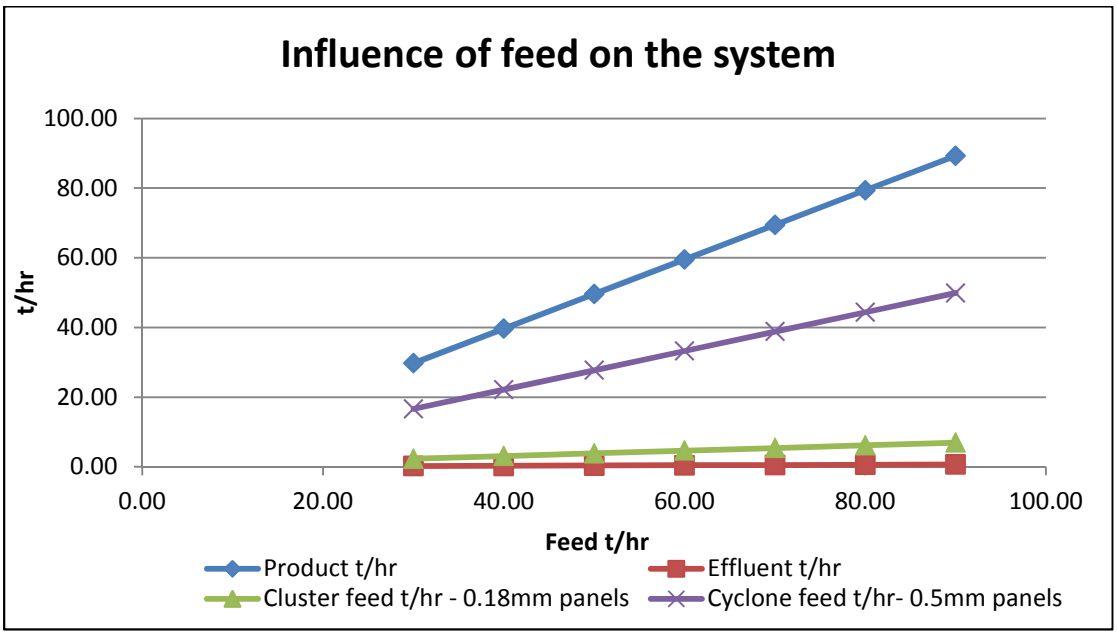

Figure 4-35: Influence of feed rate

Using 500 µm aperture panels would have a more significant impact on the cluster cyclones as the feed rate to the system increases. The 500 µm presents are greater open area allowing more drainage to the screen underflow thus having a significant impact on the cluster cyclones. The 180 µm panels would remove the majority of the solids to oversize, thus reducing the impact of solids on the cluster cyclones. This confirms that using 180 µm panels would be more beneficial than using the larger 500 µm aperture panels.

4.4.5 Scale-up and thickener impact

The Hi-G system performed better than the Daberas dewatering system in terms of dewatering the screen oversize. An average of 2.5% of the solids that were fed into the Hi-G system was lost to effluent. In the existing Daberas degrit system, about 19.6% of the material fed to the degrit section reported to the thickener as feed. Therefore installing a Hi-G Dryer as the new system layout at Daberas could mean reducing the thickener solids capacity by more than 80%. If a Hi-G Dryer system is installed, system needs will increase in capacity. The Daberas system can produce about 180 t/hr of slurry from a 400 t/hr head feed. Either a five 4x10 Hi-G screen system or one 5x14 Hi-G screen system would be able to accommodate the 180 t/hr slurry feed (see Table 4-5).

Table 4-5: Up-scaling options

	4 x 10 Hi-G screen	**5 x 14 Hi-G screen**	**Daberas system**
Feed required (t/hr)			180
Max Hi-G feed (t/hr)	40	300	
Number of Hi-G screens required to replace Daberas degrit	5	1	

The mass balance of the up-scaled system is presented in Figure 4-36. The cluster cyclones would need to be sized accordingly. Five screens would require more maintenance and a larger footprint. From a macro-techno-economic view it would be wise to rather opt for the one 5x14 Hi-G screen.

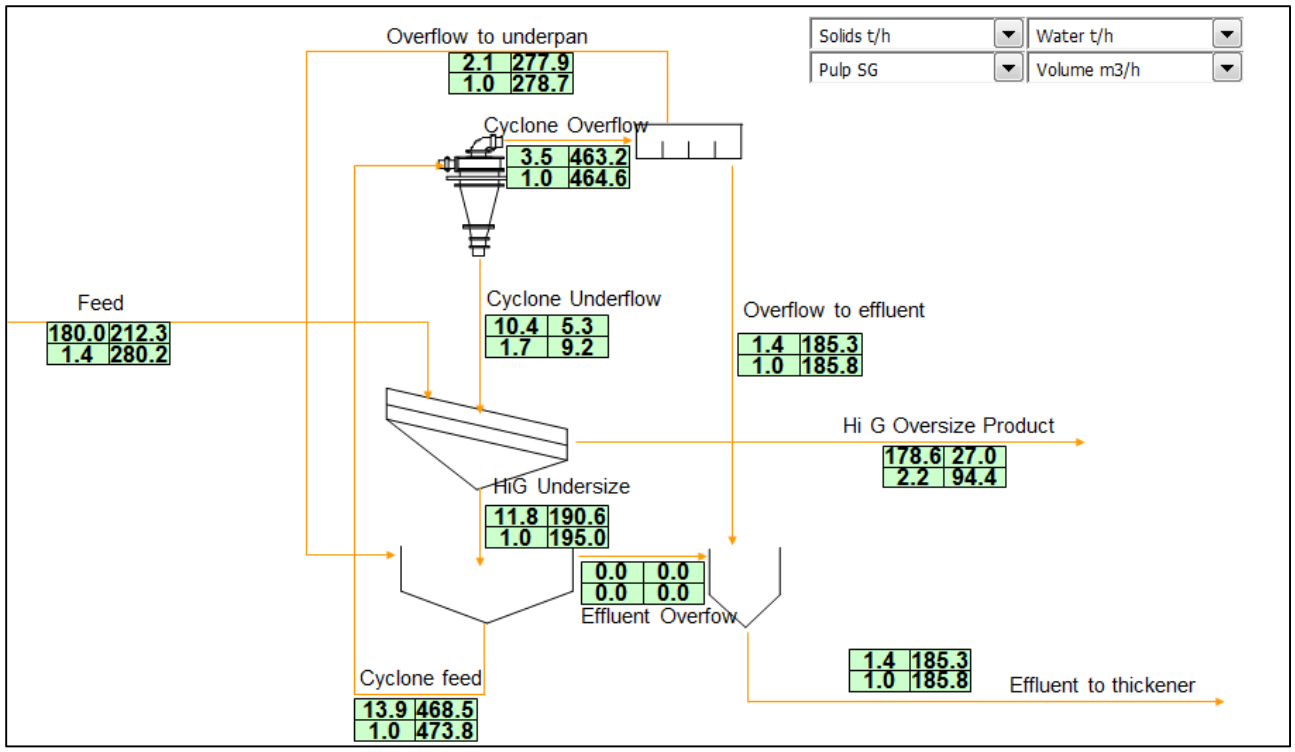

Figure 4-36: Mass balance of scale-up Hi-G Dryer system

5 Conclusion and recommendations

The objective of this project was to investigate whether the Hi-G Dryer system would be capable of producing effective dewatering results on a coarse Daberas feed slurry. In industry the Hi-G Dryer system was effectively operating with 38 µm to 75 µm particle material as feed (Bateman, 2002) (AggMan Staff, 1999). From Namdeb's perspective, this study is imperative because of the potential of reducing slimes disposal footprint especially when mining in environmentally sensitive areas. The dewatering principles were studied and effectively applied to evaluate and optimise the Hi-G Dryer system to produce the best results considering the impact of the coarse feed distribution on screen and hydrocyclone performance.

The literature study revealed the dynamics of screening and cyclone performance, and the application of the technologies within the system. Screens are ultimately utilised as a means of classification, but dewatering makes use of a slightly different convention. The purpose of dewatering is to allow most of the water to drain whilst the majority of the solids report as screen oversize. The dewatering industry uses both static screens and dynamic screens. For dynamic screens the rule of thumb is to use high-frequency, small aperture screen panels with a multi-slope or an inclined angle. The literature study also highlighted the parameters that could have an effect on dewatering, such as aperture size and shape, screen slope, screen frequency and amplitude, and PSD.

What makes Hi-G technology different is that the screen is able to run at a higher frequency than any other screen on the market. This allows more force on the slurry, breaking water tension and enhancing bed depth for better drainage. The water that is drained from the screen passes through a second processing stage by making use of hydrocyclone technology. The hydrocyclones' purpose is to remove more solids and to thicken the solids to allow the solids to be removed with the material bed.

The results revealed that the initial process layout produced an oversize solids moisture content of about 17.2% with a 98% recovery to screen oversize. The oversize product

reported to the tailings dump was stable, as confirmed by the yield stress results. Although there were some good results, the following inefficiencies were highlighted:

- The primary cyclone was constantly under roping conditions, thus misplacing a large amount of material to the overflow. Although the Imperfection of 0.2 was found which is a good efficiency it had no D_{100} thus misplacing material over the entire size range.
- The misplaced material from the primary cyclone negatively affected the cluster cyclones through blockages due to spigot crowding, resulting in misplaced material over the entire size range as well. The cluster cyclone Imperfection was calculated to 0.72 which is very poor and the partition curve had no D_{100} thus confirming the poor performance.
- Although the Hi-G screen performed well, the slurry covered more than the recommended one-third of the screen.
- A great deal of agitation in the underpan hindered settling, allowing large particles to report to the effluent.
- The water clarity indicated that there was still a large amount of ultra-fines in the effluent, which meant that it could not be used as process water.

After considering the dewatering parameters studied in the literature review, the following improvements were implemented to optimise the Hi-G Dryer system's performance:

- Bypassing the primary cyclone
- Inclining the screen at 12°
- Replacing the 500 µm aperture panels with 180 µm aperture panels

As the modifications progressed, notable improvements in the results were observed. The system produced a much dryer solids product, with an average of about 13% moisture, due to more efficient cyclone performance. No material was misplaced by the cluster cyclones and overall dewatering was very effective. The Imperfection for the cluster cyclones were calculated to 0.34 which is good, with a D_{100} of 200 µm thus proving an improvement in the performance with no misplaced material. After all the modifications

were made, the system performance exceeded the Daberas dewatering system performance. The oversize product stability also improved.

It was imperative to determine the Hi-G screen performance independently; therefore a sample of the Daberas material was sent to Buffalo, USA in order to conduct some testing under laboratory conditions. The laboratory test results together with the on-site results were used to model screen and cluster cyclone performance of the new process layout. The results were modelled in LIMN in order to comprehend the variable outputs of the system. The modelled results revealed that it is more beneficial to use the 180 µm aperture panels, because of the reduced impact on the cluster cyclones; the lower cut point would remove the majority of the material to the oversize, and it would also assist with material bed formation and dewatering.

The system can definitely reduce thickener capacity, but would not be able to replace the thickener. About 97.5% of the material that enters the Hi-G Dryer was effectively removed from the system, thus only about 2.5% of the solid material reported to the thickener. Further studies should be done to investigate the high feed densities, which is a concern. The clarity results verified that there is still a large amount of ultra-fines in the Hi-G Dryer effluent, which means that it cannot be used as process water. The benefit of the Hi-G Dryer is that a much drier and more stable product is produced to convey to a tailings dump.

The results conclude that the Hi-G Dryer Fines Recovery System is a viable dewatering system at the Daberas plant, which consists of a much coarser slurry.

Further testing on the Hi-G Dryer system is suggested to enhance performance even more as well as reveal extra benefits. The following recommendations for Hi-G Dryer testing should be investigated:

- Adjust the cluster cyclone underflow discharge to a position where it is discharged after the dewatering zone. This would prevent fluidisation of the cluster underflow and promote material bed filtration.

- Investigate the cause of the high feed densities by taking samples at different feed points.
- Investigate the Hi-G Dryer system performance by feeding the system with the Daberas thickener underflow as proposed in Figure 5-1. The Daberas thickener underflow is less than 500 µm, which is within the normal operating particle size range. Feeding the system with the thickener underflow would reveal how the system performs with a higher solids concentration.

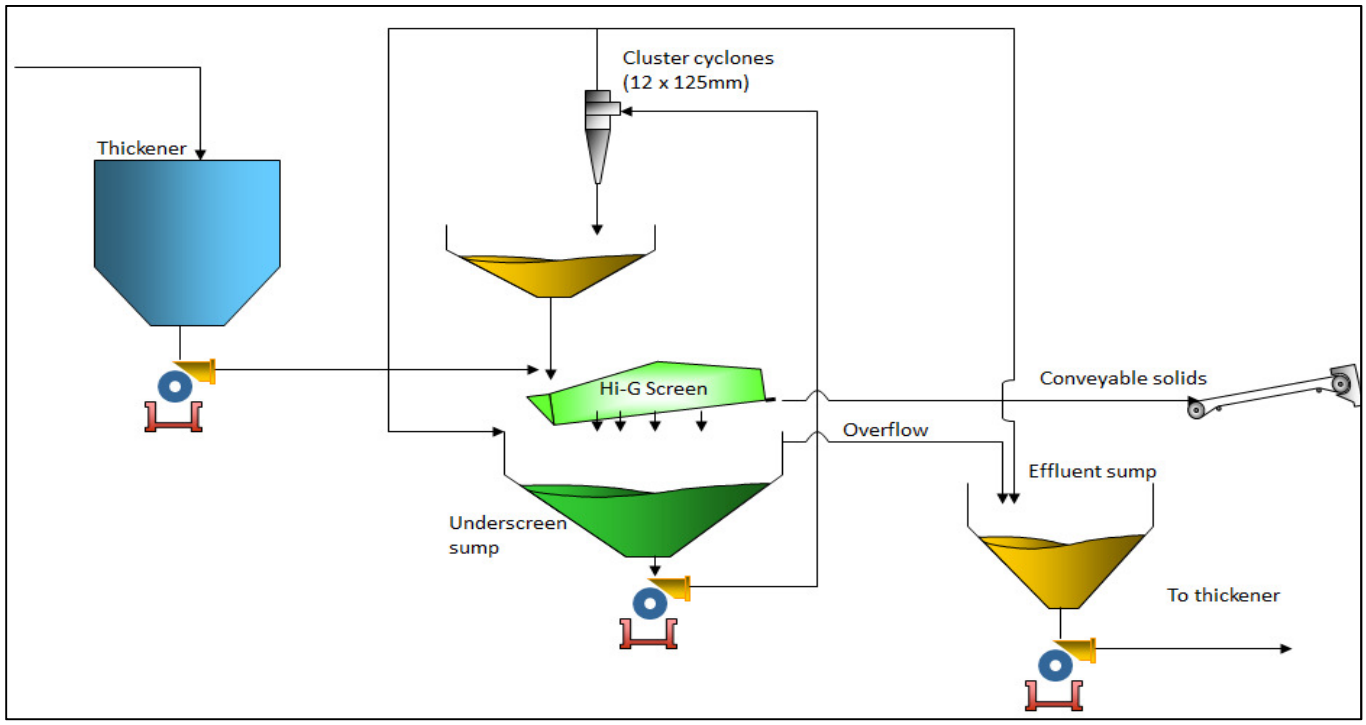

Figure 5-1: Schematic of the Hi-G Dryer system fed from the thickener underflow

6 References

AggMan Staff, 1999. ELAM S&G Streamlines Fines Management. *Aggregates Manager,* October.4(7).

Allis-Chalmers Corporation., n.d. Vibrating screen, theory and selection. *Bulletin 26M5506.* Appleton, WI

Arterburn, R. A., 1982. The Sizing and Selection of Hydrocyclones. In: A. Mular & G. Jorgensen, (eds). *Design and Installation of Comminution Circuits.* New York: AIME, pp. 592-607.

Bateman, A., 2002. Fines Recovery delivers new saleable product, reduces costs. *Aggregates & Roadbuilding,* July.pp. 2-4.

Chu, L.-Y. & Luo, Q., 1994. Hydrocyclone with High Sharpness of Separation. *Filtration & Separation,* Volume 15, pp. 733-736.

Cleary, P. W., Sinnott, M. D. & Morrison, R. D., 2009. Separation performance of double deck banana screens - Part 1: Flow and separation for different accelerations. *Minerals Engineering,* Volume 22, pp. 1218-1229.

De Pretto, R., 2000. Sizing and Screening. In: *Diamond Processing Handbook: Metallurgical Unit Process.* n.l.:n.n.

Derrick Corporation, 2008a. *Derrick Hi-G Dryer Fines Recovery System.* [Online]
Available at:
http://www.derrickcorp.com/Images/Documents/Fines%20Recovery%20System%20Rev%2010 08.pdf
[Accessed 20 March 2012].

Derrick Corporation, 2008b. *Stack Sizer: The highest Capacity, most efficient, fine wet screening machine in the world.* [Online]
Available at:
http://www.derrickcorp.com/Iimages/Documents/StackSizer%20WebBrochure%209 08.pdf
[Accessed 20 March 2012].

Derrick Corporation, 2010. *Tensionable urethane separation surfaces.* [Online]
Available at: http://www.derrickcorp.com/Images/Documents/UrethaneFlier

RevOct2010.pdf
[Accessed 20 March 2012].

Dong, K. J. & Yu, A. B., 2012. Numerical simulation of the particle flow and sieving behaviour on sieve bend/low head screen combination. *Minerals Engineering,* Volume 31, pp. 2-9.

Finch, J. A., 1983. Modelling a fish-hook in Hydrocyclone Selectivity Curves. *Powder Technology,* Issue 36, pp. 127-129.

Gaudin, A., 1939. *Principles of Mineral Dressing.* New York: McGraw-Hill.

Gupta, A. & Yan, D. S., 2006. Classification. In: A. Gupta & D. Yan, eds. *Mineral Processing Design and Operation.* Philadelphia: Elsevier, pp. 354-400.

Horton, N., 1997. New on Screen. *World Mining Equipment,* June.pp. 8-15.

Jianzhang, X. & Xin, T., 2012. Particile stratification and penetration of a linear vibrating screen by the discrete element method. *International Journal of Mining Science and Technology,* Volume 22, pp. 357-362.

Kawatra, S. K., Bakshi, A. K. & Rusesky, M. T., 1996. Effect of Viscosity on the Cutsize of Hydrocyclone Classifiers. *Minerals Engineering 9,* pp. 881-891.

Kelly, E. G. & Spottiswood, D. J., 1989. *Introduction to Mineral Processing.* 2nd ed. Denver: Mineral Engineering Services.

Kelsall, D. F., 1953. A further study of the hydraulic cyclone. *Chemical Engineering Science,* Issue 2, pp. 254-272.

Kilavuz, F. S. & Gulsoy, O. Y., 2011. The effect of cone ratio on the separation efficiency of small diameter hydrocyclones. *International Journal of Mineral Processing,* Volume 98, pp. 163-167.

Lamb, W., 2000. Dewatering. In: *Diamond Processing Handbook.* n.l.:n.n., pp. 816-832.

Linatex, 2006. *Velco Dewatering Screen,* Gallatin, TN: Linatex.

Lynch, A. J., 1965. The characteristics of hydrocyclones and their application as control units in comminution circuits. *Prog. Rep. Mining and Metallurgy,* Queensland University, Issue No. 6.

Lynch, A. J. & Rao, T. C., 1975. *Modelling and Scale-up of hydrocyclone classifiers.* In M. Carta (ed.). *Proceedings of the 11th International Mineral Processing Congress*. Cagliari, pp. 245-269.

Majumder, A. K., Yerriswamy, P. & Barnwal, J. P., 2003. The "fish-hook" phenomenon in centrifugal separation of fine particle. *Minerals Engineering,* Volume 16, pp. 1005-1007.

Meshcape Industries (Pty) Ltd, 2005. g - The Forgotten Force in Screening. *Technical Bulletin.*

Neesse, T. & Dueck, J., 2007. Dynamic modeling of hydrocyclone. *Minerals Engineering,* Volume 20, pp. 380-386.

Neesse, T., Dueck, J. & Minkov, L., 2004. Separation of finest particles in hydrocyclones. *Minerals Engineering,* Volume 17, pp. 689-696.

Osborne, D. G., 1988. Coal Preparation Technology. In: London: Graham & Trotman Limited, pp. 199-460.

Oscillation Pty Ltd, 2012. [Online]
Available at: http://www.clarometer.com/Claritywedge.html
[Accessed 3 March 2012].

Pashias, N., Summers, J., Glenister, D. J. & Boger, D. V., 1996. A fifty cent rheometer for yield stress measurement. *Journal of Rheology,* Issue 40, pp. 1179-1189.

Plitt, L. R., 1976. A Mathematical Model of a Hydrocyclone Classifier. *CIM Bulletin,* Issue 69, pp. 114-123.

Plitt, L. R. & Kawatra, S. K., 1979. Estimating the cut (d50) size of Classifiers without product particle-size measurement. *International Journal of Mineral Processing,* Volume 5, pp. 369-378.

Rogers, R. S. & Brame, K. A., 1985. An Analysis of the High-Frequency Screening of Fine Slurries. *Power Technology,* Volume 42, pp. 297-304.

Russell, A., 1991. Screens for all seasons. *Industrial Minerals,* April.pp. 39-51.

Schubert, H., 2010. Which demands should and can meet a separation model for hydrocyclone classification?. *International Journal of Mineral Processing,* Volume 96, pp. 14-26.

Soldinger, M., 1999. Interrelation of the stratification and passage in the screening process. *Minerals Engineering,* 12(5), pp. 497-519.

Soldinger, M., 2000. Influence of particle size and bed thickness on screening process. *Minerals Engineering,* March, 13(3), pp. 297-312.

Stokes, G. G., 1891. In: *Mathematical and Physical Paper III.* New York: Cambridge University Press.

Svarovsky, L., 1984. *Hydrocyclones.* 3rd ed. London: Holt Rinehart & Winston.

Tavares, L. M., Souza, L. L., Lima, J. R. & Possa, M. V., 2002. Modelling classification in small-diameter hydrocyclones under variable rheological conditions. *Minerals Engineering,* Volume 15, pp. 613-622.

Venkoba Rao, B., Kapur, P. C. & Rahul, K., 2003. Modeling the size-density partition surface of dense-medium separators. *International Journal of Mineral Processing,* 72(1-4), pp. 443-453.

Wills, B. A. & Napier-Munn, T. J., 2006. *Mineral Processing Technology: An Introduction to the Practical Aspects of Ore Treatment and Mineral Recovery.* 7th ed. Amsterdam: Elsevier Science & Technology.

7 Appendix I

Laboratory testing

LIMN mass balance

Table 7-1: Laboratory mass balance parameters

		Feed	Cyclone feed	Effluent Overfow	Cyclone Overflow	Overflow to effluent	Overflow to underpan	Cyclone Underflow	HiG Undersize	Effluent to thickener	Hi G Oversize Product
Water t/h		47.17	104.111	0.00	102.943	41.177	61.766	1.168	42.345	41.177	5.993
Size	Mean										
+4	5.66	0.038	0.00	0.00	0.00	0.00	0.00	0.00	0.00	0.00	0.038
+2.8	3.35	1.274	0.001	0.00	0.00	0.00	0.00	0.001	0.001	0.00	1.274
+2	2.37	4.545	0.027	0.00	0.00	0.00	0.00	0.027	0.027	0.00	4.545
+1.4	1.67	8.619	0.335	0.00	0.00	0.00	0.00	0.335	0.335	0.00	8.619
+1	1.18	7.644	1.147	0.00	0.00	0.00	0.00	1.147	1.147	0.00	7.644
+0.5	0.71	12.713	7.573	0.00	0.00	0.00	0.00	7.573	7.573	0.00	12.713
+0.3	0.39	3.242	5.577	0.00	0.00	0.00	0.00	5.577	5.577	0.00	3.242
+0.212	0.25	0.757	2.245	0.00	0.00	0.00	0.00	2.245	2.245	0.00	0.757
+0.15	0.18	0.338	1.427	0.00	0.00	0.00	0.00	1.427	1.427	0.00	0.338
+0.106	0.13	0.231	1.302	0.00	0.00	0.00	0.00	1.302	1.302	0.00	0.231
+0.075	0.09	0.14	0.979	0.00	0.009	0.004	0.006	0.97	0.973	0.004	0.136
+0.045	0.06	0.121	0.664	0.00	0.141	0.056	0.085	0.523	0.58	0.056	0.065
-0.045	0.03	0.337	0.899	0.00	0.741	0.296	0.445	0.157	0.454	0.296	0.04
	Total (t/hr)	40.00	22.177	0.00	0.892	0.357	0.535	21.285	21.642	0.357	39.643

Screen model

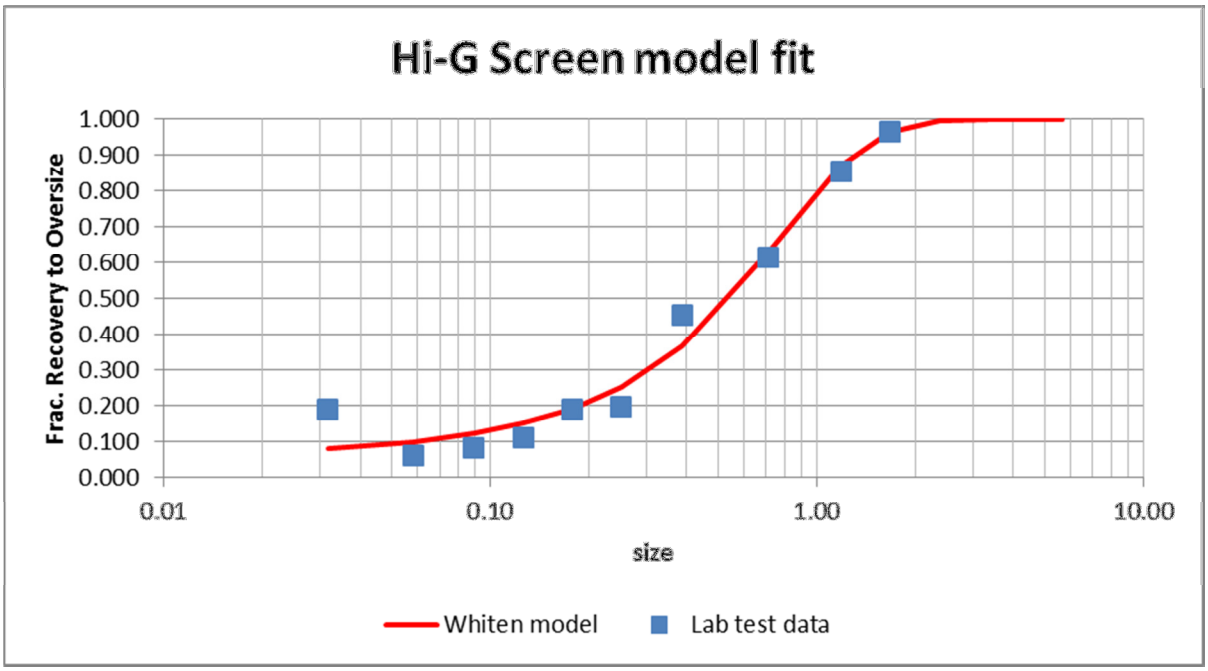

Figure 7-1: Laboratory screen parameters partition curve

Screen parameters

Table 7-2: Laboratory screen model parameters

Model parameters	
Nominal d_{50c} cut size	0.58
R_f – bypass fraction	0.06
Alpha – sharpness of cut	1.572
SSE	0.027

Cluster cyclone model

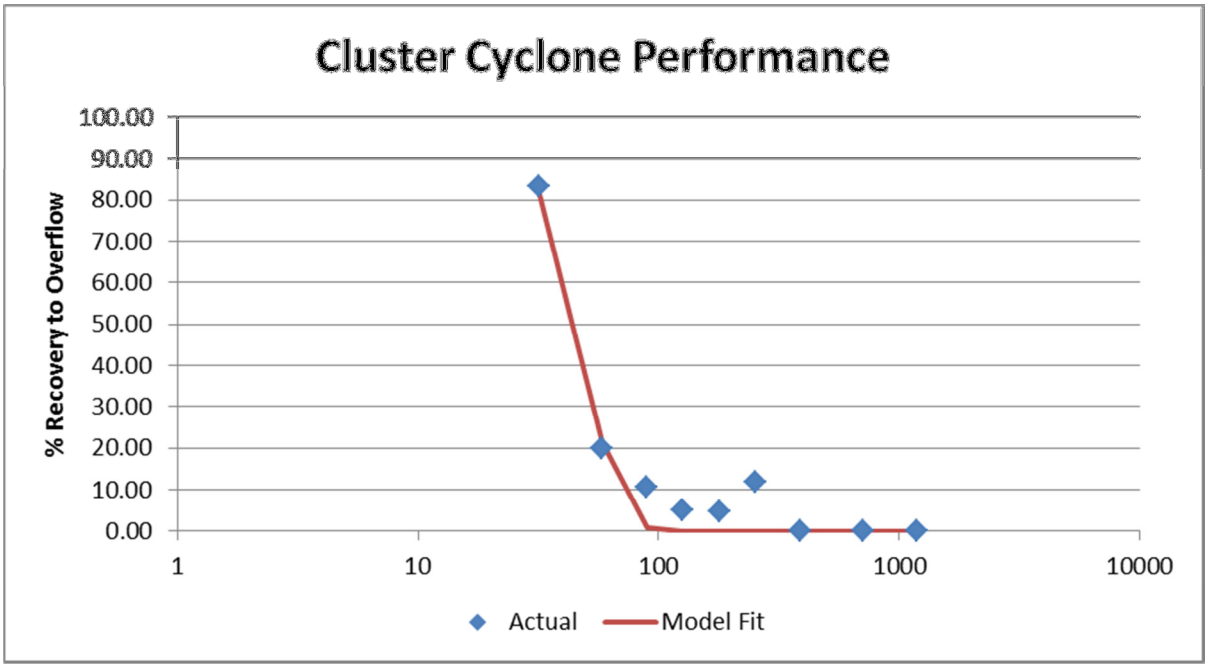

Figure 7-2: Laboratory cyclone parameters partition curve

Cluster cyclone parameters

Table 7-3: Laboratory cluster cyclone model parameters

Model parameters	
Nominal d_{50c} cut size	0.046
R_f – bypass fraction	0.00
Alpha – sharpness of cut	4.949
SSE	0.028

Daberas on-site testing

Table 7-4: Daberas on-site parameters mass balance

		Feed	Cyclone feed	Effluent Overflow	Cyclone Overflow	Overflow to effluent	Overflow to underpan	Cyclone Underflow	HiG Undersize	Effluent to thickener	Hi G Oversize Product
Water t/h		47.17	104.111	0.00	102.943	41.177	61.766	1.168	42.345	41.177	5.993
Size	Mean										
+4	5.66	0.038	0.00	0.00	0.00	0.00	0.00	0.00	0.00	0.00	0.038
+2.8	3.35	1.274	0.00	0.00	0.00	0.00	0.00	0.00	0.00	0.00	1.274
+2	2.37	4.545	0.00	0.00	0.00	0.00	0.00	0.00	0.00	0.00	4.545
+1.4	1.67	8.619	0.00	0.00	0.00	0.00	0.00	0.00	0.00	0.00	8.619
+1	1.18	7.644	0.001	0.00	0.00	0.00	0.00	0.001	0.001	0.00	7.644
+0.5	0.71	12.713	0.095	0.00	0.00	0.00	0.00	0.095	0.095	0.00	12.713
+0.3	0.39	3.242	0.406	0.00	0.00	0.00	0.00	0.406	0.406	0.00	3.242
+0.212	0.25	0.757	0.328	0.00	0.00	0.00	0.00	0.328	0.328	0.00	0.757
+0.15	0.18	0.338	0.305	0.00	0.00	0.00	0.00	0.305	0.305	0.00	0.338
+0.106	0.13	0.231	0.371	0.00	0.00	0.00	0.00	0.371	0.371	0.00	0.231
+0.075	0.09	0.14	0.357	0.00	0.001	0.00	0.001	0.355	0.356	0.00	0.14
+0.045	0.06	0.121	0.473	0.00	0.015	0.006	0.009	0.458	0.464	0.006	0.115
-0.045	0.03	0.337	1.566	0.00	0.315	0.126	0.189	1.251	1.377	0.126	0.211
	Total (t/hr)	40.00	3.901	0.00	0.332	0.133	0.199	3.57	3.702	0.133	39.867

Screen model

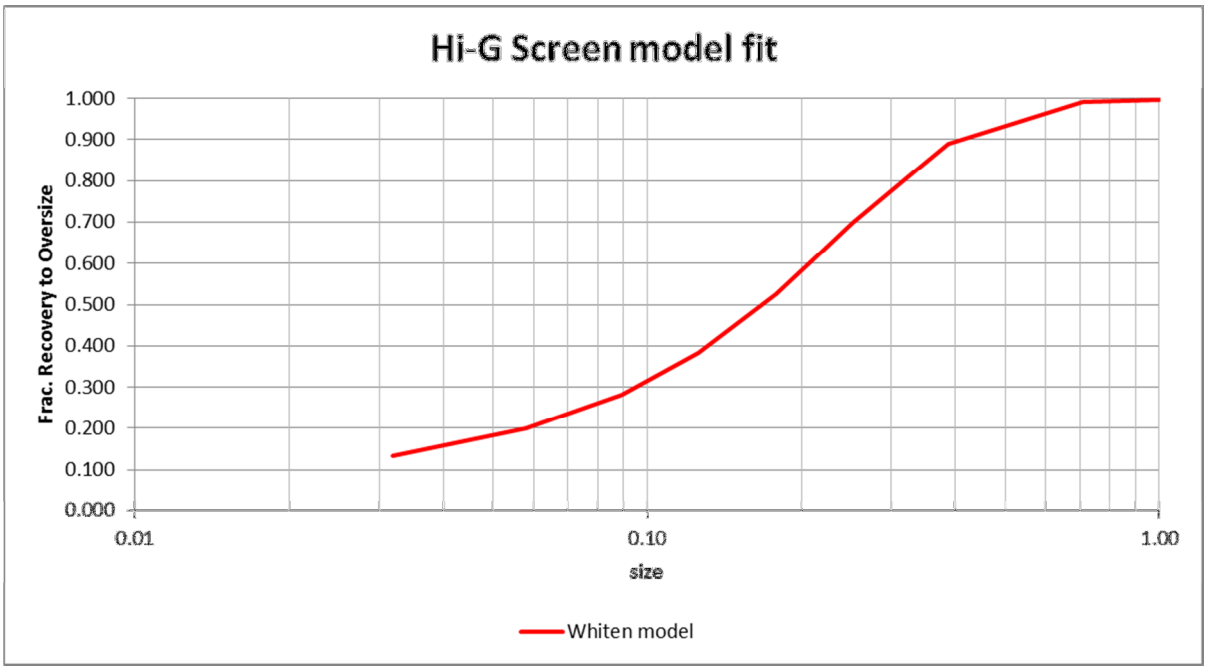

Figure 7-3: Daberas screen parameters partition curve

Screen parameters

Table 7-5: Daberas screen model parameters

Model parameters	
Nominal d_{50c} cut size	0.18
R_f – bypass fraction	0.06
Alpha – sharpness of cut	1.572
SSE	0.855

Cluster cyclone model

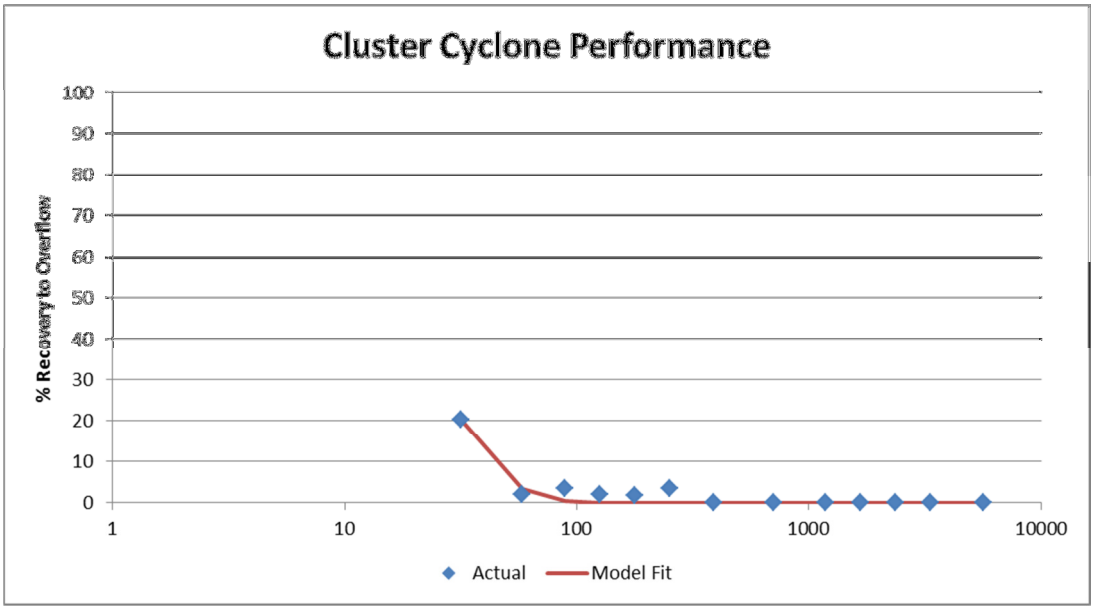

Figure 7-4: Daberas cyclone parameters partition curve

Cluster cyclone parameters

Table 7-6: Daberas cluster cyclone model parameters

Model parameters	
Nominal d_{50c} cut size	0.017
R_f – bypass fraction	0.00
Alpha – sharpness of cut	1.22
SSE	0.003

Influence of Hi-G cut size on the system

Table 7-7: Influence of d_{50} on Hi-G Dryer system

d_{50c}	Product t/hr	Cyclone feed (t/hr)	Effluent t/hr	Effluent t/hr
0.18	39.692	3.091	0.308	0.308
0.19	39.688	3.36	0.312	0.312
0.20	39.685	3.643	0.315	0.315
0.22	39.68	4.252	0.32	0.32
0.25	39.674	5.268	0.326	0.326
0.30	39.666	7.218	0.334	0.334
0.35	39.659	9.451	0.341	0.341
0.40	39.655	11.921	0.345	0.345
0.50	39.647	17.406	0.353	0.353
0.60	39.642	23.401	0.358	0.358

Influence of feed rate on the system

Table 7-8: Influence of feed rate on Hi-G Dryer system

Test selection	Feed	Product t/hr	Effluent t/hr	Cyclone feed t/hr	Vol of effluent (m^3/hr)
180 µm panel	30.00	29.769	0.231	2.318	30.97
180 µm panel	40.00	39.692	0.308	3.091	41.294
180 µm panel	50.00	49.614	0.386	3.864	51.617
180 µm panel	60.00	59.537	0.463	4.636	61.941
180 µm panel	70.00	69.46	0.54	5.409	72.264
180 µm panel	80.00	79.383	0.617	6.182	82.587
180 µm panel	90.00	89.306	0.694	6.955	92.911
500 µm panel	30.00	29.732	0.268	16.628	30.984
500 µm panel	40.00	39.643	0.357	22.171	41.312
500 µm panel	50.00	49.554	0.446	27.714	51.64
500 µm panel	60.00	59.465	0.535	33.257	61.968
500 µm panel	70.00	69.376	0.624	38.80	72.296
500 µm panel	80.00	79.286	0.714	44.343	82.624
500 µm panel	90.00	89.197	0.803	49.885	92.952

8 Appendix II

Flow diagram of overall Daberas process

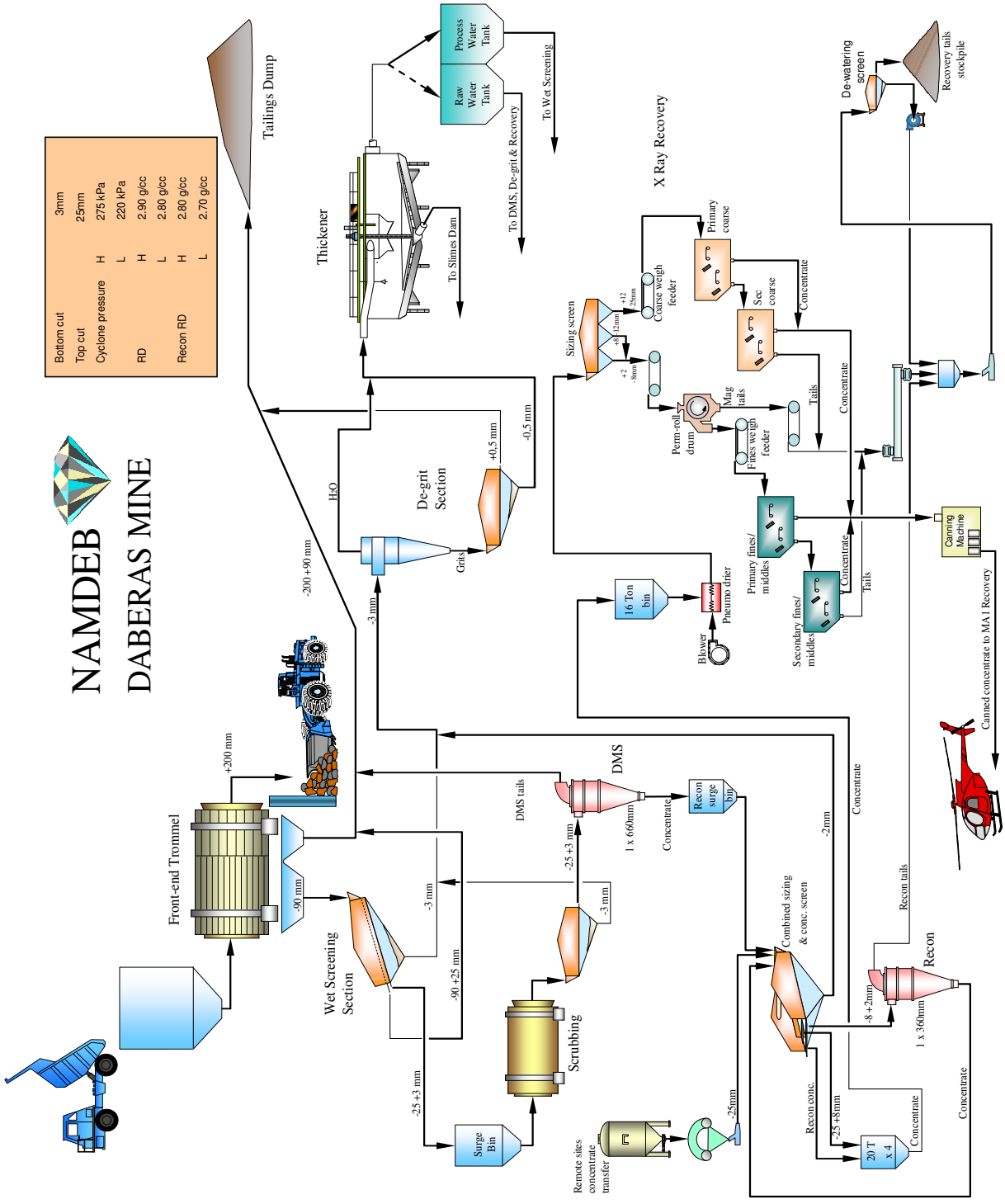

Figure 8-1: Overall Daberas plant